Chapter 17
Mass Transfer and Equilibrium Parameters on High-Pressure CO_2 Extraction of Plant Essential Oils

José M. del Valle, Juan C. de la Fuente, Edgar Uquiche, Carsten Zetzl, and Gerd Brunner

17.1 Introduction

The production of plant extracts is currently limited by safety and regulatory constraints on the concentration of toxic residues of organic solvents such as *n*-hexane or methanol (Sanders 1993). Carbon dioxide (CO_2) is an excellent alternative to these organic solvents due to its inertness, non-toxicity, non-flammability, and low cost (Brunner 1994; del Valle and Aguilera 1999). The recommended temperature in so-called supercritical fluid (SCF) extraction (SCFE) processes is slightly above the critical temperature (T_c) of the solvent so that a near-environmental temperature is applied when using CO_2 ($T_c = 304.2$ K) in SCFE, thus reducing the requirement of energy for separation as well as the thermal damage of labile bioactive compounds (Brunner 1994). Furthermore, objectionable solvent traces are eliminated from the treated substrate and the extract because, being a gas under normal environmental conditions, CO_2 is easily and fully removed following SCFE.

We would like to dedicate this chapter to the memory of our coauthors and friends Damian Cardarelli (1964–2007) and Miguel Mattea (1955–2007) who died tragically as a result of injuries sustained during a fire accident on December 5, 2007, in the pilot plant of the Facultad de Ingeniería in the Universidad Nacional de Rio Cuarto (Córdoba, Argentina). We met them either briefly (JMdV) or a long time ago (JdlF), but we were touched by their intellectual capacity, perseverance, camaraderie, and warmness.

J.M. del Valle (✉)
Departamento de Ingeniería Química y Bioprocesos, Pontificia Universidad Católica (PUC) de Chile, Avda. Vicuña Mackenna 4860, Macul, Santiago, Chile
e-mail: delvalle@ing.puc.cl

J.C. de la Fuente
Departamento de Procesos Químicos, Biotecnológicos y Ambientales, Universidad Técnica Federico Santa María, Valparaíso, Chile

E. Uquiche
Departamento de Ingeniería Química, Universidad de La Frontera, Temuco, Chile

C. Zetzl and G. Brunner
Thermische Verfahrenstechnik, Technische Universität Hamburg-Harburg (TUHH), Harburg, Germany

J.M. Aguilera et al. (eds.), *Food Engineering Interfaces*, Food Engineering Series,
DOI 10.1007/978-1-4419-7475-4_17,

Because of their high compressibility, particularly in the vicinity of the critical point, SCFs exhibit large variations in physical properties, including near-liquid solvent power and near-gas transport properties, and it is possible to take advantage of these improved properties to devise improved (medium-to-high yield, high selectivity, fast) extraction processes (Brunner 1994; del Valle and Aguilera 1999). These advantages of SCFs extend to near-critical liquids and gases. Thus, in this work the use of both supercritical CO_2 and near-critical CO_2 as extraction solvents will be covered; they will be referred to as high-pressure CO_2. The extraction process with high-pressure CO_2 will be referred as SCFE.

The typical quality fluctuations of vegetable substrates and difficulties in obtaining the standardized information required for designing selective SCFE processes make the industrial application of CO_2 as an extraction solvent for plant materials difficult (Zetzl et al. 2003). In this chapter an attempt is made to bridge the gap between scientific research and industrial application of SCFE for obtaining relevant plant extracts. Specifically, the focus will be on the SCFE of plant essential oils using high-pressure CO_2.

Two well-established SCFE applications in the food industry are the decaffeination of coffee (Lack and Seidlitz 1993) and the recovery of bitter compounds from hops to be used in improved beer-producing processes (Hubert and Vitzthum 1978; Gardner 1993). However, in this work it was felt that, viewed from a broader chemical perspective, the two most important types of components extracted from plant materials using high-pressure CO_2 are fatty oils (triglycerides) and essential oils (del Valle et al. 2005a). In the specific case of plant essential oils, SCFE allows a higher yield to be attained in a shorter time as compared to steam distillation, hydro-distillation, and conventional solvent extraction, while simultaneously avoiding thermal and hydrolytic degradation of labile compounds, as well as toxic solvent residues in the product (Stahl et al. 1988; Moyler 1993; Reverchon 1997; Mukhopadhyay 2000; Reverchon and De Marco 2006, 2008; Quirin and Gerard 2007).

Authors del Valle and de la Fuente (2006) described SCFE of fatty oils from seeds, including relevant mass transfer and equilibrium parameters. Thus, the purpose of this chapter is to provide similar information for the industrially important case of SCFE of plant essential oils. Because the solubility of essential oils in high-pressure CO_2 is great, their selective extraction from a plant requires low-to-medium densities to avoid contamination of the extract with heavier and/or more polar compounds such as, e.g., fatty oils and carotenoids. Thus, for the purpose of this chapter, plant essential oils are defined as those terpenes that can be extracted with high-pressure CO_2 at 15 MPa or less.

17.1.1 Chemistry and Localization of Essential Oils

Essential oils are complex mixtures of many volatile compounds that are responsible for the aroma of herbs and spices. As a group, essential oils do not share

common chemical properties beyond conveying the characteristic aroma of the herb or spice and consequently are used for flavoring foods, drinks, perfumes, cosmetics, incense, and bath and house-cleaning products. For applications in foods, a spice is a seed, fruit, root, bark, or leaf that is dried, ground (usually), and used in small amounts as a preservative against deleterious or harmful microorganisms, or as an additive to impart flavor or color to the food. Herbs differ from spices in that they are leafy, green plant parts that are usually chopped into smaller pieces and used in a fresh (undried) condition as food preservatives or flavor additives.

Brielmann et al. (2006) reviewed the chemistry of plant essential oils. The most volatile components in essential oils are terpenes, which are secondary plant metabolites derived from isoprene (2-methyl-1,3-butadiene), a 5-carbon unsaturated hydrocarbon molecule. Terpenes include the 2-isoprene (or 10-carbon) monoterpene hydrocarbons that typically fit a $C_{10}H_{16}$ molecular formula (e.g., *p*-cymene, limonene, α-pinene), the 3-isoprene (or 15-carbon) sesquiterpene hydrocarbons that typically fit a $C_{15}H_{24}$ molecular formula (e.g., β-caryophyllene, α-humulene), and oxygen-containing derivatives of monoterpene and sesquiterpene hydrocarbons (the so-called oxygenated monoterpenes and oxygenated sesquiterpenes, respectively) such as acetates (e.g., linalyl acetate, farnesyl acetate), alcohols (e.g., β-citronellol, geraniol, farnesol, linalool, menthol, patchoulol, verbenol), aldehydes (e.g., *p*-anisaldehyde, citral), ketones (e.g., camphor, carvone, fenchone), phenols (e.g., carvacrol, eugenol, thymol), and oxides (e.g., artemisinin, 1,8-cineole), among others. Among these compounds the oxygenated monoterpenes are especially important because they are responsible for the characteristic aroma of the herb or spice.

Plant essential oils are encapsulated in specialized secretory structures made of high-molecular-weight nonvolatile waxes (C_nH_{2n+2}) and other fatty compounds that protect them against evaporative losses and deleterious oxidative and/or hydrolytic reactions by atmospheric oxygen and water. Essential oils are secreted into specialized structures that can be located in either the surface (the so-called glandular trichomes or glands) or below the outer surface of the plant material (secretory ducts and secretory cavities) depending on the plant family and species (Denny 1991; Zizovic et al. 2007c; Stamenić et al. 2008). The leaves, terminal shoots, and flowers of aromatic herbs of the *Lamiaceae* family, such as basil (*Ocimum basilicum*), lavender (*Lavandula angustifolia*), marjoram (*Origanum majorama*), oregano (*Origanum vulgare*), pennyroyal (*Mentha pulegium*), peppermint (*Mentha* × *piperita*), rosemary (*Rosmarinus officinalis*), sage (*Salvia officinalis*), spearmint (*Mentha spicata*), thyme (*Thymus vulgaris*), and wild thyme (*Thymus serpyllum*), produce superficial oils that are stored in abundant secretory cells called glandular trichomes or glands (Zizovic et al. 2005, 2007c; Stamenić et al. 2008).

Unlike the aromatic herbs of the *Lamiaceae* family that secrete oils in superficial glands, herbs and spices of the *Apiaceae* and *Asteraceae* families secrete oils into subcutaneous ducts (Zizovic et al. 2007a,b,c; Stamenić et al. 2008). These ducts are elongated cavities that can branch out to create a network of interconnected pores extending from the roots, through the stems, and to the leaves, flowers, and fruits of the plants. In this chapter the *Apiaceae* family is

represented by anise (*Pimpinella anisum*), caraway (*Carum carvi*), celery (*Apium graveolens*), fennel (*Foeniculum vulgare*), and parsley (*Petroselinum crispum*), whereas the *Asteraceae* family is represented by candeia (*Eremanthus erythropappus*), carqueja (*Baccharis trimera*), chamomile (*Matricaria recutita*), and marigold (*Calendula officinalis*).

Other forms of subcutaneous oils are accumulated in secretory cavities, which are spherical structures lined with essential-oil-producing ephitelium cells (Zizovic et al. 2007c; Stamenić et al. 2008). Secretory cavities can be found in both aerial and underground parts of many plants including roots (valerian, *Valeriana officinalis*, *Valerianaceae*), rhizomes (ginger, *Zingiber officinale*, *Zingiberaceae*), leaves (alecrim pimenta, *Lippia sidoides*, *Verbenaceae*; boldo, *Peumus boldus*, *Monimiaceae*; cinnamon of Cunhã, *Croton zehntneri*, *Euphorbiaceae*; eucalyptus, *Eucalyptus globulus*, Myrtaceae; ho-sho, *Cinnamomum camphora*, *Lauraceae*), flower buds (clove, *Syzygium aromaticum*, *Myrtaceae*) and cones (hop, *Humulus lupulus*, *Cannabaceae*), fruit peels (orange, *Citrus sinensis*, *Rutaceae*); black pepper, *Piper nigrum*, *Piperaceae*), and seeds (nutmeg, *Myristica fragrans*, *Myristicaceae*).

17.1.2 Organization of Chapter

Figure 17.1 represents the SCFE of a solid substrate in a packed bed. As will be discussed in Sect. 17.2, the process can be modeled using a differential mass balance equation (Fig. 17.1a) coupled with a mass transfer rate equation. During SCFE of a pre-treated plant material, the partition of solutes between the solid and fluid phases (K), the actual solubility of the solutes in the solvent (C_{sat}), and various resistances to mass transfer play important roles in extraction rates. The effective diffusivity in the solid matrix (D_e), external mass transfer coefficient (k_f), and axial dispersion coefficient (D_{ax}) all influence the concentration gradient-driven mass transfer rates within the solid, the stationary SCF film surrounding each particle, and along the bed, respectively (Fig. 17.1b).

Figure 17.2 presents an integral extraction plot of solute yield versus specific solvent consumption resulting from the SCFE of the solid substrate in a packed bed. Although there might be a positive effect of superficial solvent velocity on extraction rates, integral extraction curves generally collapse to a single line, at least initially, with a slope that represents the so-called operational solubility (C_{fo}) (Fig. 17.2, zone I). Scientific research on SCFE of plant essential oils, aimed at the industrial application of the process, should result in mass transfer (k_f, D_{ax}, D_e) and phase equilibrium or pseudo-equilibrium data (K, C_{sat}, C_{fo}) that can be applied for process design purposes.

In Sect. 17.2, mathematical models are presented and discussed for the SCFE of essential oils from a packed bed of plant material, followed by a presentation of the external (k_f) and internal (D_e) mass transfer parameters that have been fitted in the literature to cumulative extraction plots of essential oil yield versus time or specific

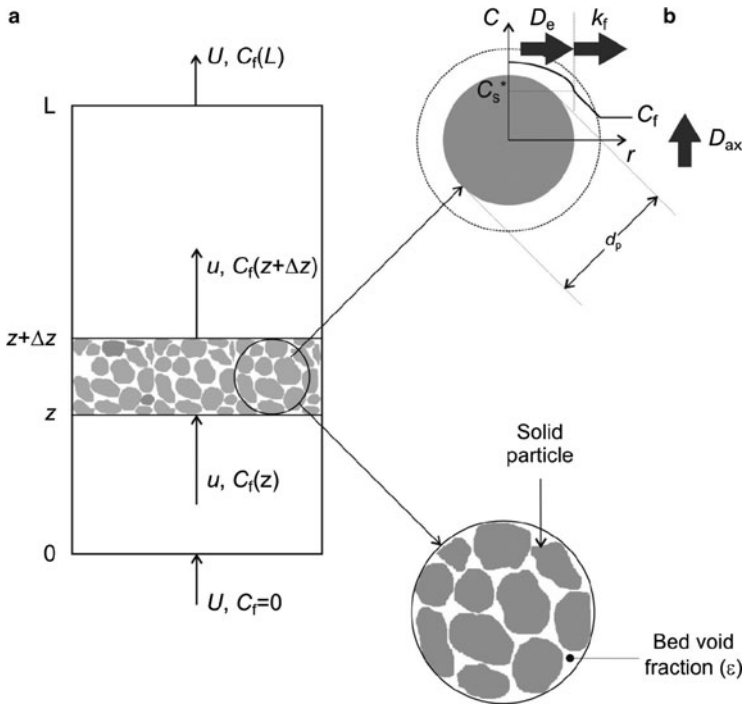

Fig. 17.1 Conceptual model of supercritical fluid extraction of solid substrates in packed beds: (**a**) differential mass balance along packed bed; and (**b**) mass transfer phenomena within solid particle (substrate), between particle and CO_2 (solvent) phase, and in CO_2 phase along bed

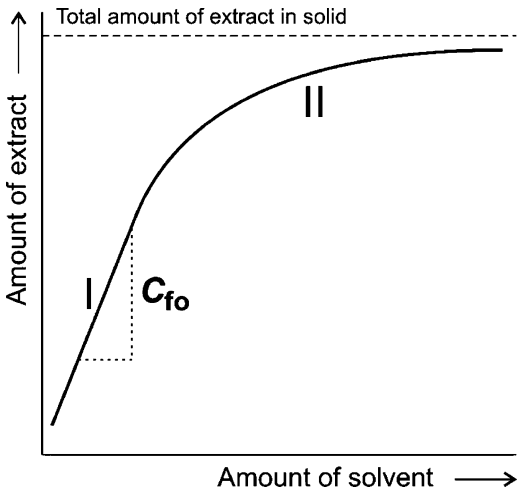

Fig. 17.2 Supercritical fluid extraction curve showing solute yield versus specific solvent consumption. Both the recovered solute and amount of CO_2 passed through the packed bed are expressed in a common base, the amount of substrate loaded into the extraction vessel

solvent consumption (Sect. 17.3). Next, reported "operational" solubility (C_{fo}) values are presented and compared to the "thermodynamic" or true solubility (C_{sat}) values of plant essential oil components in high-pressure CO_2 in binary, ternary, and more complex systems (Sect. 17.4). Some concluding remarks are made in Sect. 17.5.

17.2 Mass Transfer Models

This section presents a mathematical model that can be used as a reference to discuss the effect of mass transfer and equilibrium parameters on the SCFE of plant essential oils using high-pressure CO_2 as the solvent (Sect. 17.2.1). The so-called diffusion model assumes internal mass transfer by diffusion within solid particles, external mass transfer by convection through a static film of SCF next to the particles, and axial dispersion of dissolved solute in the SCF phase along the bed. This reference model also assumes a packed bed of spherical particles, an essential oil that can be treated as a single substance (pseudo-solute), and a constant partition coefficient for this pseudo-solute between the solid substrate and high-pressure CO_2. Discussion follows covering the effect on mass transfer rates of particle shape, localization of the solute in specialized structures within the solid matrix, actual composition of the essential oil, and its partition between the solid matrix and the CO_2 that limit the application of the diffusion model (Sect. 2.2). Finally, this section concludes with a discussion of alternative internal mass transfer mechanisms that can compliment diffusion, thus affecting the rate at which essential oils migrate through the solid substrate (Sect. 2.3).

17.2.1 Diffusion Model

The reference model used in this section will be the diffusion model of Goodarznia and Eikani (1998). The assumptions of this diffusion model are as follows: (1) the substrate particles are spherical (diameter d_p, radius $R = d_p/2$) and homogeneous; (2) the physical properties of the extract (the essential oil) are those of a representative pseudo-solute; (3) the physical properties of the SCF and the substrate remain unchanged during extraction; (4) the extract partitions between the solid and SCF phases according to a constant coefficient (K) that is concentration-independent; and (5) the solute disperses axially in the SCF as a result of irregularities in the packing of the substrate in the bed and concentration-gradient-driven diffusion of the solute along the packed bed. As a result of these assumptions, solute concentration in the solid matrix (C_s) depends on the radial position within the particle (r), the axial position along the bed (z), and the extraction time (t); whereas solute concentration in the SCF (C_f) depends only on z and t. The assumption of constant physical properties is valid when the density and viscosity of the SCF depend only on the

extraction temperature and pressure, and are unaffected by the dissolved pseudo-solute. Because of that, the variations in temperature and pressure should be negligible within the bed, and the concentration of essential oils in the loaded SCF phase should be small (selected process conditions should limit the solubility and/or availability of the solute). On the other hand, the assumption of constant physical properties of the solid phase is valid if the substrate remains unaffected (does not swell or shrink) as a result of CO_2 adsorption and solute removal, and this results in a constant bed porosity (ε) and, consequently, in a constant interstitial velocity of the SCF in the packed bed ($u = U/\varepsilon$). These assumptions are valid in the selective extraction of plant essential oils with high-pressure CO_2 for several reasons. The availability of solute is small because the content of essential oils in a typical herb or spice is limited to a few percent or below. Recommended values of extraction temperature and pressure (e.g., 323 K and 9 MPa) (Reverchon 1997) place a limit on the solubility of the essential oil in high-pressure CO_2, so as to increase the selectivity of the process. A near-environmental extraction temperature is selected to reduce thermal damage of labile compounds as well as energy requirements of the process, which reduces the exchange of heat with the environment and minimizes radial temperature gradients in the extraction vessel. Finally, as for other internally controlled mass transfer processes, small values of superficial solvent velocity ($1 \leq U \leq 5$ mm/s) (Eggers 1996) are recommended to improve economics, and these small velocities reduce losses of energy of the SCF as it passes through the bed of packed substrate, and minimize axial pressures gradients in the extraction vessel.

Equation 17.1 is a differential mass balance for the SCF surrounding the particles of substrate in the packed bed. J, the so-called source-and-transfer term (Zizovic et al. 2007c; Stamenić et al. 2008), is the flux of solute that is transferred from the solid to the SCF, and can be estimated using (17.2). On the other hand, the diffusion of the solute through the solid particles can be estimated using (17.3).

$$\frac{\partial C_\mathrm{f}}{\partial t} + u\frac{\partial C_\mathrm{f}}{\partial z} - D_\mathrm{ax}\frac{\partial^2 C_\mathrm{f}}{\partial z^2} = \frac{6}{d_\mathrm{p}}\frac{(1-\varepsilon)}{\varepsilon}J \tag{17.1}$$

$$J = -D_\mathrm{e}\frac{\partial C_\mathrm{s}}{\partial r}\bigg|_R \tag{17.2}$$

$$\frac{\partial C_\mathrm{s}}{\partial t} = \frac{D_\mathrm{e}}{r^2}\frac{\partial}{\partial r}\left(r^2\frac{\partial C_\mathrm{s}}{\partial r}\right) \tag{17.3}$$

Goodarznia and Eikani (1998) assumed constant solute concentrations in the solid matrix (initial solute content C_so) and the SCF phase (initial solute content C_fo) in the bed initially (17.4a and 17.4b, respectively), a symmetry condition for the removal of solute from the particles (17.4c), continuity in the flux of solute leaving a solid particle and entering the SCF film around it (17.4d), and the Danckwerts conditions for axial dispersion in packed beds (17.4e and 17.4f).

$$C_s = C_{so} \quad (t = 0,\ 0 \le r \le R) \tag{17.4a}$$

$$C_f = C_{fo} \quad (t = 0,\ 0 \le z \le H) \tag{17.4b}$$

$$\left.\frac{\partial C_s}{\partial r}\right|_0 = 0 \quad (t \ge 0,\ 0 \le z \le H) \tag{17.4c}$$

$$-D_e \left.\frac{\partial C_s}{\partial r}\right|_R = k_f \left(\frac{C_s|_R}{K} - C_f\right) \quad (t \ge 0,\ 0 \le z \le H) \tag{17.4d}$$

$$uC_f - D_{ax}\frac{\partial C_f}{\partial z} = 0 \quad (t \ge 0,\ z = 0) \tag{17.4e}$$

$$\frac{\partial C_f}{\partial z} = 0 \quad (t \ge 0,\ z = H) \tag{17.4f}$$

Examination of (17.1)–(17.4) suggests that variations in C_s and C_f as a function of r, z, and t depend on the initial essential oil content in the substrate (C_{so}), the geometry of the packed bed (diameter, D_E; height, H; porosity, ε) and the particles (diameter, d_p), and the conditions of the SCF (interstitial velocity, u; temperature, T; and pressure, P).

A closer examination of (17.1)–(17.4) also suggests that the extraction rate and yield depend on both kinetic (or mass transfer) parameters and equilibrium (or solubility) parameters. The former category includes an internal mass transfer coefficient (the effective diffusivity of the extract in the solid matrix, D_e), an external mass transfer coefficient (the SCF film coefficient, k_f), and an axial dispersion coefficient (D_{ax}) (Fig. 17.1b). Phase equilibrium parameters include the solubility of the essential oils in high-pressure CO_2 at T and P (C_{sat}), and their partition between the solid matrix and the SCF phase (K). Border condition 17.4b implicitly requires extraction to be preceded by a static period (unaccounted for by the model) so as to equilibrate the vessel to the required process temperature and pressure conditions, and to dissolve free solute in the solid phase. The SCF phase becomes saturated (initial solute concentration C_{sat}) only if there is enough free solute in the substrate; when there is less solute, the concentration C_{fo} is determined by the ratio between the total amount of free solute and the total void volume occupied by the SCF in the bed.

Some of the simplifications of the diffusion model applied in the literature include the following (Table 17.1): neglecting the effect of axial dispersion in mass transfer (model Diff/PF of Araus et al. 2009); treating the packed bed as a perfectly mixed extraction vessel (model Diff-Sph/PM of Reverchon et al. 1993a; models Diff-Slab/PM and Diff-Slab/IC of Gaspar et al. 2003; model Diff-Sph/IC of Campos et al. 2005); and neglecting the external resistance to mass transfer (model Diff-Slab/IC of Gaspar et al. 2003; model Diff-Sph/IC of Campos et al. 2005).

The diffusion model adopted in this chapter as the reference model (this section) makes several simplifying assumptions about the particle geometry (spherical), the

Table 17.1 Summary of mathematical models used in the literature for high-pressure CO_2 extraction of plant essential oils in packed beds

Mass transfer model	Substrate particles[a]	Hydrodynamics in packed bed[b]	External mass transfer coefficient[c]	Axial dispersion coefficient[d]	Sorption/ "operational" solubility model[e]
Diffusion (Diff or D) models					
Diff/ADPF (Goodarznia and Eikani 1998)	Sphere	Axially dispersed plug flow	Literature correlation	Literature correlation	Linear isotherm
Diff/PF (Araus et al. 2009; Uquiche et al. submitted)	Infinite slab	Plug flow	Literature correlation	Neglected	Linear isotherm
Diff-Sph/PM (Reverchon et al. 1993a)	Sphere	Perfect mixing	Literature correlation	Neglected	Neglected
Diff-Slab/PM (Gaspar et al. 2003)	Infinite slab	Perfect mixing	Literature correlation	Neglected	Neglected
Diff-Sph/IC (Campos et al. 2005)	Sphere	Perfect mixing	Neglected	Neglected	Neglected
Diff-Slab/IC (Gaspar et al. 2003; Campos et al. 2005)	Infinite slab	Perfect mixing	Neglected	Neglected	Neglected
Shrinking-Core (SC) models					
SC/ADPF (Spricigo et al. 2001; Machmudah et al. 2006)	Porous sphere	Axially dispersed plug flow	Literature correlation	Literature correlation	Limited by saturation
SC/ADPF (Steffani et al. 2006)	Porous sphere	Axially dispersed plug flow	Fitted to data	Literature correlation	Limited by saturation
SC/PF (Akgun et al. 2000; Germain et al. 2005)	Porous sphere	Plug flow	Literature correlation	Neglected	Limited by saturation
SC/PF (Germain et al. 2005)	Porous sphere	Plug flow	Fitted to data	Neglected	Limited by saturation
Desorption-Dissolution-Diffusion (DDD or D^3) models					
DDD/ADPF/BET (Ruetsch et al. 2003)	Porous sphere	Axially dispersed plug flow	Literature correlation	Literature correlation	BET isotherm
DDD/ADPF/Lang (Daghero et al. 2004)	Porous sphere	Axially dispersed plug flow	Literature correlation	Literature correlation	Langmuir isotherm
DDD/ADPF (Salimi et al. 2008)	Porous sphere	Axially dispersed plug flow	Literature correlation	Literature correlation	Several isotherms

(*continued*)

Table 17.1 (continued)

Mass transfer model	Substrate particles[a]	Hydrodynamics in packed bed[b]	External mass transfer coefficient[c]	Axial dispersion coefficient[d]	Sorption/ "operational" solubility model[e]
DDD/PM (Kim and Hong 2002)	Porous sphere	Perfect mixing	Fitted to data	Neglected	Linear isotherm, $K = 1$
Intact-and-Broken-Cell (IBC) models					
IBC-Diff (Kim and Hong 2002)	Sphere	Plug flow	Neglected	Literature correlation	Neglected
IBC/PF/PCPR (Machmudah et al. 2006; Sovová 2005; Langa et al. 2009)	Unaccounted for	Plug flow	Fitted to first stage	Neglected	PCPR isotherm
IBC/PF (Louli et al. 2004)	Unaccounted for	Plug flow	Fitted to first stage	Neglected	Limited by saturation
IBC/PFNA (Sovová et al. 1994a)	Unaccounted for	PF with no accumulation	Fitted to first stage	Neglected	Decreasing solubility
Sovová (Campos et al. 2005;Louli et al. 2004; Mira et al. (1996, 1999); Papamichail et al. 2000; Povh et al. 2001; Ferreira and Meireles 2002; Sousa et al. 2002; Martínez et al. 2003; Rodrigues et al. 2003; Sousa et al. 2005; Vargas et al. 2006; Martínez et al. 2007; Bensebia et al. 2009)	Unaccounted for	PF with no accumulation	Fitted to first stage	Neglected	Limited by saturation
Microscale (μS) models					
μS/SGl (Zizovic et al. 2005; 2007c; Stamenić et al. 2008)	Surface glands	Axially dispersed plug flow	Literature correlation	Literature correlation	Limited by saturation
μS/SDuct (Zizovic et al. 2007b, c; Stamenić et al. 2008)	Secretory ducts	Axially dispersed plug flow	Literature correlation	Literature correlation	Limited by saturation
μS/SCav (Zizovic et al. 2007a, c; Stamenić et al. 2008)	Secretory cavities	Axially dispersed plug flow	Literature correlation	Literature correlation	Limited by saturation

Diffusion models using Linear Driving Force (LDF)					
LDF/ADPF (Reverchon and Marrone 1997)	Unaccounted for	Axially dispersed plug flow	Hidden in k_g	Literature chart	Linear isotherm
LDF/ADPF (Reis-Vasco et al. 2000)	Unaccounted for	Axially dispersed plug flow	Hidden in k_g	Fitted to data	Linear isotherm
LDF/PF/CDIC (Coelho et al. 1997)	Unaccounted for	Plug flow	Hidden in variable k_g	Neglected	Limited by saturation
LDF-Sph/PF (Esquivel et al. 1996)	Sphere	Plug flow	Hidden in k_g	Neglected	Limited by saturation
LDF/PF (Reverchon et al. 1999)	Unaccounted for	Plug flow	Hidden in k_g	Neglected	Linear isotherm
LDF/IMTC (Catchpole et al. 1996b)	Sphere	Plug flow	Neglected	Neglected	Linear isotherm, $K \ll 1$
LDF-Slab/PMMS (Reverchon 1996)	Infinite slab	Perfectly mixed multistages	Hidden in k_g	Neglected	Linear isotherm
LDF/PMMS (Esquivel et al. 1996)	Unaccounted for	Perfectly mixed multistages	Hidden in k_g	Neglected	Linear isotherm
LDF/UENA (Louli et al. 2004; Papamichail et al. 2000)	Sphere	Uniform extraction NA	Hidden in k_g	Neglected	PCPR isotherm
R-SO (Louli et al. 2004; Papamichail et al. 2000; Vargas et al. 2006; Reverchon et al. 1995a; Zekovic et al. 2001; Pfaf-Šovljanski et al. 2005)	Sphere	Uniform extraction NA	Neglected	Neglected	Neglected
DDD models using LDF					
LDF-D^3/DB/BET (Goto et al. 1998)	Infinite slab	Differential bed	Literature correlation	Neglected	BET isotherm
LDF-D^3-Sph/DB (Perakis et al. 2005)	Sphere	Differential bed	Literature correlation	Neglected	Linear isotherm
LDF-D^3-Slab/DB (Sousa et al. 2005; Goto et al. 1993)	Infinite slab	Differential bed	Literature correlation	Neglected	Linear isotherm

(*continued*)

Table 17.1 (continued)

Mass transfer model	Substrate particles[a]	Hydrodynamics in packed bed[b]	External mass transfer coefficient[c]	Axial dispersion coefficient[d]	Sorption/ "operational" solubility model[e]
Equilibrium Desorption (ED), Internal-Mass-Transfer-Control (IMTC), and External-Mass-Transfer-Control (EMTC) models					
ED (Reis-Vasco et al. 2000)	Unaccounted for	Plug flow	Neglected	Fitted to data	Linear isotherm
IMTC (Ferreira et al. 1999)	Sphere	Perfect mixing	Neglected	Neglected	Limited by saturation
EMTC (Ferreira et al. 1999; Kotnik et al. 2007)	Sphere	Simplified diff. mass balance	Fitted to first stage	Neglected	Limited by saturation

[a]The particles were treated as solid or porous spheres (Sph) or infinite slabs (Slab); or else their shape as an inner structure was unaccounted for

[b]Flow conditions in extraction vessel are assumed to be axially dispersed plug flow (ADPF), plug flow (PF), perfect mixing (PM), or perfectly mixed multistages (PMMS). For simplification, the packed bed was treated as a differential bed (DB), and the differential mass balance assumed plug flow with no accumulation (PFNA) or uniform extraction with no accumulation (UENA)

[c]The external mass transfer and was estimated from correlations in the literature, then fitted to data, or neglected. The internal-mass-transfer-control (IMTC) models neglected the external resistance to mass transfer. The external mass transfer coefficient was sometimes hidden in a global mass transfer coefficient (k_g), either implicitly or explicitly; and in some cases (Reis-Vasco et al. 2000; Coelho et al. 1997; Ferreira et al. 1999; Kotnik et al. 2007) k_g was assumed to be an internal mass transfer coefficient (in IMTC models), and in others (Reverchon and Marrone 1997; Ferreira et al. 1999) (external-mass-transfer-control or EMTC models), an external mass transfer coefficient

[d]The axial dispersion coefficient was also estimated from correlations or charts in the literature, fitted to data, or neglected

[e]The equilibrium concentration of essential oils in the SCF phase was assumed to be limited by saturation (solubility), or to depend on the residual concentration of the oils in the solid substrate by a sorption isotherm given by a linear model, BET model, a Langmuir (Lang) model, or Perrut-Clavier-Poletto-Reverchon (PCPR) model of Perrut et al. (1997), among others

solid matrix (homogeneous), the localization of the solute in the solid matrix (homogeneous), the composition of the solute (fully characterized by a pseudo-solute), the partition of the solute between the solid matrix and the CO_2 (constant and independent of solute concentration), and the mass transfer mechanism for the extraction process (diffusion). As discussed in the following sections, some of these simplifying assumptions should be avoided to improve the physical picture of the extraction process.

17.2.2 Limitations of the Diffusion Model

When extracting herbs and spices it is important to consider the geometry of the tissue following application of pretreatments aimed at increasing the speed and/or final yield of the process. Mild pretreatments, such as coarse milling, are typically applied prior to SCFE to take full advantage of the natural barriers within the plant material to selectively extract the essential oils. Coarse milling of leaves and similar plant parts results in large particles having a slab rather than a spherical geometry as assumed in the diffusion model, so that the fitting of mathematical models to the data improves when using the diffusion equation for an infinite slab instead of (17.3) (Goto et al. 1993, 1998; Reverchon 1996; Gaspar et al. 2003; Araus et al. 2009). Stüber et al. (1997) derived analytical solutions for other regular geometries such as disks and cylinders having different aspect ratios by combining the analytic solutions for basic geometries such as infinite cylinders and infinite slabs using superposition theorems. However, the model for spherical particles still can be used to represent mass transfer from particles of various shapes (including disks and cylinders with different aspect ratios) if a characteristic dimension is computed as three times the volume-to-surface area ratio for a representative particle ($d_p/2$, in the case of a sphere) (Ma and Evans 1968).

When extracting herbs and spices it is important to consider the microstructure of the native tissue. Unlike the assumptions in Sect. 17.2.1, herbs and spices are heterogeneous when observed under the microscope. This is important to consider because SCFE of plant materials depends, among other factors, on the location of the solute within the plant tissue, with essential oils being encapsulated in isolated glands, secretory cells, or cavities, or in interconnected pore networks (Zizovic et al. 2007c; Stamenić et al. 2008). Furthermore, the physical properties of the solid may change during extraction as a result of impregnation of CO_2 and removal of essential oils (Eggers 1996).

Also, unlike the assumptions in Sect. 17.2.1, essential oils are not single compounds but mixtures of many different volatile terpenoids. During SCFE of herbs and spices, the waxy constituents of the specialized encapsulating structures of the essential oils are dissolved so that CO_2 extracts also include waxes and other compounds besides terpenoids. Thus, the components of CO_2 extracts of herbs and spices can be grouped as monoterpene hydrocarbons, oxygenated monoterpenes, sesquiterpene hydrocarbons, oxygenated sesquiterpenes, waxes, and other

substrate specific families of compounds such as gingerols in ginger and phenylpropanoids in parsley. In this work, for the purpose of estimating the value of physical properties of CO_2 extracts, the authors selected representative compounds of some of these groups, assigned the properties of representative compounds to whole groups, and represented extracts as pseudo-solutes whose properties were estimated as the weighted average of the properties of the representative compounds in each considered group.

The assumption of a constant coefficient for the partition of the solute (linear sorption isotherm) between the solid substrate and the high-pressure CO_2 is invalid when a fraction of the solute in the substrate, e.g., contained in broken cells or cavities, is freely available to the CO_2, so that its concentration in the fluid phase is determined by availability or solubility constraints. It is also invalid in the final stages of the extraction process, when all remaining solute is strongly bound to the solid substrate (del Valle and de la Fuente 2006). Consequently, Araus et al. (2009) claimed the necessity of relaxing the assumption of a constant partition coefficient of the pseudo-solute between the solid substrate and the CO_2 to improve modeling of SCFE of plant essential oils.

The internal mass transfer mechanism may be different from that stated in Sect. 17.2.1, since solute desorption from the solid, solubilization in the SCF, and/or migration by diffusion through the pores of the solid matrix may control mass transfer in the solid. The subject of the internal mass transfer mechanism is analyzed in the following section.

17.2.3 Alternative Internal Mass Transfer Mechanisms

Considering plant tissue as a multiphase material constituted of interconnected or isolated cells and a network of fully or partially interconnected pores (Zizovic et al. 2007c; Stamenić et al. 2008), and how its microstructure is affected by milling and other pretreatments applied prior to SCFE, alternative mass transfer models picture pretreated herbs and spices as porous solid matrices constituted of intact and broken cells (Sovová 1994, 2005; Zizovic et al. 2007c; Stamenić et al. 2008). del Valle and de la Fuente (2006) reviewed most of these models and others with alternative internal mass transfer mechanisms in detail.

When the solid matrix where mass transfer takes place is assumed to be a network of interconnected pores, two important models that can be applied are the so-called shrinking-core (SC) and desorption-dissolution-diffusion (DDD) models. The shrinking-core hypothesis assumes that the solute is retained in the pores of the solid matrix by mechanical or capillary forces, so that pore space is divided into an inner core filled with condensed solute and an outer region containing a solution of the solute in high-pressure CO_2 that are separated by a moving boundary. Roy et al. (1996) first applied the shrinking-core hypothesis to model SCFE of ginger essential and fatty oils at >15 MPa (data not included), and there are several examples in the literature on this hypothesis to model the extraction of

plant essential oils. Of these models (Table 17.1), that of Machmudah et al. (2006) is different in that they assumed that the extract is a mixture of two pseudo-components, namely the monoterpene and sesquiterpene hydrocarbons, on the one hand, and their oxygenated derivatives (oxygenated monoterpenes and sesquiterpenes), on the other hand (Sect. 17.3.2), that are extracted separately at rates defined by two independent values of D_e. Reverchon (1997) questioned the validity of the shrinking-core hypothesis to model SCFE of substrates containing little solute bound to the solid matrix, as it could be the case for essential oils in most herbs and spices, where the driving force for the extraction depends little on the solubility of the essential oil in high-pressure CO_2 under extraction conditions.

On the other hand, the desorption-dissolution-diffusion hypothesis assumes that the solute is partially adsorbed on the solid matrix within the pores, so that a fraction of the solute is adsorbed on the solid matrix and the rest is dissolved in the SCF phase within the inner pores of the solid, which are related by an equilibrium sorption isotherm (see Table 17.1 for a summary of DDD models applied in literature). Goto et al. (1993) assumed a linear sorption isotherm (or a constant equilibrium-partition coefficient K), Ruetsch et al. (2003) applied a Brunauer-Emmet-Teller (or BET) isotherm, Daghero et al. (2004) applied a Langmuir isotherm for solute concentrations below the saturation concentration in the high-pressure CO_2, and Salimi et al. (2008) compared a linear isotherm with several other sorption models including those of Langmuir, Freundlich, and Langmuir Freunlich. Kim and Hong (2002) did not differentiate between the solute adsorbed on the solid and dissolved in the gas phase within the pores, which implicitly implied a unitary equilibrium-partition coefficient ($K = 1$).

Sovová (1994) proposed the hypothesis of intact and broken cells (IBC), which assumes that as a result of a mild pretreatment such as size reduction, particles of milled plant material have broken cells on the surface, and intact cells in the interior. An external (convective) mass transfer coefficient controls transfer of solute from the broken cells to the SCF in the bed, whereas an internal (diffusive) mass transfer coefficient controls transfer of solute from the intact cells (see Table 17.1 for a summary of IBC models applied in literature). Reverchon et al. (1999) considered the simultaneous extraction of free solute and bound solute using separate coefficients for external mass transfer and internal mass transfer, respectively, and separate equilibrium-partition coefficients for free solute between the broken cells and the SCF in the bed, and between the bound solute in intact cells and the SCF in the bed. The model (LDF/PF) of Reverchon et al. (1999) (Table 17.1) is a simplification of this general IBC model, which they applied SCFE of lipids from milled fennel seeds; the simplifying assumption was that there is no free essential oil in milled fennel seeds and that all was bound to the solid matrix. Unlike Reverchon et al. (1999), Sovová (2005) and Machmudah et al. (2006) assumed that the driving force for the extraction of free essential oil is the difference between an equilibrium concentration of the oil in high-pressure CO_2 that depends on the oil concentration in broken cells according to the so-called PCPR isotherm of Perrut et al. (1997), as described in Sect. 17.4.4, and its concentration in the SCF phase, whereas the driving force for extraction of bound essential oil is the difference in oil

concentration between the intact and broken cells (model IBC/PF/PCPR in Table 17.1).

More advanced models differentiate the effect of the pretreatment on the substrate depending on the localization of the essential oil in specialized structures in the herb or spice, which are ruptured (surface glands or SGl, inner secretory ducts or SDuct, inner secretory cavities or SCav) during milling, or burst (surface glands) as a result of swelling of the glands by dissolution of high-pressure CO_2 in the gland contents (essential oils) (Zizovic et al. 2005, 2007a,b,c; Stamenić et al. 2008). Table 17.1 classifies these so-called Micro-Scale (μS) models, which are further described in Sect. 17.3.3.

Table 17.1 also summarizes several simplifications of the basic mass balance and rate equations of mass transfer models used in the literature to simulate SCFE curves of plant essential oils. Several of these simplifications pertain to the differential mass balance equation. When assuming a so-called differential bed (DB), which is valid if the height of the packed bed is comparable with the inner diameter of the extraction vessel, the second term on the right of the differential mass balance equation (17.1) is replaced by an expression reflecting a linear variation in the concentration of the solute in the SCF with the axial position along the bed (Goto et al. 1993, 1998; Perakis et al. 2005). Alternative simplifications to the differential mass balance equation include assuming that there is no accumulation (NA) of solute in the SCF phase, or neglecting the accumulation or first term on the right of (17.1) (Sovová 1994; Papamichail et al. 2000; Reverchon and Sesti Osséo 1994a); assuming a uniform extraction (UA) along the bed, or replacing the second term on the right of (17.1) by an expression reflecting a linear variation in solute concentration in SCF with the axial position along the bed, which is equivalent to assuming a "differential" bed (Papamichail et al. 2000; Reverchon and Sesti Osséo 1994a); and assuming a plug flow (PF), and/or neglecting the axial dispersion in the SCF phase or the third term on the on the right of (17.1). As summarized in Table 17.1, assuming the axially dispersed plug flow (ADPF) pattern (Reverchon and Marrone 1997; Goodarznia and Eikani 1998; Reis-Vasco et al. 2000; Spricigo et al. 2001; Ruetsch et al. 2003; Daghero et al. 2004; Zizovic et al. 2005, 2007b, c; Machmudah et al. 2006; Steffani et al. 2006; Salimi et al. 2008; Stamenić et al. 2008) that is implicit in the differential mass balance equation (17.1) presented in Sect. 2.1 is more the exception than the norm. Some authors (Reverchon et al. 1993a; Reverchon 1996; Kim and Hong 2002; Gaspar et al. 2003; Campos et al. 2005; Kotnik et al. 2007) circumvent the differential mass balance (17.1) treating the packed bed as a vessel with perfect mixing (PM), and others (Esquivel et al. 1996; Reverchon 1996; Sovová 2005) treating it as perfectly mixed multistages (PMMS) or a series of perfectly agitated mixing vessels. The perfectly mixed vessel or "hot-ball"-type model, so called because of the similitude in the mass transfer process with the cooling of a hot ball of a solid material in a fluid (Reverchon 1997), or Crank model, so called to honor the author of an influential book on diffusion in solids (Crank 1975), fail to account for the effect of the increase in solute concentration in the SCF phase along the bed in decreasing the rate of mass transfer. Models assuming several (n) perfectly mixed vessels in series approach plug flow

as the value of n increases, with the n being an indirect measurement of the axial dispersion along the packed bed; the treatment of a packed bed as a series of discrete stages does not comply with the physical situation but is commonly applied in other separation processes in packed beds such as chromatography (Martin and Synge 1941).

Besides or instead of the differential mass balance equation (17.1), some models listed in Table 17.1 simplify the so-called source-and-transfer J term (17.2) that describes the rate of transfer of essential oil between the herb or spice and the high-pressure CO_2. The linear driving force (LDF) approximation for mass transfer from the substrate to the SCF (see examples of this type of simplifying assumption in Table 17.1), which is valid when the residual solute concentration profile in the partially extracted solid substrate, $C_s(r)$, is approximately parabolic, uses a global driving force and a single global mass transfer coefficient. The global driving force for mass transfer equals the difference between the average residual concentration of solute in the solid, corrected by the equilibrium-partition coefficient $(\bar{C}_s/K)$ and the concentration of solute in the SCF (C_f). The global mass transfer coefficient (k_g, (17.5), Goto et al. 1993), on the other hand, accounts for both the internal resistance to mass transfer (related to an internal mass transfer coefficient, k_i) and external resistance to mass transfer (related to the external mass transfer coefficient, k_f):

$$k_g = \frac{k_f}{1 + \frac{Bi}{\xi}} \tag{17.5}$$

where ξ, a particle-geometry parameter, equals 10 for a sphere and equals 6 for a thin slab (for which the characteristic dimension d_p corresponds to its thickness); Bi is the dimensionless Biot number (17.6):

$$Bi = \frac{k_f d_p}{D_e} \tag{17.6}$$

When both the inner resistance to mass transfer in the plant material and the external resistance in the SCF film surrounding the particles can be neglected, it is unnecessary to include the so-called source and transfer J term in the mass balance and rate equations (17.1–17.4) because under these conditions C_f and $\bar{C}_s$ are related by equilibrium. Reis-Vasco et al. (2000) applied this simplifying assumption to the initial stages of the high-pressure CO_2 extraction of pennyroyal essential oil.

The most simple models in Table 17.1 correspond to simple steady-state approximations that assume the rate of extraction is defined by a single mass transfer controlling resistance, which switches from external control (Ferreira et al. 1999; Kotnik et al. 2007) to internal control (Kotnik et al. 2007) in a given transition time. An alternative way to account for the transition from external control to internal control in a single model is to use a concentration-dependent global mass transfer coefficient when using the linear driving force approximation to mass transfer, as done by Coelho et al. (1997). It is important to point out that some models in

Table 17.1 refer to authors who adopted them for SCFE of plant essential oils instead of the original authors who applied them for alternative SCFE applications. Specifically, these models are the Diff-Sph/IC model of Crank (1975), the EMTC model of Brunner (1984), the IMTC model of Hong et al. (1990), the LDF/PF/CDIC model of Cygnarowicz-Provost (1996), the LDF-Sph/PF model of Catchpole et al. (1994), Sovová's (1994) model, and the LDF-D^3-Sph/DB model of Skerget and Knez (2001).

Selected models that are highlighted in Table 17.1 are widely used because they have relatively simple analytical solutions and are used to best-fit model parameters with ease. The solution of the so-called Reverchon–Sesti Ossèo (R-SO) model was applied by Reverchon and Sesti Osséo (1994a), Reverchon et al. (1995a), Papamichail et al. (2000), Zekovic et al. (2001), Louli et al. (2004), Pfaf-Šovljanski et al. (2005), and Vargas et al. (2006). On the other hand, the solution of Sovová's (1994) model was applied by Mira et al. (1996, 1999), Papamichail et al. (2000), Povh et al. (2001), Ferreira and Meireles (2002), Sousa et al. (2002, 2005), Martínez et al. (2003, 2007), Rodrigues et al. (2003), Louli et al. (2004), Campos et al. (2005), Perakis et al. (2005), Vargas et al. (2006), and Bensebia et al. (2009). Sovová's model (1994) considers SCFE as a two-stage process, where the mass transfer coefficient in the first (convection-controlled) stage is k_f, whereas the mass transfer coefficient in the second (internal-diffusion-controlled) stage decreases proportionally to the difference between the solubility of the essential oil in high-pressure CO_2 and its actual concentration in the SCF phase in the bed. Povh et al. (2001) described a procedure to estimate the parameters of Sovova's model based on the fitting of an integral extraction plot of solute yield versus specific solvent consumption (Fig. 17.2) to a spline with three straight lines representing successively the constant, falling, and diffusion-controlled extraction rate periods. Sovová et al. (1994a) applied an improved version of Sovová's model (model ICB/ADPF in Table 17.1) in two aspects: they did not neglect the accumulation of essential oil in the SCF phase and they considered that the extraction was limited by a decreasing solubility (LDS) or that the saturation solubility of the essential oil in high-pressure CO_2 decreased during extraction due to the progressive enrichment of the oil remaining in the partially extracted substrate in less volatile compounds. Authors using other models include Louli et al. (2004) (LDF/UENA model of Papamichail et al. 2000), Sousa et al. (2005) (LDF-D^3-Slab/DB model of Goto et al. 1993), Campos et al. (2005) (Diff-Slab/IC model of Gaspar et al. 2003), Zizovic et al. (2007c) (μS/SGl model of Zizovic et al. 2005; μS/SCav model of Zizovic et al. 2007a; μS/SDuct model of Zizovic et al. 2007b), Stamenić et al. (2008) (μS/SCav model of Zizovic et al. 2007a; μS/SDuct model of Zizovic et al. 2007b), Langa et al. (2009) (IBC/PF/PCPR model of Sovová 2005), and Uquiche et al. (submitted) (Diff/PF model of Araus et al. 2009).

Although most authors of models in Table 17.1 applied the models to their own data, there are some exceptions. Goodarznia and Eikani (1998) modeled the data of Reverchon et al. (1993a) on SCFE of essential oils from basil, marjoram, and rosemary, as well as the data of Sovová et al. (1994a) on SCFE of caraway essential oil. Germain et al. (2005) also modeled the data of Sovová et al. (1994a) on SCFE

of caraway essential oils. Zizovic et al. (2007b) modeled data of Coelho et al. (2003) on SCFE of fennel fruit oil. Zizovic et al. (2007c) modeled literature data on SCFE of essential oils from orange peel (Mira et al. 1996), ginger rhizome (Roy et al. 1996), clove bud (Reverchon and Marrone 1997), and eucalyptus leaf (Della Porta et al. 1999). Stamenić et al. (2008) modeled the data of Machmudah et al. (2006) on SCFE of nutmeg essential oil. Finally, Araus et al. (2009) modeled literature data on SCFE of essential oils from sage (Reverchon 1996), lavender (Akgun et al. 2000), oregano (Gaspar 2002), pennyroyal (Reis-Vasco et al. 2000), and chamomile (Povh et al. 2001).

17.3 Kinetic Parameters of CO_2 Extraction of Essential Oils

Table 17.2 summarizes the conditions for the experimental studies on kinetics of mass transfer during SCFE of essential oils from herbs and spices reviewed in this chapter. Although most authors in Table 17.2 modeled the results of their own high-pressure CO_2 extraction work, there are some exceptions, including the data of Roy et al. (1996) on extraction of ginger essential oils at 313 K and 10.8 MPa, the data of Della Porta et al. (1999) on extraction of eucalyptus essential oil at 323 K and 9 MPa, the data of Coelho et al. (2003) on extraction of fennel essential oil at 313 K and 9 MPa, and the data of Gaspar (2002) on extraction of oregano essential oil under selected conditions (310 K and 8 MPa or 320 K and 20 MPa).

In this work, analysis required the estimation of the physical properties of the loaded CO_2 phase produced during the extraction of essential oils. For that purpose, the authors neglected the changes in physical properties associated with the dissolution of essential oils in the solvent under the assayed conditions, and estimated the density (ρ) and viscosity (μ) of the loaded high-pressure CO_2 as a function of the extraction temperature and pressure using the NIST (2000) database for pure CO_2 (del Valle and de la Fuente 2006). On the other hand, D_{12} was estimated using the equation of Catchpole and King (1994), which requires reduced temperature ($T_r = T/T_c$) and reduced density ($\rho_r = \rho/\rho_c$, where $\rho_c = 467.6$ kg/m^3 is the critical density of CO_2) of the SCF, and the molecular weight (MW_2) and critical volume (V_{c2}) of the pseudo-solute. As informed in Sect. 17.2.2, for the purpose of estimating MW_2 and V_{c2}, representative compounds in families of compounds were selected, such as monoterpene (MT) hydrocarbons, oxygenated monoterpene (OMT) compounds, sesquiterpene (ST) hydrocarbons, oxygenated sesquiterpene (OST) compounds, waxes, and some plant-specific compounds; properties of representative compounds to whole families were assigned; and extracts were considered as pseudo-solutes whose properties were estimated using Kay's rule as the weighted average of the properties of the representative compounds in each family (Poling et al. 2000). The composition of the essential oils was taken from the literature and was typically determined by gas chromatography analysis of the steam distillate, hydro-distillate, or CO_2-extract of the herb or spice. For calculations in this current work, only those families representing more than 1% of the

Table 17.2 Summary of extraction conditions of selected mass transfer studies on high-pressure CO_2 extraction of plant essential oils in packed beds

Substrate	Particle diameter (d_p, mm)	Temperature (T, K)	Pressure (P, MPa)	Superficial velocity (U, mm/s)	Extractor volume (V, cm^3)	L/D ratio of extractor (–)
Alecrim pimenta (Sousa et al. 2002)	0.38	298	6.7	0.12	220	27.8
Aniseed (Rodrigues et al. 2003)	0.50	303	8, 10, 14, 18	0.014–0.025	418	2.03
Basil (Reverchon et al. 1993a)	0.17	313	10	0.23	400	3.06
Black pepper (Ferreira et al. 1999; Ferreira and Meireles 2002)	0.080, 0.11	303, 313, 323	15, 20	0.018–0.20	26	29.1
Black pepper (Perakis et al. 2005)	0.18	313, 323	9, 10, 15	0.20–0.59	751	5.45
Boldo (Uquiche et al. submitted)	0.39, 0.40, 2.36	313	10	0.123	5	2.32
Caraway (Sovová et al. 1994a)	0.38	296, 313	9, 10	0.028–0.048	150	5.30
Carqueja (Vargas et al. 2006)	0.50	313, 323, 333, 343	9	0.35	4	4.09
Celery (Papamichail et al. 2000)	0.21, 0.49	318, 328	10, 15	0.167, 0.456	400	2.90
Chamomile (Povh et al. 2001)	0.30	303, 313	10, 12, 16, 20	0.030–0.087	204	4.18
Chamomile (Kotnik et al. 2007)	0.11	303, 313	10, 15	0.17–0.19	55	4.18
Cinnamon of cunha (Sousa et al. 2005)	0.52	288	6.7	0.065, 0.068	222	27.7
Clove (Reverchon and Marrone 1997)	0.37	323	9	0.244–0.488	400	3.06
Clove (Ruetsch et al. 2003)	0.79	323	9, 12	0.38, 0.76	1,500	2.62
Clove (Daghero et al. 2004)	0.79	323	9, 12	0.38, 1.52	1,500	2.62
Clove (Martínez et al. 2007)	0.86	308	10.0	0.039, 0.11	6, 133, 280	0.98, 1.05, 2.20
Eucalyptus (Della Porta et al. 1999)	0.37	323	9.0	0.514	400	6.00
Fennel (Reverchon et al. 1999)	0.37	323	9	0.20–0.61	400	3.06
Ginger (Roy et al. 1996)	0.35	313	11	0.74	2.2	6.67
Ginger (Martínez et al. 2003)	1.02	293, 303, 313	15, 20	0.091–0.12	150	13.3
Hop (Pfaf-Šovljanski et al. 2005)	0.488	313	15	0.050	200	3.98
Ho-sho (Steffani et al. 2006)	0.37, 0.50, 1.00	313, 323, 333	8, 9, 10	0.18–0.71	8	7.31
Lavender (Reverchon et al. 1995a)	1.67	321	9	0.31	400	3.06
Lavender (Akgun et al. 2000)	1.20	308, 313, 323	8, 10, 12, 14	0.44–1.4	39	50.0
Marigold (Campos et al. 2005)	0.62	313	12, 15	0.068, 0.202	139	19.1

Marjoram (Reverchon et al. 1993a)	0.15	313	10.0	0.23	400	3.06
Nutmeg (Spricigo et al. 2001)	0.30, 0.68, 1.45	296	9	0.032–0.053	35	4.76
Nutmeg (Machmudah et al. 2006)	0.56, 0.69, 2.12	313, 318, 323	1.0, 1.5	0.011, 0.068	500	1.86
Orange (Mira et al. (1996)	0.30, 0.50, 1.50, 7.50	323	15	0.084, 0.585	300	2.30
Orange (Mira et al. 1999)	0.30, 0.50, 1.50, 7.50	323	15	0.084, 0.585	300	2.30
Oregano (Esquivel et al. 1996)	1.10	298, 313	7, 10, 15	0.50–0.63	30	3.99
Oregano (Gaspar 2002)	0.36	310, 320	8, 20	0.22, 0.088	196	2.00
Oregano (Gaspar et al. 2003)	0.33, 0.36, 0.70, 1.55	300, 310, 320	7, 8, 10, 15, 20	0.017–0.058	319	0.47
Oregano (Uquiche et al. submitted)	0.35, 0.36, 2.36	313	10	0.123	5	2.32
Parsley (Louli et al. 2004)	0.29, 0.50	308, 318	10, 15	0.16–0.45	185, 209	1.34, 1.52
Pennyroyal (Reis-Vasco et al. 2000)	0.30, 0.50, 0.70	323	10	0.48–0.97	247–379	3.28–5.02
Peppermint (Goto et al. 1993)	0.12	313, 333, 353	8,8, 14.7, 19.6	0.099–0.43	21	2.17
Rosemary (Reverchon et al. 1993a)	0.23	313	10	0.23	400	3.06
Rosemary (Coelho et al. 1997)	0.72, 1.33	308, 313	10, 12.5, 20	0.11–0.43	5	12.9
Rosemary (Bensebia et al. (2009)	0.44	308, 313	10, 12, 15, 18	0.25–0.69	125	13.4
Sage (Catchpole et al. 1996b)	0.50–1.53	291	7	0.19–0.48	2,959	2.41
Sage (Reverchon 1996)	0.25–3.10	323	9	0.85–1.51	400	5.94
Sage (Langa et al. 2009)	0.3, 0.5, 0.8	313, 323	9, 10	0.15–0.34	1,000	6.00
Spearmint (Kim and Hong 2002)	0.30	312, 322	6.9, 8.5, 10.3	0.017–0.068	46	3.54
Thyme (Zekovic et al. 2001)	3.32, 1.46, 0.70	313	10	0.063	200	3.98
Valerian (Zizovic et al. 2007a)	0.40, 0.65, 0.90	313, 323	10, 15	0.072, 0.147	150	2.35
Valerian (Salimi et al. 2008)	0.59	310	17	0.233	10	12.9
Vetiver (Martínez et al. 2007)	0.12	313	20	0.054, 0.150	9, 187	1.45, 1.47
Wild thyme (Stamenić et al. 2008)	0.700	323	10	0.147	150	2.35

whole essential oil were considered, and the most concentrated four families in those cases where five or more were represented in excess of 1% each. Table 17.3 summarizes representative compounds of up to four families for essential oils in Table 17.2. As an example, the lavender essential oil of Reverchon et al. (1995a) has 3.33% MTs (main component, myrcene, representing 35.7% of all MTs), 87.9% OMTs (main component, linalyl acetate, representing 39.4% of all OMTs), 6.14% STs (main component, β-farnesene, representing 36.3 of all STs), and 2.63% OSTs (main component, bisabolol, representing 79.5% of all MTs). The values of V_c were estimated for the representative compounds in the various families using Joback's modification of the Lydersen's group-contribution method (Poling et al. 2000).

Table 17.4 summarizes the estimations of the molecular weight (MW_2) and critical volume (V_{c2}) of the pseudo-solutes representing the essential oils of the different herbs and spices reported in Table 17.3. It is clear that the properties of the pseudo-solutes vary between substrates, as expected, but also for a single substrate because of differences in the substrates or extracts. Indeed, the essential oils exhibit differences due to typical variations in biological samples associated with genetic and processing (e.g., harvest time, drying treatment, and storage condition) factors (Zetzl et al. 2003). In addition, steam distillates, hydrodistillates, and CO_2 extracts from the same substrate exhibit differences due to thermal and/or oxidative degradation of labile components during distillation, or solubilization of additional compounds in CO_2 with increased solvent power (Moyler 1993; Reverchon 1997). Figure 17.3 shows that the composition of sage essential oils extracted with high-pressure CO_2 at 313 K and 9 MPa, or 323 K and 10 MPa, changes depending on process conditions and extraction time.

17.3.1 Axial Dispersion Coefficient

Authors del Valle and de la Fuente (2006) showed consistency in the reported literature values of axial dispersion coefficients for flow of high-pressure CO_2 in a packed bed, when presenting the experimental values in a dimensionless plot of D_{ax}/D_{12} versus Pe_p where Pe_p is the Peclet number for the particle (17.7), which in turn corresponds to the product of the dimensionless numbers of Reynolds (Re, 17.8) and Schmidt (Sc, 17.9).

$$Pe_p\ (= Re \cdot Sc) = \frac{U\, d_p}{D_{12}} \tag{17.7}$$

$$Re = \frac{\rho\, U\, d_p}{\mu} \tag{17.8}$$

$$Sc = \frac{\mu}{\rho\, D_{12}} \tag{17.9}$$

Table 17.3 Summary of compositions of plant essential oils from high-pressure CO_2 extraction studies in Table 17.2. Besides the name of the main component, for each of the up to 4 fractions the compound type,* percent of fraction, and percent of the main component in the fraction are indicated within parenthesis

Plant material	Fraction 1	Fraction 2	Fraction 3	Fraction 4
Basil (Reverchon and Sesti Osséo 1994b)	Estragole (OMT/89/54)	α-*trans* Bergamotene (ST/9.0/46)	T Cadinol (ST/2.2/47)	–
Lavender I (Reverchon et al. 1995a)	Myrcene (MT/3.33/35.7)	Linalyl acetate (OMT/87.9/39.4)	*cis*-β-Farnesene (ST/6.14/36.3)	α-Bisabolol (ST/2.63/79.5)
Lavender II (Akgün et al. 2000)	Camphor (OMT/56.9)	Fenchone (OMT/43.1)	–	–
Marjoram (Jimenez-Carmona et al. 1999)	Sabinene (MT/17.7/42.3)	*cis*-Sabinene hydrate (OMT/78.9/78.6)	β-Caryophyllene (ST/3.46/100)	–
Oregano (Gaspar 2002)	γ-Terpinene (MT/6.78/79.7)	Thymol (OMT/85.8/42.4)	β-Caryophyllene (ST/7.47/100)	–
Pennyroyal (Aghel et al. 2004)	Limonene (MT/14.6/100)	Pulegone (OMT/85.4/60.9)	–	–
Peppermint (Roy et al. 1996)	Limonene (MT/2.86/45.0)	Menthol (OMT/92.8/74.5)	Germacrene (ST/4.35/57.2)	–
Rosemary (Coelho et al. 1997)	Limonene (MT/26.0/47.6)	Camphor (OMT/65.1/57.6)	α-Humulene (ST/7.23/44.1)	Caryophyllene oxide (OST/1.60/100)
Sage I (Reverchon et al. 1995b)	β-Pinene (MT/11.6/21.1)	1,8-Cineole (OMT/70.8/76.8)	β-Caryophyllene (ST/14.5/48.8)	Manool (OST/3.19/56.1)
Sage II (Langa et al. 2009) (313 K/9 MPa)	Myrcene (MT/9.08/35.9)	Camphor (OMT/80.4/62.5)	β-Caryophyllene (ST/6.19/29.2)	Viridoflorol (OST/4.35/39.8)
Sage 2 (Langa et al. 2009) (323 K/10 MPa)	Myrcene (MT/11.4/39.1)	Camphor (OMT/79.9/69.0)	β-Caryophyllene (ST/5.79/30.4)	Caryophyllene oxide (OST/2.88/15.5)
Spearmint (Özer et al. 1996)	Limonene (MT/6.42/81.9)	Carvone (OMT/90.6/89.5)	β-Bourbonene (ST/2.95/78.6)	–
Thyme (Zekovic et al. 2001)	Thymol (OMT/19.6/4.9)	β-Caryophyllene (ST/2.25/100)	Tetradecane (HC/78.2/67.1)	–
Wild thyme (Sefidkon et al. 2004) Before flowering	γ-Terpinene (MT/52.2/42.8)	Thymol (OMT/32.9/58.1)	β-Caryophyllene (ST/14.6/42)	Spathulenol (OST/0.31/33.3)

(*continued*)

Table 17.3 (continued)

Plant material	Fraction 1	Fraction 2	Fraction 3	Fraction 4
Wild thyme (Sefidkon et al. 2004) After flowering	γ-Terpinene (MT/60.20/42.7)	Thymol (OMT/32.09/66.1)	Germacrene-D (ST/6.80/85.0)	Caryophyllene oxide (OST/0.91/87.5)
Anise (Rodrígues et al. 2003) (303 K/8 MPa)	Anethole (OMT/92.0/97.7)	γ-Himachalene (ST/2.27/100)	Isoeugenyl 2-methyl-butyrate (OST/5.76/100)	
Anise (Rodrígues et al. 2003) (303 K/10 MPa)	Anethole (OMT/92.2/98.3)	γ-Himachalene (ST/2.72/100)	Isoeugenyl 2-methyl-butyrate (ST/2.72/100)	
Anise (Rodrígues et al. 2003) (303 K/14 MPa)	Anethole (OMT/91.6/98.2)	γ-Himachalene (ST/2.91/100)	Isoeugenyl 2-methyl-butyrate (OST/5.50/100)	
Caraway (Sovová et al. 1994a)	Limonene (MT/39.8)	Carvone (OMT/60.2)	–	–
Celery (Mišić et al. 2008)	Limonene (MT/28.9/91.7)	Sedanenolide (OMT/64.0/77.7)	β-Selinene (ST/4.89/73.5)	Carotol (OST/2.22/78.3)
Fennel (Simandi et al. 1999)	Limonene (MT/9.37/39.6)	Anethole (OMT/90.6/72.2)	–	–
Parsley (Louli et al. 2004) (10 MPa)	α-Pinene (MT/6.59/49.1)	Myristicin (PhPro/93.4/57.4)	–	–
Parsley (Louli et al. 2004) (15 MPa)	α-Pinene (MT/2.40/55.8)	Myristicin (MT/2.40/55.8)	–	–
Carqueja (Simões-Pires et al. 2005)	β-Pinene (MT/3.42/75.0)	Carquejyl acetate (OMT/42.7/90.7)	Ledol (OST/53.9/38.6)	–
Chamomile I (Povh et al. 2001)	β-Farnesene (ST/39.6/86.3)	α-Bisabolol (OST/60.4/47.0)	–	–
Chamomile II (Kotnik et al. 2007) (303 K/10 MPa)	Matricine (OST/100)	–	–	–
Chamomile II (Kotnik et al. 2007) (303 K/15 MPa)	Matricine (OST/96.5)	–	–	–
Chamomile II (Kotnik et al. 2007) (313 K/10 MPa)	Matricine (OST/97.3)	–	–	–
Chamomile II (Kotnik et al. 2007) (313 K/15 MPa)	Matricine (OST/96.4)	–	–	–
Marigold (Danielski et al. 2007) (313 K/12 MPa)	Tetradecanoic acid (LOHC/2.46/100)	Octacosane (HC/94.6/94.6)	Cholest-4-en-3-one-14-methyl (HOHC/2.94/40.7)	–

Marigold (Danielski et al. 2007) (313 K/15 MPa)	Octacosane (HC/98.7/43.1)	Taraxasterol (H-OHC/1.35/34.2)	–	–
Alecrim pimenta (Sousa et al. 2002)	*p*-Cymene (MT/3.22/45.0)	Thymol (OMT/74.8/67.9)	β-Caryophyllene (ST/20.0/72.2)	Caryophyllene oxide (OST/1.97/100)
Black pepper I (Ferreira et al. 1999)	Limonene (MT/66.2/30.1)	β-Caryophyllene (ST/33.8/21.8)	–	–
Black pepper II (Ferreira et al. 1999)	Limonene (MT/1.00/57.8)	β-Caryophyllene (ST/99.0/70.9)	–	–
Black pepper III (Perakis et al. 2005)	Limonene (MT/31.2/29.8)	Linalool (OMT/1.57/51.3)	β-Caryophyllene (ST/34.2/35.5)	Caryophyllene oxide (OST/33.0/51.5)
Boldo (Miraldi et al. 1996)	p-Cymene (MT/9.28/94.7)	Ascaridole (OMT/81.75/26.5)	Guaizulene (ST/8.96/100)	–
Cinnamon of Cunha (Sousa et al. 2005)	Anethole (OMT/96.5/95.8)	Germacrene (ST/3.51/35.7)	–	–
Clove (Della Porta et al. 1998)	Eugenol (OMT/86.3/77.5)	β-Caryophyllene (ST/13.7/82.2)	–	–
Eucalyptus (Della Porta et al. 1999)	α-Pinene (MT/12.2/86.1)	1,8-Cineole (OMT/67.1/93.3)	Aromadendrene (ST/12.3/65.3)	Guaiol (OST/8.40/50.0)
Ginger (Martínez et al. 2003)	Zingiberene (OMT/9.77/56.7)	α-Zingiberene (ST/45.6/35.6)	Farnesol (OST/3.73/30.3)	6-Gingerol (Ging/40.9/28.9)
Hop (Pfaf-Šovljanski et al. 2005)	α-Humulene (ST/13.5/82.4)	Isohumulone (α-acid/13.0/100)	Lupulone (β-acid/73.5/53)	–
Ho-sho (Bakkali et al. 2005)	Sabinene (MT/21.7/35.5)	1,8-Cineole (OMT/75.0/80.0)	Viridiflorol (OST/3.29/100)	–
Nutmeg I (Spricigo et al. 1999)	Sabinene (MT/78.8/51.9)	Myristicin (OMT/21.2/36.8)	–	–
Nutmeg II (Machmudah et al. 2006)	3-Cyclohexene-1-ol (LOHC/15.7/26.4)	β-Phellandrene (MT/46.3/42.9)	Myristicin (OMT/36.2/89.9)	Copaene (ST/1.83/68.9)
Orange (Budich and Brunner 1999)	Limonene (MT/98.3/97.6)	Linalool (OMT/1.75/28.8)	–	–
Valerian I (Zizovic et al. 2007a) (313 K/10 MPa)	Borneol (OMT/15.9/36.8)	Valerena-4,7(11)-diene (ST/14.1/25.7)	Valerenal (OST/67.4/19.3)	(E)-Valerenyl isovalerate (H-OHC/2.68/70.0)

(*continued*)

Table 17.3 (continued)

Plant material	Fraction 1	Fraction 2	Fraction 3	Fraction 4
Valerian II (Zizovic et al. 2007a) (313 K/10 MPa)	Isovaleric acid (LOHC/6.01/100)	Bornyl acetate (OMT/13.9/59.3)	Valerena-4,7(11)-diene (ST/13.8/17.2)	Valerianol (OST/66.2/19.7)
Valerian II (Zizovic et al. 2007a) (313 K/15 MPa)	Isovaleric acid (LOHC/7.67/100)	Bornyl acetate (OMT/10.7/61.6)	β-Bisabolene (ST/13.2/17.7)	Valerianol (OST/68.4/16.6)
Valerian II (Zizovic et al. 2007a) (323 K/10 MPa)	Isovaleric acid (LOHC/4.37/100)	Bornyl acetate (OMT/12.1/58.9)	Valerena-4,7(11)-diene (ST/13.3/17.1)	Valerianol (OST/70.2/19.2)
Valerian II (Zizovic et al. 2007a) (323 K/15 MPa)	Isovaleric acid (LOHC/3.57/100)	Bornyl acetate (OMT/10.7/59.3)	Valerena-4,7(11)-diene (ST/13.3/17.1)	Valerianol (OST/72.7/20.0)
Valerian III (Zizovic et al. 2007a)	Isovaleric acid (LOHC/9.64/100)	Bornyl acetate (OMT/16.7/52.9)	δ-Elemene (ST/28.6/26.9)	Valerenal (OST/45.0/34.9)

*MT indicates a monoterpene hydrocarbon; OMT, an oxygenated monoterpene; ST, a sesquiterpene hydrocarbon; OST, an oxygenated sesquiterpene; HC, an hydrocarbon; LOHC, a light oxygenated hydrocarbon; HOHC, a heavy oxygenated hydrocarbon; PhPro, a phenyl propanoid; and Ging, a gingerol

Table 17.4 Summary of estimated molecular weights (MW) and critical volumes (V_c) of plant essential oils in Table 17.3

Plant material	Scientific name	Family	Identified compounds (%)	Molecular weight (*MW*, Da)	Critical volume (V_c, cm^3/mol)
Basil	*Ocimum basilicum*	Lamiaceae	99.4	153.0	508.0
Lavender I	*Lavandula angustifolia*	Lamiaceae	100.1	194.5	682.6
Lavender II	*Lavandula angustifolia*	Lamiaceae	76.9	152.2	503.5
Marjoram	*Origanum majorama*	Lamiaceae	36.8	152.0	517.7
Oregano	*Origanum vulgare*	Lamiaceae	87.0	152.2	440.3
Pennyroyal	*Mentha pulegium*	Lamiaceae	100.0	149.7	504.1
Peppermint	*Mentha* × *piperita*	Lamiaceae	99.3	157.2	527.2
Rosemary	*Rosmarinus officinalis*	Lamiaceae	100.0	151.7	523.6
Sage I	*Salvia officinalis*	Lamiaceae	100.0	160.0	546.0
Sage II (313 K/9 MPa)	*Salvia officinalis*	Lamiaceae	81.4	155.2	519.8
Sage II (323 K/10 MPa)	*Salvia officinalis*	Lamiaceae	87.1	153.8	153.8
Spearmint	*Mentha spicata*	Lamiaceae	100.0	150.4	508.5
Thyme	*Thymus vulgaris*	Lamiaceae	11.9	186.8	719.0
Wild thyme, before flowering	*Thymus serpyllum*	Lamiaceae	98.0	148.1	506.6
Wild thyme, after flowering	*Thymus serpyllum*	Lamiaceae	88.2	144.3	500.4
Anise (303 K/8 MPa)	*Pimpinella anisum*	Apiaceae	99.2	152.7	500.0
Anise (303 K/10 MPa)	*Pimpinella anisum*	Apiaceae	97.7	152.5	499.6
Anise (303 K/14 MPa)	*Pimpinella anisum*	Apiaceae	97.0	152.8	500.7
Caraway	*Carum carvi*	Apiaceae	98.0	144.3	505.2
Celery	*Apium graveolens*	Apiaceae	99.8	172.7	585.9
Fennel	*Foeniculum vulgare*	Apiaceae	100.0	147.0	487.7
Parsley (10 MPa)	*Petroselinum crispum*	Apiaceae	83.4	187.1	533.1
Parsley (15 MPa)	*Petroselinum crispum*	Apiaceae	96.2	193.0	552.1
Carqueja	*Baccharis trimera*	Asteraceae	83.7	204.3	678.6
Chamomile I	*Matricaria recutita*	Asteraceae	44.4	214.9	790.6
Chamomile II (303 K/10 MPa)	*Matricaria recutita*	Asteraceae	7.56	306.4	886.5
Chamomile II (303 K/15 MPa)	*Matricaria recutita*	Asteraceae	8.42	306.4	886.5
Chamomile II (313 K/10 MPa)	*Matricaria recutita*	Asteraceae	9.74	306.4	886.5
Chamomile II (313 K/15 MPa)	*Matricaria recutita*	Asteraceae	9.65	306.4	886.5

(*continued*)

Table 17.4 (continued)

Plant material	Scientific name	Family	Identified compounds (%)	Molecular weight (*MW*, Da)	Critical volume (V_c, cm^3/mol)
Marigold (313 K/12 MPa)	*Calendula officinalis*	Asteraceae	30.9	387.9	1,565.1
Marigold (313 K/15 MPa)	*Calendula officinalis*	Asteraceae	28.2	395.2	1,601.4
Alecrim pimenta	*Lippia sidoides*	Verbenaceae	95.2	159.0	470.4
Black pepper I	*Piper nigrum*	Piperaceae	99.6	153.5	562.1
Black pepper II	*Piper nigrum*	Piperaceae	99.2	203.3	719.3
Black pepper III	*Piper nigrum*	Piperaceae	73.3	179.7	633.9
Boldo	*Peumus boldus*	Monimiaceae	98.2	166.6	525.1
Cinnamon of Cunha	*Croton zehntneri*	Euphorbiaceae	95.7	149.6	149.6
Clove	*Syzygium aromaticum*	Myrtaceae	98.5	168.8	454.7
Eucalyptus	*Eucalyptus globules*	Myrtaceae	100.0	155.0	528.6
Ginger	*Zingiber officinale*	Zingiberaceae	71.7	241.1	799.0
Hop	*Humulus lupulus*	Cannabaceae	93.3	364.5	1,224.8
Ho-sho	*Cinnamomum camphora*	Lauraceae	83.7	151.4	516.2
Nutmeg I	*Myristica fragrans*	Myristicaceae	89.6	145.2	498.9
Nutmeg II	*Myristica fragrans*	Myristicaceae	99.6	143.5	143.5
Orange	*Citrus sinensis*	Rutaceae	100	136.5	508.49
Valerian I (313 K/10 MPa)	*Valeriana officinalis*	Valerianaceae	83.5	204.6	712.1
Valerian II (313 K/10 MPa)	*Valeriana officinalis*	Valerianaceae	89.1	201.9	688.4
Valerian II (313 K/15 MPa)	*Valeriana officinalis*	Valerianaceae	86.2	199.2	683.0
Valerian II (323 K/10 MPa)	*Valeriana officinalis*	Valerianaceae	88.7	206.0	703.5
Valerian II (323 K/15 MPa)	*Valeriana officinalis*	Valerianaceae	86.4	208.3	711.8
Valerian III	*Valeriana officinalis*	Valerianaceae	82.7	190.2	662.7

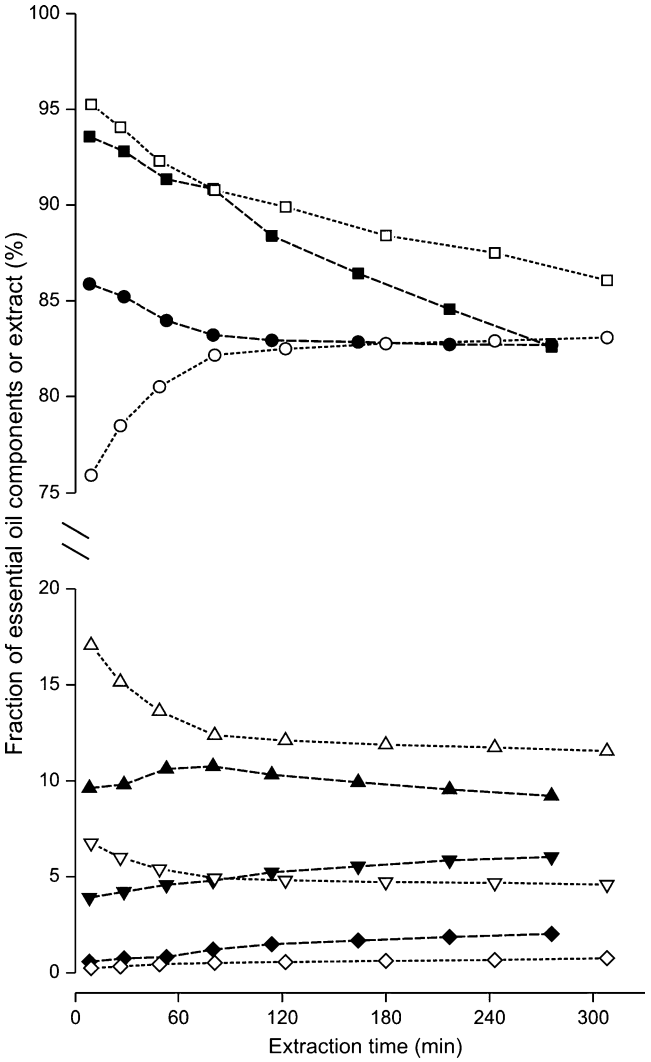

Fig. 17.3 Effect of process time and conditions on the composition of sage essential oils extracted with high-pressure CO_2: (-▲-) monoterpenes, (-●-) oxygenated monoterpenes, (-▼-) sesquiterpenes, (-◆-) oxygenated sesquiterpenes, and (-■-) total essential oil components extracted at 313 K and 9 MPa; and (···△···) monoterpenes, (···○···) oxygenated monoterpenes, (···▽···) sesquiterpenes, (···◇···) oxygenated sesquiterpenes, and (···□···) total essential oil components extracted at 323 K and 10 MPa (Adapted from Langa et al. 2009)

In a related work, del Valle and Catchpole (2005) correlated literature data for the axial dispersion of high-pressure CO_2 in packed beds (Tan and Liou 1989; Catchpole et al. 1996a; Funazukuri et al. 1998; Yu 1998; Ghoreishi and Akgerman 2004). Typical measurements in these studies were conducted by injecting a pulse

of solute (gaseous methane, volatile acetone or hexachlorobenzene, or low-volatility benzoic acid, oleic acid, or squalene) into the high-pressure CO_2 stream before a bed ($0.4 \leq D \leq 50.8$ mm) packed with different materials (sand particles, glass beads, or steel beads ranging in size from $d_p = 0.05$ to $d_p = 3.18$ mm), and evaluating the dispersion (concentration profile) of the solute in the stream leaving the bed. Different flow directions (horizontal, upward, downward) and regimes (from molecular-transport-controlled, $Pe_d \sim 9.1 \times 10^{-3}$, to convection-controlled flow conditions, $Pe_d \sim 1.2 \times 10^3$) were assayed in these studies.

Figure 17.4 summarizes the results of the correlation study of del Valle and Catchpole (2005). When dispersion is controlled by molecular transport ($Pe_d \leq 1$) the ratio D_{ax}/D_{12} has a nearly constant value (slightly below 1 in this particular case), as expected (Dullien 1992). On the other hand, under convention-controlled conditions ($Pe_d > 1$), the ratio D_{ax}/D_{12} increases exponentially with Pe_d, which results in a nearly straight line having a slope between 1 and 2 when presenting the data in a log–log plot, as also expected (Dullien 1992). Data scattering for large values of Pe_d is partially explained by the scale of the measurements; data obtained using large vessels exhibited a larger axial dispersion coefficient than data obtained using small tubes (del Valle and Catchpole 2005). Dispersion typically increases as the length of the bed (L) increases due to the increase in the residence time in the packed bed (Han et al. 1985). Dispersion also increases as the diameter of the bed (D_E) decreases because of the pronounced decrease in local porosity in the radial direction from the wall of the tube or vessel when the ratio D_E/d_p decreases, which increases concentration-gradient-driven radial diffusion and consequently increases

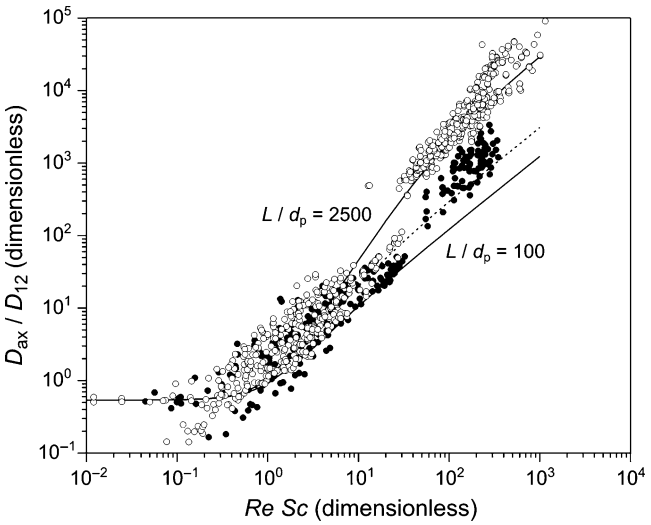

Fig. 17.4 Dimensionless plot of the axial dispersion coefficient (D_{ax}) in a packed bed operating under a high-pressure CO_2 and flow regime. The independent variable is the ratio D_{ax}/D_{12} [where D_{12} is a binary diffusion coefficient of the solute (component 2) in CO_2 (component 1)] and the dependent variable is the Peclet number for the particle (17.5)

axial dispersion of the solute (Fahien and Smith 1955). It is apparent for the results in Fig. 17.4 that the effect of an increase in L/d_p predominates over the effect of an increase in D/d_p, so that the axial dispersion is larger in large vessels than small tubes (for purposes here, $L/d_p \leq 250$ in small packed beds). Thus, del Valle and Catchpole (2005) selected Pe_d and the ratio L/d_p as the independent variables in their correlation for D_{ax}/D_{12} (17.10).

$$\frac{D_{ax}}{D_{12}} = 0.540 + \frac{0.530\left(Pe_p\right)^2}{1 + 42.8\left(\frac{Pe_p}{L/d_p}\right)}. \tag{17.10}$$

Figure 17.4 reports experimental measurements of axial dispersion using closed circles for small packed beds (experimentally $89 \leq L/d_p \leq 234$) and open circles for large beds ($295 \leq L/d_p \leq 2{,}320$), and includes the limit between the two regions predicted by (17.10) for $L/d_p = 250$ in the form of a segmented line.

In this work, the authors believe that a precise estimation of the value of the axial dispersion coefficient is less important than determining whether axial dispersion phenomena affects SCFE of plant essential oils to such an extent that the term with D_{ax} must be included in the differential mass balance equation (last term on the left of (17.1)). This determination is important because axial dispersion phenomena is typically neglected to simplify the fitting of model parameters. del Valle and de la Fuente (2006) analyzed the effect of dispersion in mass transfer for SCFE of oilseeds under typical industrial conditions based on the claim of Goto et al. (1996) that it can be disregarded in mass transfer models when the value of the Peclet number for the packed bed (Pe_L, 17.11) is above *ca.* 100.

$$Pe_L = \frac{U\,L}{D_{ax}\varepsilon} \tag{17.11}$$

Recommended conditions for SCFE of plant essential oils are 323 K and 9 MPa (Reverchon 1997), for which the following values of physical properties were estimated in this work: $\rho = 285$ kg/m^3; $\mu = 2.47 \times 10^{-5}$ Pa s; $D_{12} \cong 3.00 \times 10^{-8}$ m^2/s; and, $Sc = 2.86$. Conditions favoring axial dispersion in the extraction vessel include a large superficial solvent velocity (e.g., $U = 5$ mm/s) (Eggers 1996), a large particle size, a small bed voidage, and a tall vessel (see 17.10 and 17.11). Eggers (1996) mentioned that the aspect ratio (L/D) of a typical extraction vessel is between 4 and 6, while Reverchon (1997) specified that an industrial SCFE facility for plant essential oils (Essences, Salerno, Italy) used vessels of 0.3 m^3, so in this work a packed bed $L = 2.40$ m tall and $D = 40$ cm wide was selected for calculations ($L/D = 6$, $V = 0.3$ m^3). According to the analysis, dispersive effects can be neglected ($Pe_L \geq 100$) for small particles of $d_p \leq 0.71$ mm, but for larger particles, it is necessary to reduce the bed voidage from $\varepsilon \leq 0.59$ for $d_p = 1.0$ mm to $\varepsilon \leq 0.34$ for $d_p = 1.5$ mm.

As shown in Table 17.1, most authors neglect the contribution of axial dispersion in their SCFE models for plant essential oils from solid substrates in packed beds. There are exceptions (studies where the axial dispersion coefficient is estimated using a literature correlation) including Ruetsch et al. (2003) and Daghero et al. (2004), who used the correlation of Wakao and Kaguei (1982); Goodarznia and Eikani (1998), Spricigo et al. (2001), Gaspar et al. (2003), Steffani et al. (2006), Zizovic at al. (2005, 2007a,b,c), Salimi et al. (2008), and Stamenić et al. (2008), who used the correlation of Tan and Liou (1989); and Machmudah et al. (2006), who used the correlation of Funazukuri et al. (1998). On the other hand, Reis-Vasco et al. (2000) used D_{ax} as a fitting parameter for their experimental data, but their best-fit values decreased when the superficial solvent velocity of the CO_2 increased (which was not as expected), and were 31–138 times larger than predicted using (17.10).

17.3.2 External Mass Transfer Coefficient

There are two values of k_f (expressed in, e.g., m/s) and $k_f a_p$ (expressed in, e.g., s^{-1}) reported in the literature as external mass transfer coefficients. Thus, in this work all values were recalculated first in similar units. To do this, the specific surface (a_p), or total particle surface (S_p) per unit volume of the packed bed [$(1 - \varepsilon)\ V_p$], was estimated using (17.12):

$$a_p = \frac{\psi}{(1-\varepsilon)\ d_p}. \tag{17.12}$$

In (17.12), ψ is a factor that depends on the geometry of the particles: ψ tends to 2 for very thin slabs (approaching a so-called infinite slab geometry), for which d_p is the thickness of the slab; and $\psi = 6$ for spheres. The void fraction in the packed bed (ε) in (17.12) ranged from 0.24 for milled black pepper (Ferreira et al. 1999) to 0.901 for rapidly decompressed oregano (Uquiche et al., submitted). We assumed a typical value $\varepsilon = 0.6$ in absence of a reported value (Mira et al. 1996; Papamichail et al. 2000; Louli et al. 2004; Zizovic et al. 2007a).

Figure 17.5 summarizes corrected values of k_f from the literature in a dimensionless plot of $Sh/Sc^{1/3}$ versus Re, where Sh is the dimensionless Sherwood number defined in (17.13):

$$Sh = \frac{k_f d_p}{D_{12}} \tag{17.13}$$

Figure 17.5 also includes reference lines corresponding to correlations in the literature for the external mass transfer coefficient in packed beds operating with liquids, gases, and SCFs. The correlations include the equation of Wakao and Kaguei (1982) for mass transfer in packed beds with low-pressure liquids and

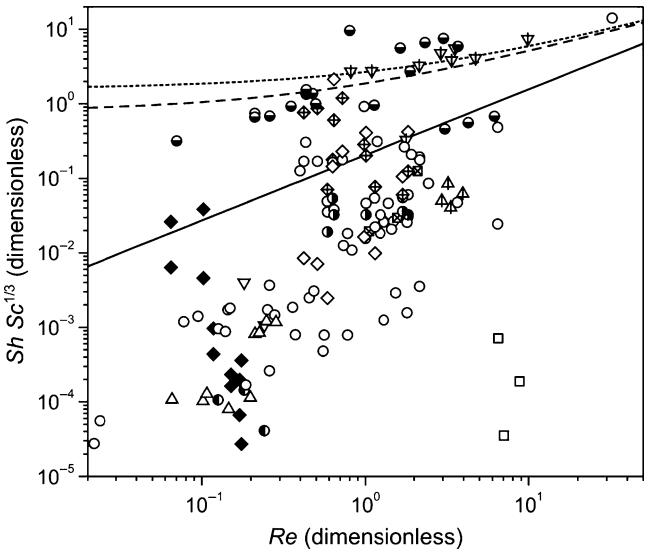

Fig. 17.5 Dimensionless plot of $Sh\ Sc^{-1/3}$ versus Re [where Sh, Sc, and Re are the dimensionless Sherwood (17.11), Schmidt (17.7), and Reynolds (17.6) numbers] for literature values of the external mass transfer coefficient (k_f) in SCFE of plant essential oils as a function of the flow regime in the packed bed. Plotted values were estimated from best-fitting parameters reported by the identified authors using the following models (model names reported in Table 17.1): (△) EMTC model applied by Ferreira et al. (1999) and Kotnik et al. (2007); (◇) R-SO model applied by Papamichail et al. (2000) and Louli et al. (2004); (⊕) LDF/UENA model applied by Papamichail et al. (2000) and Louli et al. (2004); (⧫) LDF/PF/CDIC model applied by Coelho et al. (1997); (□) LDF-Sph/PF model applied by Esquivel et al. (1996); (⊠) LDF/ADPF model applied by Reverchon and Marrone (1997); (○) Sovova's model applied by Mira et al. (1996, 1999), Papamichail et al. (2000), Povh et al. (2001), Ferreira and Meireles (2002), Sousa et al. (2002, 2005), Martínez et al. (2003, 2007), Rodrigues et al. (2003), Louli et al. (2004), Campos et al. (2005), Perakis et al. (2005), Vargas et al. (2006), and Bensebia et al. (2009); (◑) IBC/PF model applied by Louli et al. (2004); (◐) IBC/PFNA model applied by Sovová et al. (1994b); (◒) IBC/PF/PCPR model applied by Sovová (2005), Machmudah et al. (2006), and Langa et al. (2009); (◆) DDD/PM model applied by Kim and Hong (2002); (▽) SC/PF model applied by Germain et al. (2005); and (⧩) SC/ADPF model applied by Steffani et al. (2006)

gases (17.14), which is valid for $3 < Re < 3{,}000$ and $0.5 < \mathrm{Sc} < 10^4$, and the equation of Puiggené et al. (1997) for evaporation of 1,2-dichlorobenzene from glass beads into a high-pressure CO_2 stream (17.15), which is valid for $10 < Re < 100$ and $Sc < 10$.

$$Sh = 2 + 1.1\ Re^{0.6}\ Sc^{0.33} \tag{17.14}$$

$$Sh = 0.206\ Re^{0.8}\ Sc^{0.33} \tag{17.15}$$

The experimental values of Sc for the kinetic studies in Table 17.2 ranged from 2.05 to 17.0, and this result conditioned the selection of values for the two lines

corresponding to the correlation of Wakao and Kaguei (1982) in Fig. 17.5. The values of mass transfer coefficients predicted by Wakao and Kaguei (1982) for liquids and gases (17.14) are above those predicted by the literature correlations for mass transfer in packed beds operating with SCFs under forced convection (del Valle and de la Fuente 2006). Among the specific correlations for mass transfer in packed beds operating with SCFs, the predictions made in the equation of King and Catchpole (1993) are above those made in the equation of Tan et al. (1988), which are in turn above those made in (17.15) (del Valle and de la Fuente 2006). Thus, the expected estimated values of $Sh/Sc^{1/3}$ derived from the studies in Table 17.2 should be seen between the top and bottom lines in Fig. 17.5.

Figure 17.5 shows that experimental values of $Sh/Sc^{1/3}$ for the SCFE of plant essential oils exhibit considerable scattering (a span covering 3 orders of magnitude was observed, e.g., with data of Kim and Hong 2002), and are generally smaller (up to several orders of magnitude) than those predicted by the literature correlations. Most best-fit values were below the predictions of (17.15) with the exception of values of Papamichail et al. (2000) and Martínez et al. (2007), and a single value of Mira et al. (1999) using Sovová's model (Table 17.1), some values of Papamichail et al. (2000) and Louli et al. (2004) using model LDF/UENA, values of Machmudah et al. (2006) and Langa et al. (2009) using model IBC/PF/PCPR, and values of Steffani et al. (2006) using model SC/ADPF (who used (17.14) to get first guess values for k_f). Smaller best-fit values than predictions of literature correlations are probably due to a combination of several factors, including underestimation of the contribution of internal (solid phase) mechanisms to the total resistance to mass transfer, overestimation of the mass transfer area, underestimation of solvent flow heterogeneity effects, and underestimation of natural convection effects.

Some kinetic models assume that the extraction rate is controlled by external resistances to mass transfer (Ferreira et al. 1999; Kotnik et al. 2007). If this is not the case, the best-fit value of k_f would be smaller than in model systems without internal resistance to mass transfer, as those used to obtain the two correlations reported in Fig. 17.5, to compensate the contribution to the total resistance of the solid matrix (del Valle and de la Fuente 2006). This will also occur if the internal resistance to mass transfer is not neglected, but underestimated.

An overestimation of a_p would also be compensated by an underestimation of the value of k_f in cases where an overall mass transfer coefficient ($k_f a_p$) is used as a fitting parameter for experimental data (del Valle and de la Fuente 2006). In the work presented in this chapter the assumption is that the solid particles were spherical ((17.12) for $\psi = 6$), and although spheres have the smallest surface-area-to-volume ratio among regular geometric shapes, not all of the external surface of the particles is fully available for extraction due to tight packing in low-porosity beds (Marrone et al. 1998) or agglomeration of solid particles (Štastová et al. 1996; Eggers et al. 2000; del Valle et al. 2008).

Other causes of a reduction in the extraction rate and an associated reduction in the best-fitting value of k_f are irregularities in the packing of solid particles and other nonidealities that change the interstitial velocity of the high-pressure CO_2 across the extraction vessel (del Valle et al. 2004). Indeed, it is possible to have high-velocity

zones near the wall of an extraction vessel coexisting with low-velocity zones close to the axis of the vessel, with the end result of smaller extraction rates and smaller values of k_f in the axis than near the wall of the vessel (Sovová et al. 1994b; del Valle et al. 2004). These changes in velocity can be explained by the radial variations in bed porosity that result when packing comparatively large particles in small-diameter vessels (i.e., when $d_p/D < 10$ for mono-disperse particles) or radial variations in solvent viscosity when heating the packed-bed contents by conduction through the wall of the extraction vessel. Consequently with this hypothesis Brunner (1994) reported that the residual content of theobromine in ground cocoa seed shells increases when moving from the vessel wall toward the center of the extraction vessel in large-scale extraction experiments, and that these changes in residual solute content are more pronounced when the superficial velocity of high-pressure CO_2 decreases from 3.5 to <1.7 mm/s. The global effect of these changes is a reduction in the average value of the external mass coefficient (del Valle et al. 2004).

The last explanation for the differences between experimental and correlated values of k_f is neglecting the undesirable effects of natural convection on the external mass transfer. The natural convection phenomenon is important in experiments where high-pressure CO_2 moves slowly upwards in a vertical extraction vessel and against the gradient in density ($\Delta\rho = \rho_{sat} - \rho$) that develops when essential oils dissolve into the CO_2 stream, a condition under which the loaded CO_2 phase moves down under the influence of the force of gravity (Stüber et al. 1996; Puiggené et al. 1997; Germain et al. 2005). Thus, the extraction rate in a SCFE system using CO_2 upflow conditions is smaller than in a system using downflow conditions due to the negative influence of natural convection on mass transfer opposed by gravity (Sovová et al. 1994a, b; Stüber et al. 1996; Germain et al. 2005). This is important to consider in SCFE of plant essential oils because of several factors favoring undesirable convection phenomena (Germain et al. 2005): (1) the preference of solvent upflow conditions in industrial practice to improve extraction by fluidization of small particles and avoidance of compaction of the packed bed; (2) the use of near-critical conditions for extraction (Table 17.2); (3) the large solubility of essential oil components in high-pressure CO_2 under typical extraction conditions (Sect. 17.4); and (4) the use of a small superficial solvent velocity in experimental studies, as reported in the literature. Both correlations presented in Fig. 17.5 apply under forced convection conditions, but not when natural convection effects start to dominate as the ratio Gr/Re^2 increases ($>> 1$), where Gr is the dimensionless Grashof number defined in (17.16):

$$Gr = \frac{g\, d_p^3\, \rho^2\, \Delta\rho}{c_{sat}\, \mu^2}. \tag{17.16}$$

Germain et al. (2005) showed that for the extraction of caraway essential oils with high-pressure CO_2 at 313 K and 9–10 MPa ($Sc = 2.13$), another correlation of Puiggené et al. (1997) that takes into account the effect of natural convection

phenomena predicts smaller values of the external mass transfer coefficient when mass transfer is opposed by gravity (CO_2 upflow conditions) than when it is aided by gravity (CO_2 downflow conditions), whereas there are virtually no differences in $Sh/Sc^{1/3}$ for a relatively large Re (e.g., $Re \geq 50$). For a value of Re slightly below ($Re \approx 10$) the value of $Sh/Sc^{1/3}$ drops pronouncedly; this drop is only slightly dependent on the value of Gr (for $10 < Gr < 38{,}000$), but shifts to smaller values of Re as the value of Sc decreases (e.g., $Re \approx 2.5$ for $Sc = 34.4$). This helps to explain some of the experimental results reported in Fig. 17.5.

In selected cases, the value of k_f was not fitted to a cumulative extraction plot, but instead adopted from a literature correlation for forced convection. Goto et al. (1993, 1998), Spricigo et al. (2001), and Steffani et al. (2006) used the equation of Wakao and Kaguei (1982). Several authors used the equation of Tan et al. (1988), including Reverchon et al. (1993a), Reverchon (1996), Goodarznia and Eikani (1998), Perakis et al. (2005), Zizovic et al. (2005, 2007a,b,c), Salimi et al. (2008), and Stamenić et al. (2008). Catchpole et al. (1996b), Gaspar et al. (2003), Ruetsch et al. (2003), Daghero et al. (2004), and Machmudah et al. (2006) used the equation of King and Catchpole (1993). Araus et al. (2009) and Uquiche et al. (submitted) used the equation of Puiggené et al. (1997). It is relevant to mention that in most of these studies, the selected equations were applied for values of Re below the limit where the natural convection effects must be taken into account. Two exceptions where natural convection phenomenon was accounted for are the works of Akgun et al. (2000), who used the equation of Lee and Holder (1995), and Germain et al. (2005), who use an equation of Puiggené et al. (1997).

17.3.3 Effective Diffusivity in the Solid Matrix

To compare the best-fit internal mass transfer parameters in the reviewed studies in this work, the value of a microstructural factor F_M (17.17) that embodies all effects of the substrate and its pretreatment on inner mass transfer was estimated (Aguilera and Stanley 1999; del Valle and de la Fuente 2006; Araus et al. 2009; Uquiche et al. submitted):

$$F_M = \frac{D_{12}}{D_e}. \tag{17.17}$$

The term F_M gives the retarding effect of the solid matrix on the mass transfer rate by indicating how many times smaller the effective diffusivity of the essential oil is in the treated plant material than its binary diffusion coefficient in high-pressure CO_2. It is convenient to use F_M instead of D_e in modeling SCFE processes because it is independent of extraction temperature and pressure, interstitial solvent velocity, and substrate particle size (Araus et al. 2009).

There are some problems in expressing the internal mass transfer parameters as reported in the literature in consistent units. For example, some contributions

describe the best-fit value of an internal mass transfer coefficient k_i (expressed in, e.g., m/s) (Reverchon et al. 1999; Reis-Vasco et al. 2000) or the product $k_i a_p$ (expressed in, e.g., s^{-1}) (Sovová et al. 1994a; Esquivel et al. 1996; Mira et al. 1996, 1999; Coelho et al. 1997; Ferreira et al. 1999; Papamichail et al. 2000; Povh et al. 2001; Ferreira and Meireles 2002; Sousa et al. 2002, 2005; Martínez et al. 2003, 2007; Rodrigues et al. 2003; Louli et al. 2004; Campos et al. 2005; Perakis et al. 2005; Sovová 2005; Machmudah et al. 2006; Vargas et al. 2006; Bensebia et al. 2009; Langa et al. 2009), and in these cases the effective diffusivity was computed using the relationship between D_e and the reciprocal of $k_i a_p$ (or the so-called internal diffusion time t_i, s) proposed by Villermaux (1987) and reported in (17.18):

$$D_e = \frac{k_i d_p}{(1-\varepsilon)\,\xi} \tag{17.18}$$

where the particle-geometry parameter ξ was defined in connection with (17.5) in Sect. 2.3 (ξ = 10 for a sphere, ξ = 6 for a for thin slab).
When values of the effective diffusivity were reported, those cases were distinguished where they referred to the movement of the pseudo-solute in the solid (e.g., diffusion model), from those referring to movement in the fluid phase trapped in the solid (e.g., DDD models, SC models). Under the latter conditions, the values of D_e can be estimated according to (17.19) (del Valle and de la Fuente 2006):

$$D_e = D'_e K \tag{17.19}$$

where D'_e(the effective diffusivity of the pseudo-solute in the fluid trapped within the pores of the solid matrix) is the reported value, and K, the partition of the pseudo-solute between the SCF and the herb or spice which, in absence of a reported value (Sovová et al. 1994a; Mira et al. 1996, 1999; Coelho et al. 1997; Ferreira et al. 1999; Papamichail et al. 2000; Povh et al. 2001; Ferreira and Meireles 2002; Martínez et al. 2003, 2007; Rodrigues et al. 2003; Louli et al. 2004; Campos et al. 2005; Perakis et al. 2005; Vargas et al. 2006; Bensebia et al. 2009), is estimated using (17.20):

$$K = \frac{C_{fo}}{C_{so}} \tag{17.20}$$

Table 17.4 is an example of computed values of F_M in the case of SCFE of essential oils from oregano bracts, reporting the effect on F_M of different independent variables such as extraction temperature, extraction pressure, superficial velocity of the CO_2, sample pretreatment, and sample particle size. It is important to note that in those experiments where Esquivel et al. (1996), Gaspar (2002) (data modeled by Araus et al. 2009), and Gaspar et al. (2003) studied the effect of extraction temperature and/or extraction pressure, they also changed the superficial

velocity of the CO_2, because they kept the mass flow rate constant instead. Indeed, the superficial velocity of the CO_2 (U) depends not only on its mass flow rate (Q), but also on its density (ρ) under process conditions, which is a strong function of the extraction temperature and pressure, especially under near-critical conditions, according to (17.21):

$$U = \frac{4\,Q}{\pi\,D_E^2\,\rho} \tag{17.21}$$

As proposed by Araus et al. (2009), it was expected that the values of F_M are dependent on sample pretreatment, but independent of process temperature, process pressure, CO_2 superficial velocity, and substrate particle size, but clearly this is not the case (Table 17.4). Some of the differences can be imputed to typical variations in biological materials associated with differences in genetic makeup, growing environment, and harvest time (Zetzl et al. 2003). Although some differences were expected between the samples assayed by Esquivel et al. (1996), Gaspar (2002), Gaspar et al. (2003), and Uquiche et al. (submitted), which explains why the differences were smaller between experiments in a single study than among the four studies, the percent differences in estimated values of F_M between experiments in single studies were clearly still large. The very large difference in values of F_M between the sample with $d_p = 1.55$ mm (untreated sample) and all other samples in the study of Gaspar et al. (2003) can be explained by the positive effect of sample milling in reducing internal resistance to mass transfer. Uquiche et al. (submitted) also imputed the differences in values of F_M between their samples to microstructural differences caused by conventional milling, low-temperature milling, and rapid decompression of oregano and provided microscopy evidence of these differences. In work presented in this chapter the composition of the essential oil sample of oregano reported by Gaspar (2002) was used as representative of the extracts obtained in all experiments (Table 17.5); however, this assumption may be erroneous because of the aforementioned variability exhibited by biologic materials, as well as the variability in extract composition with process temperature and process pressure (i.e., extracts obtained using higher density CO_2 are expected to contain heavier and more polar compounds than the sample analyzed by Gaspar). As it will be analyzed later in this section, the errors introduced when not accounting for the actual composition are not as large as those observed in Table 17.5 and, in addition, differences were not expected in extract composition as used in experiments done by Gaspar et al. (2003) to assess the effect on extraction kinetics of the superficial solvent velocity, or the size of milled particles (Table 17.5). In this work, the authors believe mathematical models adopted and their ability to fit the physical picture of the actual extraction process explain the differences among estimated values of F_M reported in Table 17.5 to a large extent. For example, in the work of Gaspar et al. (2003) average values of F_M were 7.32×10^5 (range of value between 2.65×10^5 and 5.72×10^6) using model IBC-Diff (Table 17.5), 4.28×10^5 (range: 1.46×10^5 to 3.81×10^6) using model Diff-Slab/IC, and 4.19×10^5

Table 17.5 Values of microstructural factor for high-pressure CO_2 extraction of essential oils from oregano in selected studies from Tables 17.1 and 17.2 as a function of extraction conditions (system temperature and pressure, superficial velocity) and sample pretreatment and particle size

Studied effect	Independent variable	Microstructural factor (F_M, –)	Reference
Process conditions[a]	$T = 298$ K/$P = 7$ MPa	34,900	Esquivel et al. (1996)
	$T = 313$ K/$P = 10$ MPa	3,600	
	$T = 313$ K/$P = 15$ MPa	1,880	
Process pressure[b]	$P = 7$ MPa	409,000	Gaspar et al. (2003)
	$P = 8$ MPa	313,000	
	$P = 10$ MPa	265,000	
	$P = 15$ MPa	277,000	
Process temperature[c]	$T = 300$ K	277,000	Gaspar et al. (2003)
	$T = 310$ K	308,000	
	$T = 320$ K	390,000	
Superficial solvent velocity[d]	$U = 0.017$ mm/s	593,000	Gaspar et al. (2003)
	$U = 0.029$ mm/s	542,000	
	$U = 0.040$ mm/s	519,000	
	$U = 0.052$ mm/s	479,000	
Sample particle size[e]	$d_p = 0.330$ mm	440,000	Gaspar et al. (2003)
	$d_p = 0.360$ mm	440,000	
	$d_p = 0.700$ mm	477,000	
	$d_p = 1.550$ mm	5,720,000	
Sample pretreatment[f]	Conventionally milled ($d_p = 0.354$ mm)	2,650	Uquiche et al. (submitted)
	Low-temperature-milled ($d_p = 0.339$ mm)	2,540	
	Rapidly decompressed ($d_p = 0.844$ mm)	1,000	

[a] $_p = 1.10$ mm/$Q = 8.33$ g CO_2/min
[b] $d_p = 0.36$ mm/$T = 300$ K/$Q = 8.33$ g CO_2/min
[c] $d_p = 0.36$ mm/$P = 15$ MPa/$Q = 8.33$ g CO_2/min)
[d] $d_p = 0.36$ mm/$T = 310$ K/$P = 10$ MPa
[e] $T = 300$ K/$P = 7$ MPa/$U = 0.017$ mm/s
[f] $T = 313$ K/$P = 10$ MPa/$U = 1.234$ mm/s

(range: 1.38×10^5 to 3.81×10^6) using model Diff-Slab/PM. Furthermore, values of F_M for a selected experiment of Gaspar et al. (2003) – $d_p = 0.360$ mm/$T = 300$ K/$P = 8$ MPa/$Q = 8.33$ g CO_2/min – differed by a factor of more than 10 depending on the model: 3.13×10^5 using model IBC-Diff (Gaspar et al. 2003) and 2.64×10^5 using model Diff-PF (Araus et al. 2009).

Table 17.6 supports the claim that mathematical models and their ability to fit the physical picture of the actual extraction process explain the differences among estimated values of F_M to a great extent in the case of four different substrates. For basil, marjoram, and rosemary average values of F_M were approximately 1.5 times larger using model Diff-Sph/PM (Reverchon et al. 1993a) than model Diff-ADPF (Goodarznia and Eikani 1998), and approximately 70 times larger using model Diff-ADPF than model μS/SGl (Zizovic et al. 2005). For caraway, values of F_M were 20–110 times larger using model IBC/PFNA (Sovová et al. 1994a) than model

Table 17.6 Values of microstructural factor for high-pressure CO_2 extraction of plant essential oils in selected studies from Tables 17.1 and 17.2. All reported values for a single substrate and extraction condition were based on single experiments from an original publication, and fitted by individual authors to different models

Substrate	Original Study	Goodarznia and Eikani (1998)	Zizovic et al. (2005)	Sovová (2005)	Contribution of the authors
Basil (Reverchon et al. 1993a)	91,200	72,000	675	–	–
Marjoram (Reverchon et al. 1993a)	97,100	59,100	894	–	–
Rosemary (Reverchon et al. 1993a)	48,400	28,800	891	–	–
Caraway (Sovová et al. (1994a), extraction at 313 K and 9 MPa)	2,180,000	20,000	–	–	1,860 (Germain et al. 2005)
Caraway (Sovová et al. (1994a), extraction at 313 K and 10 MPa)	680,000	36,000	–	–	3,620 (Germain et al. 2005)
Pennyroyal (Reis-Vasco et al. (2000), d_p = 0.3 mm)	280	–	–	–	436 (Araus et al. 2009)
Pennyroyal (Reis-Vasco et al. (2000), d_p = 0.5 mm)	168	–	–	817	436 (Araus et al. 2009)
Pennyroyal (Reis-Vasco et al. (2000), d_p = 0.7 mm)	120	–	1,278	–	436 (Araus et al. 2009)

Diff-ADPF (Goodarznia and Eikani 1998), and approximately 10 times larger using model Diff-ADPF than model SC/PF (Germain et al. 2005). Finally, for pennyroyal values of F_M were 1.5–3.5 times larger using model Diff-PF (Araus et al. 2009) than model LDF/ADPF (Reis-Vasco et al. 2000), and for selected experiments 6.8 times larger using model IBC/PF/PCPR (Sovová 2005) or 10.7 times larger using model μS/SGl (Zizovic et al. 2005) than using model LDF/ADPF (Reis-Vasco et al. 2000).

Table 17.7 reports the interval of F_M-values estimated for all mass transfer studies in Tables 17.1 and 17.2 that inform best-fit values of internal mass transfer parameters, with the exception of studies in Tables 17.5 and 17.6. The results of the single experiments were collated using the same material based on this chapter's hypothesis that the values of F_M depend on the sample and its pretreatment, but do not depend on the extraction temperature and pressure, CO_2 superficial velocity, and particle diameter (del Valle and de la Fuente 2006; Araus et al. 2009; Uquiche et al. submitted). Explanations of the observed variations in the form of wide intervals for the values of F_M were advanced in the previous paragraphs in explaining some differences in Tables 17.5 and 17.6.

According to (17.17), the validity of reported values of the microstructural correction factor in Tables 17.5–17.7 depends partially on the values of the binary diffusion coefficient (D_{12}) estimated in this chapter using the equation of Catchpole and King (1994). This equation was developed with a large database that did not include typical components in plant essential oils. Table 17.8 displays estimated

Table 17.7 Summary of values of the microstructural factor for high-pressure CO_2 extraction of plant essential oils in studies from Tables 17.1 and 17.2 that are not included in Tables 17.4 or 17.5

Substrate	Pretreatment	Model name[a]	Microstructural factor (F_M, –)
Black pepper (Ferreira and Meireles 2002)	Milled	Sovová	(230–2.40) × 10^7
Black pepper (Perakis et al. 2005)	Milled	Sovová	(12.5–1.47) × 10^3
Valerian II (Zizovic et al. 2007a)	Milled	μS/SCav	(218–6.79) × 10^5
Valerian I (Zizovic et al. 2007a)	Milled	μS/SCav	(7.25–3.58) × 10^6
Valerian III (Zizovic et al. 2007a)	Milled	μS/SCav	(4.63–2.99) × 10^6
Spearmint (Kim and Hong 2002)	Milled	DDD/PM	(30.1–4.17) × 10^4
Marigold (Zizovic et al. 2007a)	Milled	Sovová	(68.2–4.06) × 10^3
Marigold (Zizovic et al. 2007a)	Milled	Diff-Slab/PM	(11.2–4.99) × 10^4
Sage (Reverchon 1996)	Milled	LDF-Slab/PMMS	5.54 × 10^4
Sage (Araus et al. (2009)	Milled	Diff/PF	(39.5–3.95) × 10^3
Sage (Catchpole et al. 1996b)	Chopped	LDF/IMTC	2.52 × 10^3
Sage (Langa et al. 2009)	Milled	IBC/PF/PCPR	49.9–3.75
Rosemary (Coelho et al. 1997)	Milled	LDF/PF/CDIC	(16.9–7.39) × 10^2
Rosemary (Bensebia et al. 2009)	Milled	Sovová	(4.34–1.26) × 10^2
Hop (Pfaf-Šovljanski et al. 2005)	Milled	R-SO	3.20 × 10^4
Aniseed (Rodrigues et al. 2003)	Milled	Sovová	(30.5–2.09) × 10^3
Eucalyptus (Zizovic et al. 2007c)	Milled	μS/SCav	1.58 × 10^4
Chamomile (Povh et al. 2001)	Milled	Sovová	(14.7–7.97) × 10^3
Chamomile (Araus et al. 2009)	Milled	Diff/PF	1.08 × 10^4
Chamomile (Kotnik et al. 2007)	Milled	EMTC	(6.65–3.53) × 10^3
Thyme (Zekovic et al. 2001)	Milled	R-SO	(13.9–1.2) × 10^3
Orange peel (Mira et al. 1996)	Milled	Sovová	(13.5–1.15) × 10^3
Orange peel (Mira et al. (1999)	Milled	Sovová	4290–7.29
Orange peel (Zizovic et al. 2007c)	Milled	μS/SCav	1.68 × 10^2
Ginger (Martínez et al. 2003)	Milled	Sovová	(11.1–2.21) × 10^3
Alecrim pimenta (Sousa et al. 2002)	Triturated	Sovová	1.03 × 10^4
Ho-sho (Steffani et al. 2006)	Milled	SC/ADPF	(83.1–4.44) × 10^2
Parsley (Louli et al. 2004)	Milled	Sovová	(7.53–2.23) × 10^3
Parsley (Louli et al. 2004)	Milled	Sovová	(7.5–2.54) × 10^3
Lavender (Reverchon et al. 1995a)	Milled	R-SO	6.41 × 10^3
Lavender (Akgun et al. 2000)	Manually crushed	SC/PF	(36.8–9.25) × 10^2
Lavender (Araus et al. 2009)[7]	Milled	Diff/PF	2.03 × 10^2
Cinnamon of cunha (Sousa et al. 2005)	Triturated	Sovová	(6.17–4.62) × 10^3
Boldo (Uquiche et al. submitted)	Rapidly decompressed	Diff/PF	5.66 × 10^3
Boldo (Uquiche et al. submitted)	Conventionally milled	Diff/PF	4.75 × 10^3
Boldo (Uquiche et al. submitted)	Low-temperature-milled	Diff/PF	4.18 × 10^3
Nutmeg (Spricigo et al. 2001)	Milled	SC/ADPF	(56.5–3.39) × 10^2
Nutmeg (Machmudah et al. 2006)	Milled	–	–
Fennel (Reverchon et al. 1999)	Milled	LDF/PF	(2.25–2.37) × 10^2
Celery (Papamichail et al. 2000)	Milled	Sovová	(15.1–2.04) × 10^2
Celery (Zizovic et al. 2005)	Milled	μS/SDuct	1.28 × 10^3

(*continued*)

Table 17.7 (continued)

Substrate	Pretreatment	Model name[a]	Microstructural factor (F_M, –)
Carqueja (Vargas et al. 2006)	Milled	Sovová	(4.25–1.79) × 10^2
Carqueja (Vargas et al. 2006)	Milled	R-SO	(8.30–1.58) × 10^2
Clove (Martínez et al. 2007)	Milled	Sovová	84.2–69.6

[a]Model names are specified in Table 17.1

variations in the D_{12} of typical components in plant essential oil extracts in high-pressure CO_2 as a function of CO_2 density and system temperature. Values of D_{12} decrease when decreasing the temperature (a 6.4% decrease from 333 to 313 K), or increasing the density of the CO_2 (a 60% decrease from 285 to 683 kg/m^3), or increasing the size of the solute. However, changing D_{12} to a considerable extent demands extreme changes in extract composition; the reduction is limited to 25% between the heaviest OST (the 17-C farnesyl acetate) and lightest MT (the 10-C limonene), 40% between the wax (the 28-C *n*-octacosane) and limonene, and 56% between the triglyceride (the 57-C triolein) and limonene. According to this analysis, the discrepancies in D_{12} associated with the use of the equation of Catchpole and King (1994) and the adoption of an erroneous pseudo-solute could result in discrepancies that are substantially smaller than discrepancies in values of F_M reported in Tables 17.5–17.7.

Another factor that is partially responsible for errors in the estimation of F_M, according to (17.19), is the erroneous estimation of the partition K of the pseudo-solute between the solid and the fluid. A discussion of errors in the estimation of K can be found in Sect. 4.4.

There are some reports on the estimation of D_e for a porous solid as a function of D_{12} and the inner porosity (ε_p) of the solid substrate (Goto et al. 1993; Ruetsch et al. 2003; Daghero et al. 2004; Perakis et al. 2005). According to the equation of Wakao and Smith (1962), (17.22), F_M can be estimated as follows:

$$F_M = \frac{1}{\varepsilon_p^2} \tag{17.22}$$

Considering that in these studies, inner porosity values for the substrates ranged from $\varepsilon_p = 0.487$ for black pepper (Perakis et al. 2005) to $\varepsilon_p = 0.537$ for peppermint (Goto et al. 1993), the values of F_M estimated using (17.22) ranged from 4.0 to 4.2. Thus, (17.22) produces smaller values of F_M than those reported in Tables 17.5–17.7. Ruetsch et al. (2003) and Daghero et al. (2004) did not measure ε_p, but assumed a value $\varepsilon_p = 0.5$. On the other hand, Perakis et al. (2005) estimated the porosity from experimental values of the true density (ρ_p) of ground particles of black pepper, and the bulk density (ρ_p) of a packed of the particles according to (17.23):

$$\varepsilon = 1 - \frac{\rho_b}{\rho_p} \tag{17.23}$$

Table 17.8 Predicted binary diffusion coefficient D_{12} ($m^2/s \times 10^8$) of selected components in plant essential oils (component 2) in supercritical CO_2 (component 1) as a function of system temperature and CO_2 density

Solute	MW_2 (Da)	V_{c2} (cm^3/mol)	ρ = 285.0 (kg/m^3)			ρ = 682.6 (kg/m^3)		
			313 K (8.1 MPa)	323 K (9.0 MPa)	333 K (9.9 MPa)	313 K (10.0 MPa)	323 K (12.8 MPa)	333 K (15.7 MPa)
Limonene	136.2	507.5	3.38	3.49	3.60	1.37	1.41	1.45
Linalool	154.3	565.5	3.22	3.32	3.42	1.30	1.34	1.38
Linalyl acetate	196.3	682.5	2.95	3.04	3.13	1.19	1.23	1.26
β-Caryophyllene	204.4	722.5	2.88	2.97	3.06	1.16	1.20	1.23
Farnesol	222.4	837.5	2.71	2.79	2.88	1.09	1.13	1.16
Farnesyl acetate	264.4	954.5	2.55	2.63	2.71	1.03	1.061	1.09
n-Octacosane	394.8	1,603.5	2.04	2.11	2.17	0.824	0.850	0.877
Triolein	885.5	3,233.5	1.49	1.54	1.59	0.603	0.622	0.642

The problem with using (17.21) to estimate the inner porosity of the substrate is that ε is the total porosity of the bed instead of ε_p, which is smaller. (17.24) relates the inner porosity of the substrate (ε_p) with the total porosity (ε) and the interparticle porosity of the particles in the packed bed (ε_b):

$$\varepsilon_p = \frac{\varepsilon - \varepsilon_b}{1 - \varepsilon_b} \tag{17.24}$$

Considering that randomly packed spherical particles in a dense bed have a large ratio, D/d_p, for which the expected value of interparticle porosity is $\varepsilon_b = 0.36$ (Carman 1937), it can be estimated using (17.24) that $\varepsilon_p = 0.198$ for $\varepsilon = 0.487$, and then using (17.22) that $F_M = 25.4$, which is still small but closer to the experimental values reported in Tables 17.5–17.7.

This chapter's analysis of the inner mass transfer within the solid substrate up to this point has implicitly considered that the substrate is a homogeneous material. Tables 17.5–17.7 include examples of materials being considered as being composed of broken superficial cells and intact inner cells, and total mass transfer in these heterogeneous materials considers separate extraction of the two fractions according to different controlling mechanisms, respectively external resistance to mass transfer, and internal (diffusive) resistance to mass transfer. These models usually use the ratio of broken to intact cells or the fraction of free solute (α) in the pretreated substrate as a fitting parameter; however, this ratio has to agree with the microstructure of the biological substrate, particularly of the specialized secretory structures where plant essential oils are encapsulated. For a spherical particle obtained by milling of a parenquimatous tissue, α is given by (17.25):

$$\alpha = 1 - \left(1 - \frac{d_c}{d_p}\right)^3 \tag{17.25}$$

where the thickness of a superficial layer of ruptured cells is closely related to the diameter (d_c) of the specialized secretory structure, and d_p is the diameter of the milled particle.

Figure 17.6 shows the effect of the ratio between cell diameter and particle diameter (d_c/d_p) on the best-fit values of fractions of broken cells (α) in milled herbs or spices containing superficial glands, including oregano bracts (Gaspar et al. 2003), pennyroyal leaves (Sovová 2005), rosemary leaves (Bensebia et al. 2009), and sage leaves (Langa et al. 2009); secretary ducts, including caraway fruits (Sovová et al. 1994a), celery seeds (Papamichail et al. 2000), chamomile flowers (Povh et al. 2001), aniseed fruits (Rodrigues et al. 2003), parsley seeds (Louli et al. 2004), and marigold flowers (Campos et al. 2005); or secretory cavities, such as orange peels (Mira et al. 1996, 1999). For calculations, the cell diameters (d_c) estimated from microphotographs in the literature were as follows: for oregano, $d_c = 78$ μm (Svoboda and Svoboda 2000); for pennyroyal, $d_c = 52.5$ μm (Zizovic et al. 2007c); for rosemary, $d_c = 85$ μm (Svoboda and Svoboda 2000); for sage,

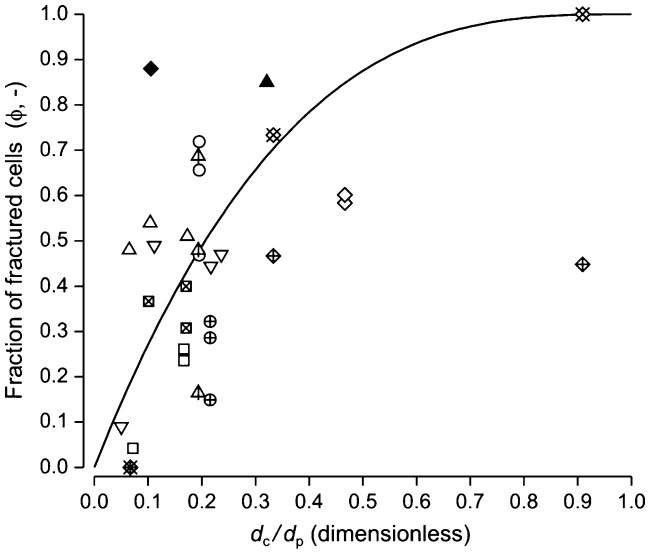

Fig. 17.6 Effect of particle diameter on the best-fit values of the fraction of broken cells in milled herbs or spices. Calculations were made from data of (▲) caraway (Sovová et al. 1994a), (⊕) orange peel (Mira et al. 1996), (⊗) orange peel (Mira et al. 1999), (□) celery (Papamichail et al. 2000), (◇) chamomile (Povh et al. 2001), (▽) oregano (Gaspar et al. 2003), (⊕) aniseed (Rodrigues et al. 2003), (⍋) marigold (Campos et al. 2005), (◆) pennyroyal (Sovová 2005), (⊠) parsley (Louli et al. 2004), (○) rosemary (Bensebia et al. 2009), and (△) sage (Langa et al. 2009)

$d_c = 52$ μm (Serrato-Valenti et al. 1997); for caraway, $d_c = 123$ μm (Svoboda and Svoboda 2000); for celery, $d_c = 35$ μm (Stamenić et al. 2008); for chamomile, $d_c = 140$ μm (Zizovic et al. 2007c); for aniseed, $d_c = 108$ μm (Zizovic et al. 2007c); for parsley, $d_c = 50$ μm (Podlaski et al. 2003); for marigold, $d_c = 120$ μm (Zizovic et al. 2007c); and for orange peels, $d_c = 500$ μm (Svoboda and Svoboda 2000). The line in Fig. 17.6 corresponds to (17.25) which is only valid for size reduction relying on impact or attrition mechanisms that fracture surface cells only. Figure 17.6 shows that (17.25) only partially explains the best-fit values of broken cells reported in the literature, possibly because of differences between the assumed and actual particle shape, microstructure, and fracturing mechanism of the specialized secretory structures in the plant materials.

Zizovic et al. (2005, 2007a, b, c) have contributed a series of studies on the mathematical modeling of SCFE of plant essential oils at the micro-scale that demonstrate the need to include a description of the encapsulating secretory structures in plant tissue to improve the predictive capacity of the model. These structures (glandular trichomes or glands, large or small secretory cavities, and secretory ducts) (Sect. 17.1.1), are not equally affected by pre-treatment, nor by the extraction process. For example, milling causes partial destruction of glandular trichomes or glands in the surface of leaves, terminal shoots, and flowers of *Laminaceae* herbs, and subsequent SCFE causes partial destruction of the

remaining glands by a mechanism involving diffusion of CO_2 through the gland wall, its dissolution into the essential oil, and swelling the CO_2-saturated mixture to the extent of rupturing the gland. Zizovic et al. (2005) obtained microscopical evidence of the rupture of a fraction $\phi \sim 0.35$ of the glands during milling of dried mentha leaves to a final particle diameter of 0.5–1 mm, as well as of the rupture of about $\varphi \sim 0.39$ of the glands after contacting unmilled leaves with high-pressure CO_2 at 313 K and 10 MPa for 1 h. Zizovic et al. (2005) hypothesized that all glands cracked during the process as a result of swelling of the gland contents, become disrupted upon saturation of the essential oil with the CO_2 at a single time that is determined by diffusion of CO_2 through the gland wall, but later Stamenić et al. (2008) proposed a cracking time distribution based on microscopical evidence gathered by exposing wild thyme leaves to high-pressure CO_2 at 313 K and 10 MPa different times between 20 min and 100 min. These models were applied to basil, rosemary, marjoram, and pennyroyal by Zizovic et al. (2005) and to wild thyme by Stamenić et al. (2008).

Unlike superficial glands that can rupture upon swelling of the gland contents by dissolution of CO_2 into the essential oil, inner secretory cavities in plant tissue are ruptured only as a result of a size-reduction pretreatment, with the probability of rupture being dependent on the relative sizes of secretory cavities and milled particles. Since the physical picture for the extraction of essential oil from secretory cavities at the microscale is similar to that of intact and broken cells proposed by Sovová (1994) (Sect. 17.2.3), the mathematical model in this particular case considered simultaneous extraction of essential oils from disrupted cavities controlled by an external mass transfer coefficient, and of essential oils from nondisrupted cavities controlled by a best-fit internal mass transfer coefficient. Zizovic et al. (2007a) estimated the fraction of disrupted cavities in milled valerian roots as the ratio between the cavity diameter (determined by microscopy) and the particle diameter (determined by sieving). Zizovic et al. (2007a) estimated the mean diffusion pathway in nondisrupted cells as half the difference between the particle diameter and cavity diameter, but they did not explain the basis for this assumption. This model was applied to valerian roots by Zizovic et al. (2007a), and to clove buds, ginger rhizomes, and eucalyptus leaves by Zizovic et al. (2007c). Consequently, Zizovic et al. (2007c) developed a separate model for SCFE of plant materials with large secretory cavities, such as citrus peels, where most cavities are cracked.

In the case of plant material with secretory ducts, the size-reduction pretreatment opens each duct on two opposite sides of the particle. The essential oil in the duct becomes saturated with CO_2 during extraction and the swelling of the mixture results in a superficial layer of oil embedding the whole particle. SCFE can be pictured as a two-stage process. In the first stage, when the mass transfer area is the external surface of the particle, the extraction of essential oil is defined by convection of the superficial oil to the CO_2 (mass transfer coefficient from a literature correlation). In the second stage, when the mass transfer area diminishes to that fraction of the external surface of the particle covered with openings of secretory ducts, the essential oil moves from a receding boundary in the pore to the pore

opening by unimpeded diffusion (defined by the binary diffusion coefficient of the oil in CO_2), and then by convection (the same mass transfer coefficient from the first stage) from the pore opening to the bulk of the high-pressure CO_2 phase; the diffusion path for the essential oil in this second stage is half the particle diameter. Zizovic et al. (2007b) proposed a fully predictive mathematical model for SCFE plant material with secretory ducts, which used the diameter of the secretory ducts and their superficial density (number of ducts per unit surface area) as microstructural parameters. The model was applied for fruits of celery (Stamenić et al. 2008), and fruits of fennel, and flowers of chamomile and marigold (Zizovic et al. 2007b).

17.4 Phase Equilibrium Effects in Essential Oil Extraction, Fractionation, and Recovery

In this section, the effect of phase equilibrium on the extraction, fractionation, and recovery of plant essential oils using high-pressure CO_2 is discussed. Firstly, the variations in the solubility of essential oil components in high-pressure CO_2 are discussed as a function of system temperature and pressure (Sect. 17.4.1). Secondly, there is discussion of the selective removal of high-solubility MTs from the remaining OMTs so as to produce citrus essential oils with an improved functionality (more intense aroma, less off-flavors, increased solubility in water) based on high-pressure phase equilibrium data for ternary CO_2 + MT + OMT and more complex systems (Sect. 17.4.2). Next, the thermodynamic solubility in CO_2 of complex essential oil mixtures is compared with the "operational" solubility of the CO_2 extract of the corresponding herb or spice under comparable temperature and pressure (Sect. 17.4.3). Finally, the effect of sorption phenomena on the aforementioned "operational" solubility (Sect. 17.4.4) is discussed.

17.4.1 Solubility in CO_2 of Essential Oil Components in Model (Binary) Systems

There are many experimental studies about the solubility of selected essential oil components in CO_2 as a function of system temperature and pressure, as shown in Table 17.9. The data include four different solute families and CO_2 conditions that span from subcooled liquid, to superheated vapor, and to SCF (equilibrium temperatures of 296–373 K, and equilibrium pressures of 0.81–30.9 MPa). There is abundant information in the literature about the solubility of limonene in high-pressure CO_2, but virtually none about other 10-carbon MT compounds, the only exceptions being *p*-cymene and α-pinene (Table 17.9). On the other hand, there is extensive information on the solubility of OMT compounds in high-pressure CO_2, including anisaldehyde, camphor, carvacrol, carvone, 1,8-cineole (eucalyptol),

Table 17.9 Summary of high-pressure equilibrium CO_2 + plant essential oil component binary systems. The essential oil components were classified as monoterpene hydrocarbons, oxygenated monoterpenes, sesquiterpene hydrocarbons and oxygenated sesquiterpenes, and waxy compounds

Solute	Data points	Temperature(s) or temperature range (K)	Pressure(s) or pressure range (MPa)	Solubility range (mg solute/g CO_2)
Monoterpenes				
p-Cymene (Wagner and Pavlicek 1993)	16	313–323	3.855–9.829	6.73–41.7
Limonene (di Giacomo et al. 1989)	26	308, 315, 323	3.0–10.0	0.681–142
Limonene (Matos et al. 1989)	14	318, 323	8.6–9.8	12.4–106
Limonene (Marteau et al. 1995)	29	310, 320, 323	6.96–9.85	5.58–73.2
Limonene (Iwai et al. 1996)	15	313, 323, 333	3.94–10.26	3.41–24.3
Limonene (Akgun et al. 1999)	22	313, 323, 333	7.04–11–20	1.24–54.8
Limonene (Chang and Chen 1999)	28	314, 323, 333	0.83–11.00	1.55–47.2
Limonene (Vieira de Melo et al. 1999)	16	323, 333, 343	7.00–10.55	4.96–88.2
Limonene (Kim and Hong 1999)	11	312, 322	6.2–9.3	3.10–79.4
Limonene (Berna et al. 2000)	8	318	6.9–10.5	5.27–1,202
Limonene (Gamse and Marr 2000)	42	304, 314, 324	3.1–8.4	2.79–65.4
Limonene (Benvenuti and Gironi 2001)	8	315	3.05–8.50	5.89–18.4
Limonene (Leeke et al. 2001)	15	318, 323	7.32–10.05	2.79–81.3
Limonene (Francisco and Sivik 2002)	8	313, 333	8–25	12.4–89.2
Limonene (Fonseca et al. 2003)	4	323	8.3–9.5	130–244
α-Pinene (Pavlicek and Richter 1993)	72	313, 323, 328	3.25–9.75	3.60–54.3
α-Pinene (Richter and Sovová 1993)	24	296–335	6.14, 7.65	4.15–102
α-Pinene (Akgun et al. 1999)	19	313, 323, 333	7.15–10.93	5.27–53.5
α-Pinene (Francisco and Sivik 2002)	8	313, 333	8–25	9.32–82.7
Oxygenated monoterpenes				
p-Anisaldehyde (Mukhopadhyay and De 1995)	13	323, 373	5.5–13.7	0.619–43.9
Camphor (Akgun et al. 1999)	39	313, 323, 333	7.51–12.61	2.98–139
Camphor (Carvalho et al. 2006)	15	314, 324, 334, 354	8.65–15.71	32.5–275
Carvacrol (Leeke et al. 2001)	49	313, 323	7.70–30.85	9.59–740
Carvone (Kim and Hong 1999)	13	312, 322	6.2–9.6	0.307–59.0
Carvone (Gamse and Marr 2000)	31	304, 314, 324	2.0–10.0	0.683–50.9
1,8-Cineole (Matos et al. 1989)	15	318, 323	7.75–9.80	14.1–82.5
1,8-Cineole (Francisco and Sivik 2002)	8	313, 333	8.0–25.0	10.5–86.2
Citral (di Giacomo et al. 1989)	29	308, 315, 323	3.0–11.0	0.104–78.9
Citral (Marteau et al. 1995)	26	310, 320, 330	7.94–11.93	2.42–4.85
Citral (Benvenuti and Gironi 2001)	10	315	4.70–9.58	0.692–36.0
Citral (Fonseca et al. 2003)	4	323	8.7–10.3	32.5–143
β-Citronellol (Tufeu et al. 1993)	15	309, 316, 321	8.46–15.70	25.8–160
Eugenol (Cheng et al. 2000)	21	308, 318, 328	1.480–12.512	4.48–61.8
Fenchone (Akgun et al. 1999)	21	313, 323, 333	7.04–11.50	1.04–1.04
Geraniol (Tufeu et al. 1993)	9	309, 316, 321	10.82–16.27	37.9–120
Linalool (Chang and Chen 1999)	29	313, 323, 333	0.81–11.06	1.05–35.4
Linalool (Vieira de Melo et al. 1999)	3	323	7.49–8.37	1.75–4.56
Linalool (Berna et al. 2000)	13	318, 328	7.1–11.1	2.39–1,381

(*continued*)

Table 17.9 (continued)

Solute	Data points	Temperature(s) or temperature range (K)	Pressure(s) or pressure range (MPa)	Solubility range (mg solute/g CO_2)
Linalool (Fonseca et al. 2003)	3	323	8.6–9.4	132–196
Linalool (Iwai et al. 1994)	14	313, 323, 333	4.00, 10.96	1.05–27.9
Linalool (Raeissi and Peters 2005)	12	319–348	9.355–13.705	71.5
Menthol (Carvalho et al. 2006)	12	323, 343	6.5–13.5	0.256–218
Menthol (Sovová and Jež 1994)	40	308, 313, 318, 323, 328	6.52–11.56	0.782–47.1
Menthol (Sovová et al. 2007)	47	303, 313, 323, 333	6.64–14.37	1.24–147
Thymol (Carvalho et al. 2006)	12	323, 343	6.5–13.5	19.6–497
Verbenol (Richter and Sovová 1993)	73	313, 323, 328	5.09–13.78	0.208–194
Sesquiterpenes and oxygenated sesquiterpenes				
β-Caryophyllene (Michielin et al. 2009)	86	303, 313, 323, 333, 343	4.5–19.2	18.7–522
Artemisinin (Xing et al. 2003)	36	310, 318, 328, 338	10.0–27.0	0.628–17.1
Farnesol (Núñez et al. 2010)	58	313, 323, 333	9.7–26	0.657–9.67
α-Humulene (Michielin et al. 2009)	77	303, 313, 323, 333, 343	4.7–19.2	18.7–521
Patchoulol (Hybertson 2007)	8	313, 323	10.0–25.0	2.17–48.0
Typical wax component				
Octacosane (Reverchon et al. 1993b)	28	308, 313, 318	8.0–27.5	0.110–3.50
Octacosane (Stassi and Schiraldi 1994)	3	308–318	25	0.610–3.36
Octacosane (Chandler et al. 1996)	14	308, 318	10.0–24.0	0.170–4.22

citral, β-citronellol, eugenol, fenchone, geraniol, linalool, menthol, thymol, and verbenol (Table 17.9). There is less solubility information about the 15-carbon terpene compounds, which is limited to artemisinin (OST), β-caryophyllene (ST), farnesol (OST), α-humulene (ST), and patchoulol (OST). Finally, although there is extensive information in the literature on the solubility of waxy compounds in high-pressure CO_2, Table 17.9 is limited to experimental works with octacosane. Literature on the solubility of waxy compounds includes *n*-alkanes having 9–36 carbon atoms under typical CO_2 extraction conditions, as well as long-chain *n*-alkanes under typical gas-processing conditions (Stassi and Schiraldi 1994; Chandler et al. 1996; Reverchon et al. 1993b). Stahl et al. (1988) conducted a systematic study on the solubility of essential oil components in high-pressure CO_2 including data for limonene, anethole (OMT), carvone, eugenol, β-caryophyllene, and valeranone (OST). This chapter does not include the results of Stahl et al. (1988) in Table 17.9 since they reported trend lines instead of actual experimental data, so their results are of less value for quantitative comparison purposes.

Solubility values of selected essential oil components in high-pressure CO_2 vary widely, as exemplified in Fig. 17.7 for the solubility of limonene in high-pressure

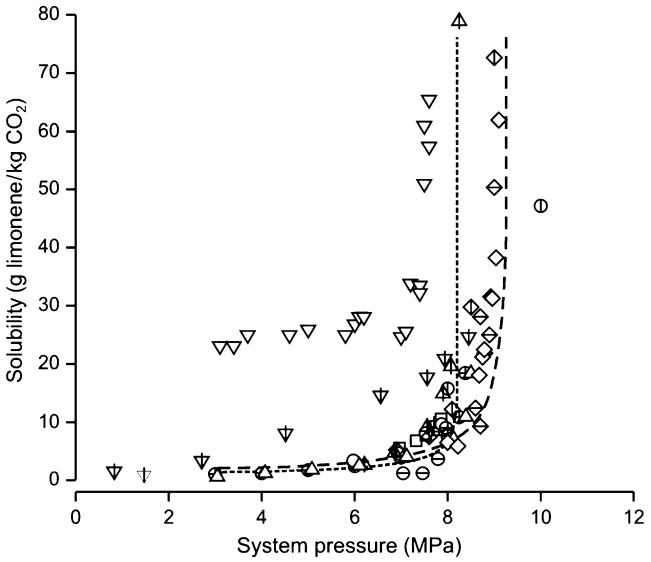

Fig. 17.7 Solubility of limonene in supercritical CO_2 as a function of system pressure (approximately between 1 MPa and 10 MPa) as reported by (⊕) di Giacomo et al. (1989) at 313 K, (◈) Matos et al. (1989) at 318 K, (□) Marteau et al. (1995) at 310 K, (○) Iwai et al. (1996) at 313 K, (⊖) Akgun et al. (1999) at 313 K, (▼) Chang and Chen (1999) at 314 K, (▲) Kim and Hong (1999) at 312 K, (◈) Berna et al. (2000) at 318 K, (▽) Gamse and Marr (2000) at 314 K, (△) Benvenuti and Gironi (2001) at 315 K, (◇) Leeke et al. (2001) at 318 K, and (⊙) Francisco and Sivik (2002) at 313 K. Lines represent the solubility isotherms at (– – –) 311 and (-------) 318 K predicted using the Peng-Robinson-Mathias-Copeman equation of state with the modified Huron-Vidal (MHV1) – UNIFAC mixing rules and model parameters in database of PE 2000 (Pfohl et al. 2000), a shareware software for modeling high-pressure phase equilibria

CO_2 at approximately 313 K (310–318 K) and as a function of system pressure, due to the inherent limitations of methodologies applied to assess phase equilibrium (Raal and Mühlbauer 1998). Limonene is the most abundant MT in plant essential oils, representing >90% (w/w) of some of them, because it acts typically as a carrier of other compounds (mainly OMTs) that impact more definitely on plant aroma. The experimental methods can be broadly classified as analytic (if one or both phases in equilibrium are sampled and analyzed to determine composition) or synthetic (if the global composition of the system is predetermined, and the conditions of the system are changed so as to reach a phase boundary). These broad classes, in turn, can be implemented in static or dynamic equilibrium cells, depending on agitation. In dynamic cells, the time to reach equilibrium is shortened by agitation of the cell contents, or recirculation of one or the two phases in the cell (the so-called multi-pass dynamic systems, where sampling is done in recirculation loops). Measurements using all methods are susceptible to error if true equilibrium conditions are not reached, and no single method is more questionable in this regard than the one-pass dynamic method (di Giacomo et al. 1989; Kim and Hong 1999;

Gamse and Marr 2000; Benvenuti and Gironi 2001; Fonseca et al. 2003). Observation of the cell contents through a window-cell helps to ascertain the quality of stirring and the number and nature of phases in the system. In the case of analytical methods, where system temperature and pressure are kept constant, sampling and analysis of one phase as a function of equilibration time can help to ascertain whether equilibrium conditions have been reached. Another problem with analytic methods occurs when an incomplete picture of the equilibrium is achieved when only the CO_2-rich phase is sampled, and when CO_2 transfers to the solute-rich phase (Matos et al. 1989; Berna et al. 2000). A final problem when using an analytic system is the disturbance of system conditions and the associated shift in equilibrium during sampling, which causes a drop in pressure (Iwai et al. 1996; Vieira de Melo et al. 1999). Since these disturbances are unavoidable, users of analytical methodologies try to minimize the negative effects of sampling by using large cells (Akgun et al. 1999; Leeke et al. 2001), or by reducing the size of the sampled aliquot by coupling the cell with a high-sensitivity instrument such as an infrared absorption device (Marteau et al. 1995), a densitometer (Chang and Chen 1999), or a chromatograph (Francisco and Sivik 2002).

The sampling problem inherent in analytic methods can be avoided by using synthetic methods. Synthetic systems use a variable volume cell to change system pressure while keeping the temperature and global composition constant. Raising the pressure (reducing the inner volume of the cell) to make the CO_2-rich phase collapse to a single bubble (as is the case when the composition of the liquid phase equals the global composition of the system) determines the bubble pressure at the test temperature. Alternatively, decreasing the pressure (increasing the inner volume of the cell) to cause the solute-rich phase collapse to a single drop (as is the case when the composition of the vapor phase equals the global composition of the system) determines the dew point at the test temperature. A problem of the synthetic method is the inherent difficulty in reaching and determining both bubble and dew point conditions for binary and more complex systems (Marteau et al. 1995).

The solubility of limonene in supercritical CO_2 at 313 K increases steadily with system pressure at low pressures ($P < 8$ MPa) and then increases sharply at high pressures ($P > 8$ MPa), with the transition between steady and sharp increase occurring close to the critical point of the mixture (Fig. 17.7). The reported critical point of CO_2 + limonene mixtures at 313 K is 8.3 MPa (Matos et al. 1989) or 8.5 MPa (Tufeu et al. 1993), and under these conditions the composition of the liquid phase coincides with that of the SCF phase (35.1 g limonene/kg CO_2). The binary CO_2 + limonene system exhibits a temperature crossover at ~8 MPa (Akgun et al. 1999; Berna et al. 2000). Thus, as the temperature increases isobarically, solubility of limonene in CO_2 decreases at $P < 8$ MPa due to reduction in the density and solvent power of CO_2, whereas solubility increases at $P > 8$ MPa due to the rise in vapor pressure and volatility of limonene. There is a general consistency between experimental solubility data for <8.5 MPa and for <80 g limonene/kg CO_2, but the data of Chang and Chen (1999) and Gamse and Marr (2000) are ~3 times and ~10 times, respectively, above the general trend. The results of Francisco and Sivik (2002) are questionable because they report limited solubility

of limonene in CO_2 under conditions where the two components are mutually miscible (at 313 K and well above the critical pressure of the CO_2 + limonene mixture). The data are more diverse at pressures >8.5 MPa due to experimental difficulties in measuring solubilities under conditions near the critical point of a mixture.

Figure 17.7 also includes the solubility isotherms at 310 and 318 K of limonene in high-pressure CO_2 predicted using the computer program PE 2000 (Pfohl et al. 2000). PE 2000 models liquid–vapor equilibrium by searching the phase transition corresponding to the bubble-point curve of the CO_2 + limonene system. Phase equilibrium was modeled using the modification of Mathias-Copeman of the Peng-Robinson (PR) equation of state (EoS), or the so-called PR-Mathias-Copeman EoS (Poling et al. 2000), and the first modification (or Modification 1, M1) of the Huron-Vidal (HV) mixing rules with the activity coefficients estimated using UNIFAC, or the so-called MHV1-UNIFAC mixing rules (Poling et al. 2000). The database of PE 2000 included all model parameters for the CO_2 + limonene system. Figure 17.7 shows a reasonable agreement between the predictions of the model and the experimental measurements, including the temperature cross-over at ~8 MPa. This finding is important because the selected model is of a predictive nature, in that the model parameters for the binary system are not estimated using phase equilibrium data; this chapter will expand on the implications of this feature when comparing the solubilities in high-pressure CO_2 of other compounds in Table 17.9.

Table 17.10 compares the solubilities in high-pressure CO_2 of selected solutes from each component family in Table 17.9 to those of limonene, under selected system conditions (313 K and 8 or 9–10 MPa). The density of the CO_2 under the selected system conditions bracket the interval proposed by Reverchon (1997) for SCFE of plant essential oils (250–500 kg/m^3). At the lower end of recommended CO_2 density, ~260 kg/m^3 (at 313 K and 8 MPa), the solubility of limonene in high-pressure CO_2 is approximately 6 g/kg, which is about 50% lower than the solubility of α-pinene reported by Akgun et al. (1999), probably because of the increased volatility (larger vapor pressure) of α-pinene as compared to limonene at 313 K (Table 17.10). The oxygen-bearing functional groups in OMTs increase their molecular weight and polarity, and decrease their vapor pressure as compared to MTs, which causes the solubility of OMTs in high-pressure CO_2 at 313 K and 8 MPa to be about 50% of that of limonene. At the upper end of recommended CO_2 density, ~410 kg/m^3 (at 313 K and 9 MPa), the binary systems of MTs and CO_2 are above their critical points, thus MTs are fully miscible with CO_2. Tufeu et al. (1993) reported the critical points at 314 K of the binary CO_2 + citral (8.76 MPa, 36.4 g citral/kg CO_2) and CO_2 + linalool (8.66 MPa, 11.5 g linalool/kg CO_2) systems, and these critical point values bring into question the limited solubility of citral in high-pressure CO_2 at 313 K and 9 MPa as reported by Benvenuti and Gironi (2001) (Table 17.10). The solubilities in high-pressure CO_2 at 313 K and ~9 MPa of the two OMTs in Table 17.10 (camphor and menthol) are approximately 1 order of magnitude larger than the corresponding solubilities of the ST (β-caryophyllene) and OSTs (artemisinin, farnesol, patchoulol), also included in Table 17.10, which are in turn approximately 2 orders of magnitude above the corresponding solubility

Table 17.10 Solubilities of selected plant essential oil components in high-pressure CO_2 at 313 K and relatively low (approximately 8 MPa) or relatively high pressure (8.6–10 MPa). Essential oil component included representative monoterpene hydrocarbons (limonene and α-pinene) and oxygenated monoterpenes (citral, linalool, and menthol), a sesquiterpene hydrocarbon (β-caryophyllene), an oxygenated sesquiterpene (farnesol), and a hydrocarbon (octacosane)

Compound	Molecular weight (*MW*, Da)	Vapor pressure (P_v, Pa)	Low-pressure			High-pressure		
			Pressure (*P*, MPa)	CO_2 density (ρ, kg/m^3)	Solubility (C_{sat}, mg/g CO_2)	Pressure (*P*, MPa)	CO_2 density (ρ, kg/m^3)	Solubility (C_{sat}, mg/g CO_2)
Limonene (Benvenuti and Gironi 2001)[a]	136.2	515 (Espinosa-Díaz et al. 1999)	8.13	295.6	7.04	9.0	408.4	CM[c]
α-Pinene (Richter and Sovová 1993)	136.2	1,440 (Richter and Sovová 1993)	7.74	252.7	60.1	9.0	408.4	CM
α-Pinene (Akgun et al. 1999)	136.2	1,440 (Richter and Sovová 1993)	7.74	252.7	60.1	–	–	–
Camphor (Akgun et al. 1999)	152.2	133 (Espinosa-Díaz et al. 1999)[b]	7.97	276.1	3.60	8.8	436.1	98.9
Citral (Benvenuti and Gironi 2001) [a]	152.2	30 (Stull 1947)	8.00	261.3	1.30	9.0	408.4	7.66
Linalool (Iwai et al. 1994)	154.2	95 (Espinosa-Díaz et al. 1999)	7.99	278.3	5.27	–	–	–
Menthol (Sovová and Jež 1994)	156.3	<133 (Stull 1947)[b]	7.86	264.3	3.31	9.02	497.9	50.8
β-Caryophyllene (Michielin et al. 2009)	204.4	0.018 (The Good Scents Company 2009a)	–	–	–	8.6	375.9	18.65
Farnesol (Núñez et al. 2010)	222.4	0.192 (The Good Scents Company 2009b)	–	–	–	9.73	609.3	4.29
Octacosane (Chandler et al. 1996)	394.3	~7×10^{-6} (Chandler et al. (1996)	–	–	–	10.0	631.7	0.170

[a]At 315 K
[b]Sublimation pressure
[c]Completely miscible

of a typical wax (*n*-octacosane), 0.015 g/kg CO_2, which is as expected because of the differences in molecular weight (increasing) between OMT compounds, ST/OST compounds, and waxes.

Figure 17.8 expands the results in Table 17.10 to show solubility isotherms of selected compounds in a wider pressure range, together with the estimates of the predictive model in this chapter. In order to use the PR-Mathias-Copeman EoS in PE 2000, an adjustment was made of the so-called model parameters c_1, c_2, and c_3, to vapor pressure data for α-pinene (Daubert and Danner 1989), citral (Hall 2001), linalool (Espinosa-Díaz et al. 1999), β-caryophyllene (Helmig et al. 2003; The Good Scents Company 2009a), farnesol (Helmig et al. 2003; The Good Scents Company 2009b), and *n*-octacosane (Daubert and Danner 1989; Chandler et al. 1996). Other parameters required were the normal boiling point, critical temperature, critical pressure, and acentric factor for the pure compounds. In those cases where no reliable values for these properties were available, values were estimated using group contribution methods. The normal boiling point of *n*-octacosane was

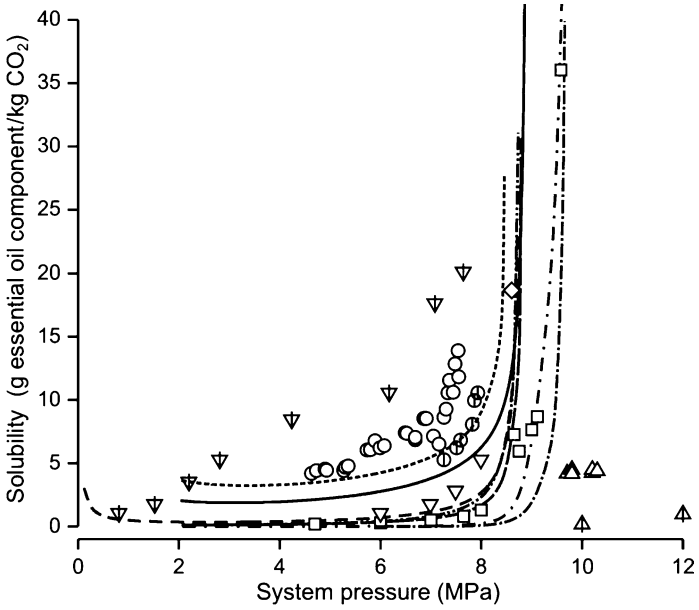

Fig. 17.8 Solubilities of selected plant essential oil components in supercritical CO_2 as a function of system pressure (approximately between 1 MPa and 12 MPa), including (——) limonene at 315.7 K; α-pinene at 313 K, data of (----○) Richter and Sovová (1993) and (----⊕) Akgun et al. (1999); (—-□) citral at 315 K, data of Benvenuti and Gironi (2001); linalool at 313 K, data of (– –▽) Iwai et al. (1994) or (– –▽) Chang and Chen (1999); (–··–◇) caryophyllene at 313 K, data of Michielin et al. (2009); (– · –△) farnesol at 313 K, data of Núñez et al. (2010); and (–··–⏃) octacosane at 313 K, data of Chandler et al. (1996). Lines represent the solubility isotherms at corresponding temperatures predicted by the Peng-Robinson-Mathias-Copeman equation of state with the modified Huron-Vidal (MHV1) – UNIFAC mixing rules using PE 2000 (Pfohl et al. 2000). The solubility isotherm for (——) limonene in supercritical CO_2 at 315.7 K predicted by PE 2000 is included as a reference

estimated using Joback's method (Poling et al. 2000). On the other hand, the critical temperature and critical pressure of citral, linalool, β-caryophyllene, farnesol, and *n*-octacosane were also estimated using Joback's method (Poling et al. 2000), whereas the acentric factor of these same solutes was estimated using the method of Lee-Kesler (Poling et al. 2000). PE 2000 includes all of these group-contribution algorithms for the estimation of physical properties. Figure 17.8 shows that the predictive model implemented in PE 2000 gives values of solubility for typical essential components in high-pressure CO_2 under typical extraction conditions for herbs and spices that are only qualitatively correct; thus, it can be only moderately appropriate for the purpose of discussing equilibrium effects on mass transfer kinetics as attempted in this chapter. An advantage of the method is that it is fully predictive if a group contribution method is applied to estimate the effect of temperature on the vapor or sublimation pressure of the solutes. Obviously, the predictive capabilities of the model improve when including experimental instead of estimated values of relevant physical properties, as suggested by the better fit of the model to experimental solubility data for limonene (Fig. 17.7) than higher molecular solutes such as STs, OSTs, and waxes (Fig. 17.8 compares the experimental data and predicted solubility isotherms for β-caryophyllene, farnesol, and *n*-octacosane).

Differences in solubility between solutes using data for binary CO_2 + solute systems suggest the possibility of selectively recovering a single solute or mixture of solutes in a complex essential oil sample. A general application of this type of fractionation process is the deterpenation of essential oils, which consists of the selective elimination of oxidation-prone and water-immiscible MTs that mask the characteristic aroma of OMTs in an herb or spice, and cause a haze in aqueous essential oil solutions (Stahl et al. 1988; Temelli et al. 1990; Reverchon 1997). Mukhopadhyay and De (1995) proposed the selective recovery of menthol from peppermint oil based on the solubility isotherms at 323 and 343 K of the binary CO_2 + menthol (component 2) and CO_2 + thymol (component 3) systems at pressures ranging from 6.5 to 13.5 MPa. They computed the values of the separation factor between menthol and thymol, R_{23} (17.26), as a function of system temperature and pressure,

$$R_{23} = \frac{y_2}{y_3}, \tag{17.26}$$

and found that $3.37 \leq R_{23} \leq 6.12$, which suggests that it is possible to enrich menthol in the high-pressure CO_2 phase. Mukhopadhyay and De (1995) neglected the molecular interactions between menthol and thymol, which may affect the separation factor, as exemplified next for the separation of limonene and linalool using high-pressure CO_2. It is also important to mention that using the separation factor to draw conclusions about the selective recovery of a component in a binary or multicomponent mixture has limitations in that the analysis should be made by comparing of concentration ratios between the two components in two phases (liquid, SCF) in equilibrium; if these concentration ratios coincide in the two

phases, then it is not possible to selectively recover one of the components using high-pressure CO_2 as the separating agent. Thus, the selectivity of the separation between menthol and thymol, α_{23} (17.27), instead of the separation factor R_{23} should be computed, where:

$$\alpha_{23} = \frac{y_2/y_3}{x_2/x_3} \tag{17.27}$$

Chafer et al. (2001) used composition information from the vapor phase for the ternary CO_2 (1) + limonene (2) + linalool (3) system to estimate the separation factor R_{23} so as to evaluate the possibility of recovering a linalool-enriched fraction. They concluded that the deterpenation of linalool was possible based on R_{23} values of ~2 for mixtures of limonene and linalool containing about 90–95% (mol/mol) of limonene, but also observed that the values of R_{23} were approximately four times higher when estimated on the basis of binary equilibrium data, which reveals a loss of information when solute–solute interactions in the more complex systems are not accounted for. Because of the requirement of ternary data to assess the fractionating capabilities of high-pressure CO_2, this subject is discussed next.

17.4.2 Essential Oil Fractionation in Model (Ternary) Systems and Complex Mixtures

Two CO_2-containing tertiary systems of practical importance that have been extensively analyzed in the literature are CO_2 + limonene + citral and CO_2 + limonene + linalool, because limonene and citral (a mixture of two isomers, geranial and neral) are the key MT and OMT, respectively, in lemon essential oil (Gironi and Maschietti 2008), and linalool replaces citral as the key OMT in orange essential oil (Budich and Brunner 1999). High-pressure CO_2 fractionation allows deterpenation of citrus oils so as to improve their shelf life, solubility in water, and aroma (Stahl et al. 1988; Temelli et al. 1990; Reverchon 1997), and the designing of these two deterpenation processes demands phase equilibria data for the aforementioned model systems (Budich et al. 1999; Gironi and Maschietti 2008).

The phase equilibria of the ternary CO_2 (1) + limonene (2) + citral (3) system was studied by Benvenuti and Gironi (2001) at 315 K and 8.4 or 9.0 MPa, and by Fonseca et al. (2003) at 323 K and 9.5, 9.7, or 10.3 MPa. Fonseca et al. (2003) reported that the selectivity α_{23} for the separation between limonene and citral varied between 1.72 and 2.00, which indicates that the vapor (or CO_2-rich) phase is enriched in limonene, whereas citral remains in the liquid (or essential oil-rich) phase. This agrees with the vapor pressure ratio between limonene and citral, ${P_2}^{Sat}/{P_3}^{Sat} = 17$ (Benvenuti and Gironi 2001), which defines separation under low-solubility (relatively small pressure) conditions. The selectivity α_{23} did not depend on system pressure (9.5–10.3 MPa), nor the composition of the essential oil model mixture (49–73% w/w limonene) (Fonseca et al. 2003). On the other hand, values of

α_{23} estimated by Benvenuti and Gironi (2001) at 315 K ranged from 1 to 62 depending on the limonene content in the CO_2-rich phase and the system pressure (limonene content in a CO_2-free basis ranged 36–90% mol/mol at 8.4 MPa, and 26–74% mol/mol at 9 MPa).

The vapor–liquid equilibria of the CO_2 (1) + limonene (2) + linalool (3) ternary system has been studied by Morotomi et al. (1999) at 313 K and 6.9 MPa, 333 K and 6.9 MPa, or 333 K and 10.0 MPa, by Vieira de Melo et al. (1999) at 323 K and 7.54, 8.08, 8.76, or 8.90 MPa, and by Chafer et al. (2001) at 318 or 328 K, pressures between 7 and 11 MPa, and mixtures having 40% or 60% (w/w) limonene in a CO_2-free basis. The selectivity for the separation between limonene and linalool is $\alpha_{23} > 1.2$ (Morotomi et al. 1999), which suggests the possibility of enriching limonene in the vapor phase, thus making the isolation of linalool in the liquid phase feasible, particularly in essential oil mixtures enriched in oxygenated compounds. Vieira de Melo et al. (1999) reported that α_{23} decreases from 3.75 to 2.14 as the pressure increases from 7.54 to 8.90 MPa, probably as a result of the increase in the solvent power of high-pressure CO_2 for OMTs. The apparent selectivity at 323 K and 8 MPa based on binary data ($\alpha_{23} = 4.6$) was larger than the true selectivity based on ternary data ($\alpha_{23} = 3.6$), thus confirming the need for ternary equilibrium data for the design of deterpenation process (Vieira de Melo et al. 1999). Chafer et al. (2001) reported the composition of the vapor phase only; thus, it was not possible to estimate values of selectivity for the separation of limonene and linalool based on their data.

The use of model systems with a limited number of components is appropriate only as a rough estimate of the behavior of more complex natural mixtures. Because of that, Budich and Brunner (1999) and Budich et al. (1999) recommended the estimation of separation factors and other design parameters for the high-pressure CO_2 deterpenation process by using actual essential oil mixtures. Cold-pressed orange oil is constituted by about 200 components, mainly MTs (~95% w/w) and OMTs. Temelli et al. (1990) measured the solubility in CO_2 of this oil at 313, 323, 333, and 343 K and 8.3, 9.7, 11.0, and 12.4 MPa using a one-pass dynamic method. Experimental results confirmed that CO_2 preferably solubilizes MTs so that the selectivity α_{23} for the separation between limonene (2) and linalool (3), the key components in the MT and OMT fractions, respectively, ranged from 1.10 to 2.83 within the experimental region. Under isothermal conditions, α_{23} reached a maximum at 9.7 MPa and then decreased to a minimum at 12.4 MPa. Temelli et al. (1990) also reported an unusual increment in solubility at 313 K and 12.4 MPa, which they attributed to the formation of a liquid phase, a common occurrence in systems of high-pressure CO_2 and complex liquid mixtures.

Budich and Brunner (1999) studied the equilibrium of CO_2 + orange peel oil at 323, 333, or 343 K and 8–13 MPa. For data analysis they assumed orange peel oil as a binary mixture of 98.25% (w/w) terpenes (*T*, 96.7% w/w limonene) and 1.75% (w/w) oxygenated aroma compounds (*A*, 28.8% w/w linalool). The solubility of the essential oil in high-pressure CO_2 was similar to that of pure limonene, probably because of the elevated content of limonene in orange peel oil. The selectivity α_{TA} ranged from 1.3 to 3.2, which suggests the possibility of

removing the MT fraction using high-pressure CO_2. Under isothermal conditions, α_{TA} decreases as the pressure increases. For low-solubility values (<10 g extract/kg CO_2) α_{TA} decreases with temperature under isobaric conditions because of a more limited increase in the vapor pressure of the OMTs than MTs; for high-solubility values (>50 g extract/kg CO_2) α_{TA} increases with temperature due to the reduction in the density and solvent power of the CO_2; in the intermediate range (10–50 g extract/kg CO_2) there is not a definite trend for the variations in α_{TA} with temperature.

Figure 17.9 compares the values of selectivity measured by Budich et al. (1999) for the multicomponent CO_2 + orange peel oil system at 323 and 333 K with those reported for the CO_2 + limonene + citral or CO_2 + limonene + linalool model systems. For all temperature-solubility pairs, $\alpha_{23} < \alpha_{TA}$, e.g., at 323 K the values of α_{23} reported by de Vieira de Melo et al. (1999) are 25% of the values of α_{TA}, whereas the values of α_{23} reported by de Fonseca et al. (2003) are ~40% of the values of α_{TA}, and at 333 K Morotomi et al. (1999) report values of α_{23} ranging from 16% to 51% of corresponding values of α_{TA} at 333 K. Budich et al. (1999) reported that values of α_{TA} at 333 K and 10 MPa decreased pronouncedly as the content of terpenes in the liquid phase increased, or when replacing the real OMT fraction (α_{TA} ~ 2.2 for a 98.3% w/w MT content in the liquid phase) by pure

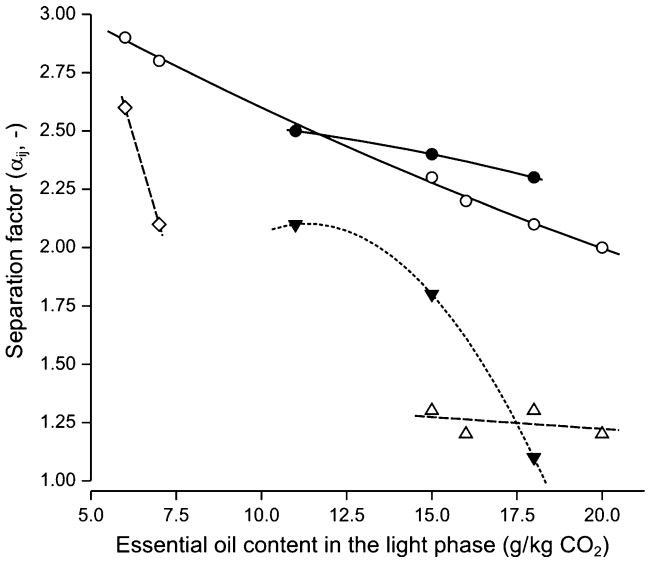

Fig. 17.9 Separation factors between terpenes and aroma (oxygenated) compounds in model and real systems as a function of essential oil concentration in the CO_2 phase: α_{23} for the separation at 323 K of limonene and linalool in a ternary CO_2 + limonene + linalool system reported by (--◇--) Vieira de Melo et al. (1999) and (--△--) Morotomi et al. (1999); (···▼···) α_{23} for the separation at 333 K of limonene and citral in a ternary CO_2 + limonene + citral system (Fonseca et al. 2003); and α_{TA} for the separation at (—○—) 323 K or (—●—) 333 K between terpene and aroma (oxygenated) compounds in orange peel oil (Budich et al. 1999)

linalool ($\alpha_{TA} \sim 1.2$). This result is consistent with the value $\alpha_{23} \sim 1.1$ reported by Morotomi et al. (1999) for the model limonene + linalool system containing 85% w/w MT in the liquid phase. Based on data in Fig. 17.9, Budich et al. (1999) recommended deterpenation of orange oil at $\geq$ 333 K, where both α_{TA} (=1.5) and the solubility of the oil in high-pressure CO_2 are high enough to make the process economical.

17.4.3 Thermodynamic and Operational Solubility in the CO_2 Extraction of Essential Oils

There have been few publications on high-pressure phase equilibria between CO_2 and complex mixtures other than those of Temelli et al. (1990) with cold-pressed orange oil, and those of Budich and Brunner (1999) with orange peel oil. Reported equilibrium isotherms include those of clove bud oil at 303, 308, 313, 318, and 328 K for 5.8–10.8 MPa (Souza et al. 2004); of fennel seed oil at 303, 313, 323, and 333 K for 4.74–21.0 MPa (Moura et al. 2005); of vetiver (*Vetiveria zizanioides*) root oil at 303, 318, and 333 K for 5–30 MPa (Takeuchi et al. 2008); of candeia (*Eremanthus erythropappus*) bark oil at 313, 323, and 333 K for 6.27–25.2 MPa (Teixeira de Souza et al. 2008); and of priprioca (*Cyperus articulatus*) rhizome oil at 313, 323, and 333 K and 4.42–29.9 MPa (Moura et al. 2005). These measurements are usually performed using synthetic methods (Sect. 17.4.1), and are difficult to set up, in that bubble and dew or cloud points are not easily visually identified for complex mixtures of CO_2 and natural extracts. With the exception of vetiver root and priprioca rhizome, these studies complement other studies on SCFE (Table 17.1). Furthermore, besides assisting the analysis of the extraction process, the results of these studies can help to optimize the condition of the separation step of the entire SCFE process. Indeed, the high-pressure phase equilibrium for complex CO_2 + essential oil systems under typical separation conditions in a SCFE plant (e.g., 273–288 K and 2–9 MPa, Reverchon and De Marco 2008) determines the residual solute content in a recycled CO_2 stream, which affects the extraction rate (del Valle et al. 2004), as well as the residual content of CO_2 in the extract, which affected solvent losses during the process (Takeuchi et al. 2008).

Table 17.11 presents the solubilities of essential oil extracts of orange peel, clove bud, fennel seed, and candeia bark under selected temperature and pressure conditions, as taken from the publications of Budich and Brunner (1999), Souza et al. (2004), Moura et al. (2005), and Teixeira de Souza et al. (2008), respectively. Specifically referred to are the values from the *P-y* branch of isotherms in equilibrium diagrams under the conditions where only two phases (a CO_2-rich vapor phase and an essential oil-rich liquid phase) were at equilibrium, which forced the neglect of many data points under conditions where the authors reported partial liquid miscibility. Liquid immiscibility conditions in complex systems result from

Table 17.11 Comparison of estimated thermodynamic solubility and operational solubility for selected studies on high-pressure CO_2 extraction of plant essential oils

Extract	Temperature (T, K)	Pressure (P, MPa)	Solubility (C_{sat}, mg solute/g CO_2)
Orange peel oil			
Limonene (Iwai et al. (1994)	313	7.17	6.2
Linalool (Iwai et al. 1994)	313	7.17	2.1
Model oil mixture[a]	313	7.17	6.0
Actual essential oil (Budich and Brunner 1999)	313	7.17	5.1
Actual essential oil (Budich and Brunner 1999)	313	15	CM*
Ibid. in the presence of substrate (Mira et al. 1996, 1999)	313	15	13.2–19.3
Clove oil			
Eugenol (Cheng et al. 2000)	313	8.06	5.6
β-Caryophyllene (Stahl et al. 1988)	313	8.06	2.3
Model oil mixture[b]	313	8.06	5.0
Actual essential oil (Souza et al. 2004)	313	8.06	11
Ibid. in the presence of substrate (Martínez et al. 2007)	308	10	230
Fennel oil			
Limonene (Iwai et al. 1994)	313	8.02	9.6
Anethole (Stahl et al. 1988)	313	8.02	6
Model oil mixture[c]	313	8.02	5
Actual essential oil (Moura et al. 2005)	313	8.02	26
Ibid. in the presence of substrate (Reverchon et al. 1999)	313	9	2
Candeia oil			
Actual essential oil (Teixeira de Souza et al. 2008)	313	6.17	111
Ibid. in the presence of substrate (Teixeira de Souza et al. 2008)	313	10	4.5

[a]Ideal solubility estimated neglecting interactions between solutes and assuming orange peel oil as a mixture of 98% (w/w) limonene and 2% (w/w) linalool
[b]Ideal solubility estimated neglecting interactions between solutes and assuming clove oil as a mixture of 86% (w/w) eugenol and 14% (w/w) β-caryophyllene
[c]Ideal solubility estimated neglecting interactions between solutes and assuming fennel oil as a mixture of 9% w/w limonene and 91% w/w anethole
*Complete miscibility between the essential oil and high-pressure CO_2

interactions between minor components in the essential oil mixture, and those interactions have large effects on the actual equilibrium. One such effect is a limited dependence on temperature of the equilibrium concentration of the essential oil in the high-pressure CO_2-rich phase. Another effect is unusual variations in essential oil solubility as a function of system temperature and pressure, such as the increase in solubility of cold-pressed orange oil in high-pressure CO_2, as reported by Temelli et al. (1990) at 313 K and 12.4 MPa. Taking further advantage of equilibrium data of essential oils in high-pressure CO_2 collected up to now demands more detailed experimental evidence.

The thermodynamic solubility values reported in Table 17.11 are different from those expected based on measurements for model binary systems of CO_2 and the main MT, OMT, and ST/OST in the actual essential oils. The belief here is that this

finding is due to the effect of minor components in the essential oils which, as mentioned before, interact with each other and the major components in the mixture, thus strongly affecting the equilibrium, as exemplified in the following paragraph.

In general, the solubility of a particular substance in high-pressure CO_2, such as MT or OMT, may be affected by the presence of other substances in the natural product, such as a wax or a triglyceride, which may exhibit a higher or lower solubility in the CO_2. The example of a major MT and a wax is relevant in the particular case of essential oils because, as previously mentioned, they are usually encapsulated within specialized wax-made structures that serve a protective function in herbs (Gaspar et al. 2001). Sovová et al. (2001) reported high-pressure phase equilibria data for a ternary CO_2 + limonene + blackcurrant oil system at 313 K and 8–12 MPa, and showed that the solubility of limonene in high-pressure CO_2 decreased in the presence of triglycerides for pressures up to 20% higher than the critical pressure of the CO_2 + limonene binary mixture ($P_{cm} = 8.44$ MPa).

17.4.4 Operational Solubility and Sorption Phenomena in the CO_2 Extraction of Essential Oils

Figure 17.1b defines the "operational" solubility of plant essential oils as the concentration of the essential oil in high-pressure CO_2 at the outlet of the extraction vessel, provided that CO_2 and the herb or spice reach equilibrium conditions as the CO_2 travels along the vessel, and there is some free solute in the substrate. The initial slope of the cumulative plot of solute yield versus specific CO_2 consumption may represent the actual "operational" solubility only if extraction is preceded by an initial static period to achieve steady temperature and pressure conditions and equilibration between the substrate and the high-pressure CO_2. Table 17.11 shows that the operational solubility (in the presence of the solid substrate) of selected essential oils in high-pressure CO_2 is smaller than the thermodynamic solubility (in the absence of the solid substrate) under equivalent conditions, probably due to binding of the essential oils to the solid matrix or an insufficient amount of essential oils in the herb or spice to saturate the CO_2 (del Valle et al. 2005; Sovová 2005).

Figure 17.10 shows selected values of operational solubility C_{fo} as a function of the ratio between C_{so} and ρ, together with trend lines that can be explained on the basis of either limited availability of the essential oil in the solid matrix or a sufficient amount to saturate the high-pressure CO_2 phase in a case where the essential oil is not bound to the solid matrix. If the porosity of an extraction vessel with an inner volume V packed with a milled herb or spice of inner porosity ε_p is ε, the vessel will contain $V\,[\varepsilon + (1 - \varepsilon)\,\varepsilon_p]\,\rho$ of high-pressure CO_2 at system temperature and pressure (at those conditions the density of the CO_2 is ρ). If the substrate loaded in the extraction vessel (a total weight $V\,(1 - \varepsilon)$

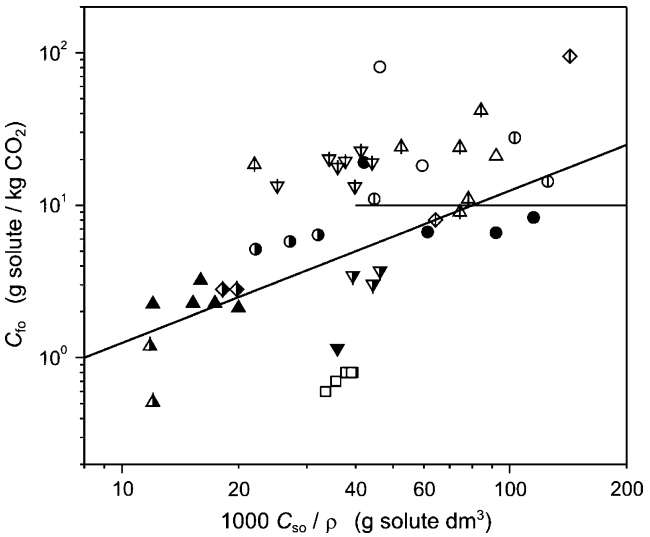

Fig. 17.10 Best-fit values of operational solubility of essential oils in high-pressure CO_2 as a function of the initial essential oil content in the herb or spice. Plotted values include substrates with light essential oils ($v_c \leq 550$ cm^3/mol) extracted with low-density ($\rho \leq 650$ kg/m^3) CO_2 –(○) caraway (Sovová et al. 2004), (△) nutmeg (Machmudah et al. 2006), and (□) sage (Langa et al. 2009) – or high-density ($\rho > 650$ kg/m^3) CO_2 – orange peel (Mira et al. 1996, 1999), (◭) nutmeg (Spricigo et al. 2001; Machmudah et al. 2006), (▽) alecrim pimenta (Sousa et al. 2002), and (◍) aniseed (Rodrigues et al. 2003), as well as substrates with heavy essential oils ($v_c > 550$ cm^3/mol) extracted with low-density ($\rho \leq 650$ kg/m^3) CO_2 –(▼) chamomile (Povh et al. 2001), (●) carqueja (Vargas et al. 2006), and (▲) valerian (Zizovic et al. 2007a) or high-density ($\rho > 650$ kg/m^3) CO_2 (▼) chamomile (Povh et al. 2001), (◑) ginger (Martínez et al. 2003), (◆) marigold (Campos et al. 2005), and (▲) valerian (Zizovic et al. 2007a)

ε_p ρ_s, where ρ_s is the true density of the solid matrix) initially contains a concentration C_{so} of essential oil in a solute-free basis, in a situation where there is not enough solute to saturate the CO_2 following a static extraction period, (17.28) defines the operational solubility:

$$C_{fo} = \frac{1}{\frac{1}{\varepsilon_p}\left(\frac{\varepsilon}{1-\varepsilon}\right) + 1} \frac{\rho_s}{\rho} C_{so} \tag{17.28}$$

where the term $\varepsilon/(1 - \varepsilon)$ represents the ratio of interparticle void volume to apparent particle volume. Equation 17.28 suggests that a plot of C_{fo} versus (C_{so}/ρ) (Fig. 17.10) will result in a straight line with a slope m (17.29):

$$m = \frac{\rho_s}{\frac{1}{\varepsilon_p}\left(\frac{\varepsilon}{1-\varepsilon}\right) + 1} \tag{17.29}$$

On the other hand, if there is enough solute to saturate the CO_2 phase (C_{so}/ρ large), C_{fo} will reach an asymptotic value C_{sat} (the thermodynamic solubility of the complex essential oil mixture in the CO_2 under process conditions). It is difficult to compute the slope m in the absence of precise measurements of the bed porosity (ε), the interparticle porosity (ε_p), and the true density of the matrix (ρ_s), which may vary depending on the substrate and its pretreatment, but the data in Fig. 17.10 were plotted under the simplifying assumption that m changes little between substrates. Regarding the horizontal asymptote, it is important to stress that C_{sat} is a strong function of the essential oil mixture and the system conditions characterized by the temperature and density of the CO_2 (Chrastil 1982).

Figure 17.10 presents selected data that follow the trend suggested by the hypothesis of limited solute in a noninteracting solid matrix. A log–log plot was made to allow a wide range of experimental values in a single plot, and under those conditions a linear relationship such as (17.28) (power relationship with an exponent one) follows a straight line with a unitary slope (such as the trend line included in Fig. 17.10 for values of C_{so}/ρ below 0.05 g dm^3). Fig. 17.10 includes essential oils with relatively low values of critical volume ($V_c \leq 550$ cm^3/mol) enriched in monoterpene hydrocarbons, oxygenated monoterpenes, and related compounds such as those of aniseed, caraway, alecrim pimenta, nutmeg, orange peel, and sage, and extracts with larger values of critical volume ($V_c > 550$ cm^3/mol) that are instead enriched in heavier sesquiterpenes, waxes, and related compounds, such as the extracts of carqueja, chamomile, ginger, marigold, and valerian. Apparently, heavy extracts and essential oils behave the same for low solute contents ($C_{so}/\rho \leq 0.05$ g dm^3) in the solid matrix, as expected; only for high solute contents ($C_{so}/\rho > 0.05$ g dm^3) do the values for heavy extracts level off to an apparent solubility of $C_{sat} \sim 10$ g/kg. Another trend that is apparent in Fig. 17.10 is that the values of C_{fo} for low CO_2 density ($\rho \leq 650$ kg/m^3) tend to be below the values C_{fo} for higher CO_2 densities ($\rho > 650$ kg/m^3), particularly in the upper end of values of C_{so}/ρ, as expected for an increase in solubility with the solvent power of CO_2.

Table 17.12 complements Fig. 17.10, providing values of operational solubility (C_{fo}) reported from studies in Table 17.2 reviewed in this chapter. The data in Fig. 17.10 exhibit scattering because of variations in substrates and their pretreatments, extraction temperatures, and CO_2 densities that are not fully accounted for in the plot, and some additional values in Table 17.12 are not fully consistent with the aforementioned trends. Of all single-measurement C_{fo} values reported in Table 17.12 (boldo, cinnamon of Cunha, fennel, oregano, and pennyroyal), only the one for pennyroyal does not follow the general trends in Fig. 17.10. In the case of rosemary, the data of Coelho et al. (1997) and Bensebia et al. (2009) are inconsistent, and only the C_{fo} values of Coelho et al. (1997), higher, follow the trend lines in Fig. 17.10. The data on clove by Ruetsch et al. (2003) and Martínez et al. (2007) are outside (above and/or to the right) the upper limits selected for Fig. 17.10 and are inconsistent; only the C_{fo} values of Martínez et al. (2007) follow the general trends in Fig. 17.10. The data of Perakis et al. (2005) on black pepper, to the right of the upper limit of C_{so}/ρ (> 0.05 g m^3) in Fig. 17.10, are only slightly below the top

Table 17.12 Summary of operation solubility values in high-pressure CO_2 extraction of plant essential oils studies from Tables 17.1 and 17.2, as a function of the extraction conditions and the initial solute content of the substrates

Substrate	Temperature (T, K)	CO_2 density (ρ, kg/m^3)	Initial solute content (C_{so}, mg solute/g solute-free)	Operational solubility (C_{fo}, mg solute/g CO_2)
Clove (Martínez et al. 2007)	306	713	157	230
Clove (Ruetsch et al. 2003)	323	581	212	34.0
Clove (Ruetsch et al. 2003)	323	288	212	2.50
Orange peel (Mira et al. 1996)	323	700	100.0	95.0
Orange peel (Mira et al. 1996)	323	700	45.0	8.00
Black pepper (Ferreira and Meireles 2002)	313	780	35.8	93.2
Black pepper (Ferreira et al. 1999)	303, 323	698, 847	35.8	89.0–85.8
Black pepper (Ferreira et al. 1999)	303–323	698–847	14.7	35.3–24.2
Black pepper (Perakis et al. 2005)	313, 323	384–780	92.0–155	3.80–2.50
Caraway (Sovová et al. 1994a)	313	623	28.8	80.9
Caraway (Sovová et al. 1994a)	313	484	28.8	18.2
Nutmeg (Spricigo et al. 2001)	296	819	18.0–69.0	67.5
Nutmeg (Machmudah et al. 2006)	313–323	629–780	58.0	24.0–9.00
Parsley (Louli et al. 2004)	318	742	650	33.0
Parsley (Louli et al. 2004)	308, 318	498, 713	120	8.302.80
Cinnamon of Cunhã (Sousa et al. 2005)	288	851	38.5	28.3
Aniseed (Rodrigues et al. 2003)	313	700–836	31.3–105	27.7–11.0
Alecrim pimenta (Sousa et al. 2002)	283–298	728–891	22.4–34.0	22.7–13.2
Carqueja (Vargas et al. 2006)	313–343	208–486	17.5–24.0	19.1–6.60
Celery (Papamichail et al. 2000)	348, 328	498–742	500	8.31–2.12
Celery (Papamichail et al. 2000)	318	498	62.0	2.12
Ginger (Martínez et al. 2003)	293–313	847–905	20.0–25.0	6.41–5.15
Chamomile (Povh et al. 2001)	303, 313	623–809	22.4–34.2	3.71–1.15
Valerian (Zizovic et al. 2007a)	313, 323	384–780	6.14–12.6	3.22–0.511
Marigold (Campos et al. 2005)	313	718, 780	14.2	2.80
Fennel (Reverchon et al. 1999)	323	288	18.3	2.00
Rosemary (Coelho et al. 1997)	308, 313	629–777	7.05	1.98–1.65
Rosemary (Bensebia et al. 2009)	313, 333	290–780	32.0	0.356–0.238
Boldo (Uquiche et al. submitted)	313	632	13.1	1.75
Pennyroyal (Reis-Vasco et al. 2000)	323	384	25.3	1.16
Sage (Langa et al. 2009)	313, 323	384, 486	12.9–19.2	0.800–0.600
Lavender (Akgun et al. 2000)	323	220–670	15.3	0.418–0.234
Oregano (Uquiche et al. submitted)	313	632	6.02	0.390

solubility $C_{sat} \sim 10$ g/kg for heavy extracts. Finally, the data of operational solubility C_{fo} of Ferreira et al. (1999) and Ferreira and Meireles (2002) for black pepper are irregularly high, whereas the data of initial solute content C_{so} of Papamichail et al. (2000) for celery and of Louli et al. (2004) for parsley are too high, considering the typical amount of extractible compounds in those substrates (Moyler 1993).

Goto et al. (1998) showed that the operational solubility of menthol (the main component in the essential oil of mint leaves) is smaller than its thermodynamic solubility in high-pressure CO_2 at 313 K and 13.6 MPa, and suggested that the transfer of menthol to the CO_2 phase was limited by strong interactions between the essential oil and solid matrix. They also claimed weaker interactions between *n*-triacontane (the main component in the cuticular waxes of mint leaves) with the solid matrix than between menthol and the solid matrix because the operational solubility of *n*-triacontane was closer to its thermodynamic solubility than the operational solubility of menthol. As shown in Sect. 17.4.3, solute–solute interactions between the components of the mint leaf extract may be partially responsible for a reduction in the apparent solubilities of menthol and *n*-triacontane in CO_2 when they are a part of a complex essential oil mixture as compared with their corresponding thermodynamic solubilities in the binary CO_2 + menthol or CO_2 + *n*-triacontane systems, but this does not negate the possibility of a reduction in their apparent solubility due to some additional interactions between the solutes and the solid matrix.

The effect of solute binding by the solid matrix, which affects solute availability in SCFE, can be accounted for by an equilibrium sorption isotherm that relates the concentration of solute in the high-pressure CO_2 phase with the residual content of solute in the solid phase (the pretreated herb or spice) under equilibrium conditions. Some authors hypothesize that the operational solubility C_{fo} depends on the substrate and extraction conditions, but does not depend on the solute content in the substrate, as reported in Table 17.12. Other authors hypothesize a constant partition coefficient K (17.20) for essential oils between the high-pressure CO_2 phase and the solid phase, which may correspond to a linear sorption isotherm (17.30a), derived from (17.20) or the initial slope of another sorption isotherm model for a low essential oil content in the pretreated herb or spice, such as the Freundlich (17.30b), Langmuir (17.30c), or Brunauer-Emmett-Teller (BET, (17.30d) models. Finally, selected authors combine the possibility of a constant C_{sat} for large concentrations of essential oil in the solid matrix ($C_{so} > C_{lim}$) and a constant partition coefficient for smaller values of C_{so} ($\leq C_{lim}$) using the so-called isotherm of Perrut et al. (1997). Table 17.13 summarizes the values of the linear partition coefficient K (or equivalent partition coefficient, (17.31)), as reported in studies from Table 17.2 reviewed in this chapter.

The mathematical models for the linear, Freundlich, Langmuir, and BET's sorption isotherms are, respectively, as follows:

$$\bar{C}_s = \frac{C_f}{K} \tag{17.30a}$$

Table 17.13 Summary of values of solute partition coefficients in high-pressure CO_2 extraction of plant essential oils in studies from Tables 17.1 and 17.2, as a function of the extraction conditions and the initial solute content of the substrates

Substrate	Temperature (T, K)	CO_2 density (ρ, kg/m^3)	Initial solute content (C_{so}, mg solute/g solute-free)	Solute partition coefficient (K, –)
Cinnamon of Cunhã (Sousa et al. 2005)	288	851	38.5	2.38–2.00
Carqueja (Vargas et al. 2006)	313	486	20.4	0.813
Carqueja (Vargas et al. 2006)	323	285	17.5	0.694
Carqueja (Vargas et al. 2006)	333	235	21.7	0.104
Carqueja (Vargas et al. 2006)	343	208	24.0	0.067
Clove (Ruetsch et al. 2003)	323	288, 581	212.1	0.314
Clove (Daghero et al. 2004)	323	288, 581	212.1	0.022–0.008
Nutmeg (Machmudah et al. 2006)	313	780	58.0	0.300–0.150
Nutmeg (Machmudah et al. 2006)	323	700, 780	58.0	0.300–0.100
Nutmeg (Machmudah et al. 2006)	318	742	58.0	0.200
Boldo (Uquiche et al. submitted)	313	632	13.1	0.134
Parsley (Louli et al. (2004)	308	713	120	0.067[a]
Parsley (Louli et al. (2004)	318	498, 742	650, 120	0.051–0.023[a]
Parsley (Louli et al. (2004)	308	713	63	0.0099[b]
Parsley (Louli et al. (2004)	318	498, 742	63, 450	0.0076–0.0038[b]
Celery (Papamichail et al. 2000)	328	654	500	0.0605[a]
Celery (Papamichail et al. 2000)	318	498, 742	63, 270	0.0585–0.0471[a]
Celery (Papamichail et al. 2000)	328	654	417	0.0046[b]
Celery (Papamichail et al. 2000)	318	498, 742	417, 476	0.0041–0.00001[b]
Oregano (Uquiche et al. submitted)	313	632	6.02	0.0647
Peppermint (Goto et al. 1993)	313	445, 777	–	0.0506–0.0202
Peppermint (Goto et al. 1993)	333	228, 594	–	0.0331–0.0113
Peppermint (Goto et al. 1993)	353	184, 415	–	0.0248–0.0066
Sage (Langa et al. 2009)	313	486	17.3–19.2	0.047–0.042
Sage (Langa et al. 2009)	323	384	12.9	0.033
Black pepper (Perakis et al. 2005)	313	486, 629	93.0, 134.0	0.0090–0.0025
Black pepper (Perakis et al. 2005)	323	384	84.0	0.0063
Pennyroyal (Sovová 2005)	323	384	25.3	0.063

[a]Sovová's model, model R-SO
[b]Model LDF-UENA

$$\bar{C}_s = \frac{(C_f)^n}{k} \tag{17.30b}$$

$$\bar{C}_s = \frac{k\, C_m C_f}{1 + k\, C_f} \tag{17.30c}$$

$$\bar{C}_s = \frac{k\, C_m C_f}{(C_{sat} - C_f)[C_{sat} + (k-1)C_f]} \tag{17.30d}$$

where k and n are empirical sorption energy parameters, and C_m (the so-called monolayer coverage of the solid surface) is the maximal amount of essential oil that can hold the solid matrix. Ruetsch et al. (2003) and Daghero et al. (2004) arbitrarily assumed that the monolayer coverage corresponded to the initial solute content ($C_m = C_{so}$) in clove. The sorption isotherm models (17.30a–17.30d) are written with C_s instead of C_f as the independent variable because they are adapted from the literature on adsorptive separations. In adsorptive separation processes, where the solute in a fluid phase transfers to a solid phase, there is no upper limit to solute concentration in the fluid phase (for all practical purposes, solute and mobile or fluid phases are mutually miscible), and eventual saturation of the solid matrix imposes an upper limit on the concentration of the solute in the solid for high concentration in the fluid under equilibrium conditions. Depending on the herb or spice and its pretreatment, this upper limit in concentration of solute in the solid substrate is not reached when the concentration of the essential oil in the CO_2 is limited by its solubility under process conditions. Because of that, Ruetsch et al. (2003), Daghero et al. (2004), and Salimi et al. (2008) imposed an upper limit ($C_f \leq C_{sat}$) to the value of solute concentration in the CO_2 phase for high concentrations of solute in the solid phase (Fig. 17.11). Equation 17.31 defines the limit value of K for small value of C_s ($C_s \to 0$) for both Langmuir's and BET's sorption isotherm models (Frendlich's isotherm model predicts limit values, $K = 0$ for $n > 1$ and $K \to \infty$ for $n < 1$):

$$K = \frac{1}{k\, C_m} \tag{17.31}$$

Observation did not reveal special trends in values of the linear partition coefficients (Table 17.13) as a function of the substrate and its essential oil content, the temperature of the system, or the density of the CO_2 (plots not shown). Based on (17.28) for a noninteracting solid matrix, for a packed bed with porosity $\varepsilon = 0.6$, a solid substrate with true density $\rho_s = 1{,}000$ kg/m^3, an inner porosity $\varepsilon_p = 0.1$, and high-pressure CO_2 at 323 K and 9 MPa ($\rho = 287.5$ kg/m^3), the expected value of the partition coefficient in a situation of limited essential oil content in the plant material would be $K = 0.222$, which is between upper and lower limit values reported in Table 17.13. No evidence was found that K increases as the initial essential oil content in the herb or spice increases. Also, no evidence was found that

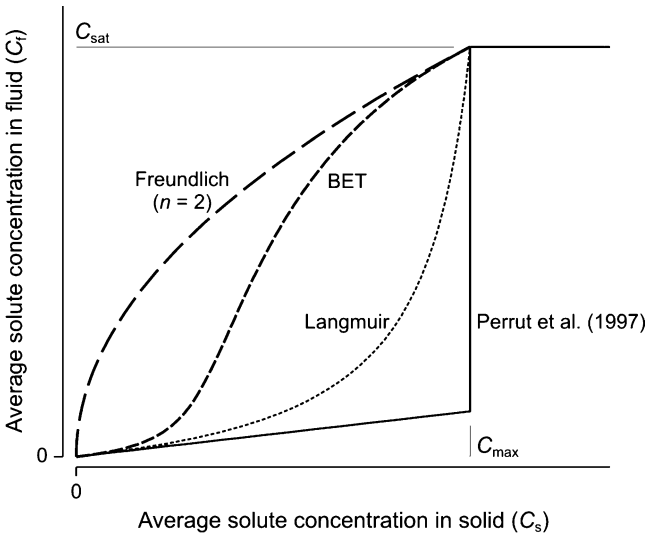

Fig. 17.11 Sorption isotherm models for equilibrium partition of essential oil between high-pressure CO_2 and an herb or a spice as a function of the solute content in the substrate under equilibrium conditions at constant system temperature and pressure

K decreases as the density of the CO_2 increases, as expected (a comparison of (17.28), (17.29), and (17.30a) suggests that $K = m/\rho$ for a situation where the essential oil does not interact with the solid matrix).

17.5 Concluding Remarks

This chapter reviewed mass transfer and phase equilibrium parameters that can be used to design industrial SCFE processes for plant essential oils. Relevant mass transfer parameters include an axial dispersion coefficient (D_{ax}) for the migration of the solute in the SCF along the bed; an external mass transfer coefficient (k_f) for its movement through the stationary SCF film surrounding the solid particles; and an effective diffusivity (D_e) for its movement through the solid matrix, which were computed in the form of a so-called microstructural factor (F_M). This review suggests neglecting axial dispersion effects to simplify the mass transfer models.

Based on this review, it is recommended that SCFE experiments be carried out under forced convection conditions, and that the external mass transfer coefficient (k_f) be estimated using a literature-based correlation between dimensionless variables valid for mass transfer in packed beds operating with SCFs. Best-fitting usually provides underestimations of k_f because of the underestimation of internal resistances to mass transfer, overestimation of the specific surface of the solid

substrate, neglecting of solvent flow heterogeneity effects when using a small D/d_p ratio, and/or neglecting of natural convention effects when using low-*Re* flow conditions.

The values of the microstructural factor for inner mass transfer in the herb or spice estimated in this chapter ranged from $F_M = 10^2$ to $F_M = 10^5$, which suggested pronounced limitations to mass transfer within the solid matrix in the high-pressure CO_2 extraction of plant essential oils. The estimated values of F_M, unlike those expected, depended on the system (temperature, pressure) conditions, the superficial velocity of the CO_2, and/or the particle size of the substrate. Furthermore, for equivalent experiments, the best-fit values of F_M changed dramatically depending on the applied mathematical model, which raised questions about the validity of some of the hypotheses of these mass transfer models. To improve the modeling of high-pressure CO_2 extraction of plant essential oils, extraction experiments should be complemented by measurements using microscopy and allied/complementary techniques to fully characterize the pretreated solid matrix at a relevant scale (Aguilera and Stanley 1999; Zizovic et al. 2005, 2007a, b, c; Stamenić et al. 2008). Such measurements would result in microstructure– extractability relationships, which could be taken advantage of to optimize the pretreatment of the herb or spice samples prior to SCFE.

Regarding phase equilibrium data for designing industrial SCFE processes for plant essential oils, the conclusion here is that their "operational" solubility in high-pressure CO_2 depends markedly on the availability of the solute (the complex essential oil mixture) and its partition between the solid matrix (the herb or spice) and the SCF. The reviewed literature included several phase equilibrium studies using binary systems CO_2 + pure essential oil (mainly MT and OMT) component, few studies using ternary CO_2 + limonene + citral/linalool systems, and limited studies using CO_2 and complex essential oil mixtures (low-pressure CO_2 extracts of herbs or spices). Further advancements in this field will require additional fluid phase equilibrium measurements using binary mixtures of CO_2 and ST or OST compounds, CO_2 + MT + OMT model ternary mixtures representing plant essential oils other than citrus oils, or CO_2 + complex essential oil mixtures. Furthermore, given that the "operational" solubility of essential oils in high-pressure CO_2 does not depend solely on thermodynamic solubility, quantifying the effect of the availability and binding of the solute to the herb or spice demands additional measurements of the solid-SCF phase equilibrium in addition to the aforementioned fluid phase equilibrium data. Because there is no real evidence in the literature that the solute partition between the solid substrate and the SCF is constant, sorption isotherms should be experimentally measured instead of assuming a sorption pattern and achieving best-fit model parameters as part of the data analysis process.

Acknowledgments The present work was funded by the Chilean agency Fondecyt (Regular project 105–0675 and International Cooperation project 703–0033). We are indebted to Verónica Glatzel (PUC) for recalculating from the literature some of the values of external mass transfer coefficient (k_f), and effective diffusivities (D_e) that we report in Sect. 17.3.2 and 17.3.3, respectively; and to Gustavo Lozano (TUHH) for simulating the solubility isotherms for selected

essential oil components included in Figs. 17.7 and 17.8 using the predictive methodology described in Sect. 17.4.1 in PE 2000.

References

Aghel N, Yamini Y, Hadjiakhoondi A, Pourmortazavi SM (2004) Supercritical carbon dioxide extraction of *Mentha pulegium* L. essential oil. Talanta 62:407–411

Aguilera JM, Stanley DW (1999) Microstructural principles of food processing and engineering, 2nd edn. Aspen Publishers, Gaithersburg, MD

Akgun M, Akgun NA, Dincer S (1999) Phase behaviour of essential oil components in supercritical carbon dioxide. J Supercrit Fluids 15:117–125

Akgun M, Akgun NA, Dincer S (2000) Extraction and modeling of lavender flower essential oil using supercritical carbon dioxide. Ind Eng Chem Res 39:473–477

Araus K, Uquiche E, del Valle JM (2009) Matrix effects in supercritical CO_2 extraction of essential oils from plant material. J Food Eng 92:438–447

Bakkali F, Averbeck S, Averbeck D, Zhiri A, Idaomar M (2005) Cytotoxicity and gene induction by some essential oils in the yeast *Saccharomyces cerevisiae*. Mutat Res 585:1–13

Bensebia O, Barth D, Bensebia B, Dahmani A (2009) Supercritical CO_2 extraction of rosemary: Effect of extraction parameters and modelling. J Supercrit Fluids 49:161–166

Benvenuti F, Gironi F (2001) High-pressure equilibrium data in systems containing supercritical carbon dioxide, limonene, and citral. J Chem Eng Data 46:795–799

Berna A, Chafer A, Monton JB (2000) Solubilities of essential oil components of orange in supercritical carbon dioxide. J Chem Eng Data 45:724–727

Brielmann HL, Setzer WN, Kaufman PB, Kirakosyan A, Cseke LJ (2006) Phytochemicals: The chemical components of plants. In: Cseke LJ, Kirakosyan A, Kaufman PB, Warber S, Duke JA, Brielmann HL (eds) Natural products from plants, 2nd edn. CRC Press, Boca Raton, FL, pp 1–49

Brunner G (1984) Mass transfer from solid material in gas extraction. Ber Bunsen Ges Phys Chem 88:887–891

Brunner G (1994) Gas extraction: an introduction to fundamentals of supercritical fluids and the application to separation processes. Springer, New York

Budich M, Brunner G (1999) Vapor–liquid equilibrium data and flooding point measurements of the mixture carbon dioxide + orange peel oil. Fluid Phase Equilib 158–160:759–773

Budich M, Heilig S, Wesse T, Leibküchler V, Brunner G (1999) Countercurrent deterpenation of citrus oils with supercritical CO_2. J Supercrit Fluids 14:105–114

Campos LMAS, Michielin EMZ, Danielski L, Ferreira SRS (2005) Experimental data and modeling the supercritical fluid extraction of marigold (*Calendula officinalis*) oleoresin. J Supercrit Fluids 34:163–170

Carman PC (1937) Fluid flow through granular beds. Trans Inst Chem Eng 15:150–166

Carvalho RN Jr, Corazza ML, Cardozo-Filho L, Meireles MAA (2006) Phase equilibrium for (camphor + CO_2), (camphor + propane), and (camphor + CO_2 + propane). J Chem Eng Data 51:997–1000

Catchpole OJ, King MB (1994) Measurement and correlation of binary diffusion coefficients in near critical fluids. Ind Eng Chem Res 33:1828–1837

Catchpole OJ, Andrews EW, Toikka GN, Wilkinson GT (1994) Mathematical models for the extraction of oils from plant matrices using near-critical solvent. In: Perrut M, Brunner G (eds) Proceedings of the third symposium on supercritical fluids, vol 2. Institut National Polytechnique de Lorraine, Lorraine, France, pp 47–52

Catchpole OJ, Bernig R, Bott MB (1996a) Measurement and correlation of packed-bed axial dispersion coefficients in supercritical carbon dioxide. Ind Eng Chem Res 35:824–828

Catchpole OJ, Grey JB, Smallfield BM (1996b) Near-critical extraction of sage, celery, and coriander seed. J Supercrit Fluids 9:273–279

Chafer A, Berna A, Monton JB, Mulet A (2001) High pressure solubility data of the system limonene plus linalool plus CO_2. J Chem Eng Data 46:1145–1148

Chandler K, Pouillot FLL, Eckert CA (1996) Phase equilibria of alkanes in natural gas systems. 3. Alkanes in carbon dioxide. J Chem Eng Data 41:6–10

Chang CMJ, Chen CC (1999) High-pressure densities and *P–T–x–y* diagrams for carbon dioxide + linalool and carbon dioxide + limonene. Fluid Phase Equilib 163:119–126

Cheng K-W, Kuo S-J, Muoi Tang M, Chen Y-P (2000) Vapor–liquid equilibria at elevated pressures of binary mixtures of carbon dioxide with methyl salicylate, eugenol, and diethyl phthalate. J Supercrit Fluids 18:87–99

Chrastil J (1982) Solubility of solids and liquids in supercritical gases. J Phys Chem 86: 3016–3021

Coelho JAP, Mendes RL, Provost MC, Cabral JMS, Novais JM, Palavra AMF (1997) Supercritical carbon dioxide extraction of volatile compounds from rosemary. In: Abraham MA, Sunol AK (eds) Supercritical fluids. Extraction and pollution prevention. American Chemical Society, Washington, DC, pp 101–109

Coelho JAP, Pereira AP, Mendes RL, Palavra AMF (2003) Supercritical carbon dioxide extraction of *Foeniculum vulgare* volatile oil. Flavour Frag J 18:316–319

Crank J (1975) The mathematics of diffusion, 2nd edn. Oxford University Press, New York

Cygnarowicz-Provost M (1996) Design and economic analysis of supercritical fluid extraction processes. In: King JW, List GR (eds) Supercritical fluid technology in oil and lipid chemistry. AOCS Press, Champaign, IL, pp 155–179

Daghero J, Ruetsch L, Zacchi P, Mattea M (2004) Supercritical CO_2 extraction of herbaceous matrices. Pilot plant experiments and modeling. V Encuentro Brasileño sobre Fluidos Supercríticos (EBFS 2004), Florianopolis, Brasil

Danielski L, Campos LMAS, Bresciani LFV, Hense H, Yunes RA, Ferreira SRS (2007) Marigold (*Calendula officinalis* L.) oleoresin: solubility in SC-CO_2 and composition profile. Chem Eng Process 46:99–106

Daubert TE, Danner RP (1989) Physical and thermodynamic properties of pure chemicals: data compilation. Hemisphere Publishers, New York

del Valle JM, Aguilera JM (1999) Extracción con CO_2 a alta presión. Fundamentos y aplicaciones en la industria de alimentos. Food Sci Technol Int 5:1–24

del Valle JM, Catchpole OJ (2005) Transferencia de masa en lechos empacados operando con fluidos supercríticos. I. Correlación de coeficientes de dispersión axial. XVI Congreso Chileno de Ingeniería Química, Pucón, Chile

del Valle JM, de la Fuente JC, Cardarelli DA (2005) Contributions to supercritical extraction of vegetable substrates in Latin America. J Food Eng 67:35–57

del Valle JM, de la Fuente JC (2006) Supercritical CO_2 extraction of oilseeds: Review of kinetic and equilibrium models. CRC Crit Rev Food Sci Nutr 46:131–160

del Valle JM, Rivera O, Mattea M, Ruetsch L, Daghero J, Flores A (2004) Supercritical CO_2 processing of pretreated rosehip seeds: Effect of process scale on oil extraction kinetics. J Supercrit Fluids 31:159–174

del Valle JM, Mena C, Budinich M (2008) Extraction of garlic with supercritical CO_2 and conventional organic solvents. Braz J Chem Eng 25:535–542

Della Porta G, Taddeo R, D'urso E, Reverchon E (1998) Isolation of clove bud and star anise essential oil by supercritical CO_2 extraction. Lebensm Wiss Technol 31:454–460

Della Porta G, Porcedda S, Marongiu B, Reverchon E (1999) Isolation of eucalyptus oil by supercritical fluid extraction. Flavour Frag J 14:214–218

Denny EFK (1991) Field distillation for herbaceous oils, 2nd edn. Denny, McKenzie Associates, Lilydale (Tasmania), Australia

di Giacomo G, Brandani V, del Re G, Mucciante V (1989) Solubility of essential oil components in compressed supercritical carbon dioxide. Fluid Phase Equilib 52:405–411

Dullien F (1992) Porous media. Fluid transport and pore structure, 2nd edn. Academic, San Diego, CA

Eggers R (1996) Supercritical fluid extraction of oilseeds/lipids in natural products. In: King JW, List GR (eds) Supercritical fluid technology in oil and lipid chemistry. AOCS Press, Champaign, IL, pp 35–64

Eggers R, Ambrogi A, von Schnitzler J (2000) Special features of SFC solid extraction of natural products: Deoling of wheat gluten and extraction of rose hip oil. Braz J Chem Eng 17:329–334

Espinosa-Díaz MA, Guetachew T, Landy P, Jose J, Voilley A (1999) Experimental and estimated saturated vapor pressure of aroma compounds. Fluid Phase Equilib 157:257–270

Esquivel MM, de Sousa CL, Ribeiro MA, Bernardo-Gil MG (1996) Mathematical models for supercritical extraction of oregano "*Origanum virens* L.". In: von Rohr PR, Trepp C (eds) High pressure chemical engineering. Elsevier, Amsterdam, The Netherlands, pp 525–530

Fahien RW, Smith JM (1955) Mass transfer in packed beds. Am Inst Chem Eng J 1:28–37

Ferreira SRS, Meireles MAA (2002) Modeling the supercritical fluid extraction of black pepper (*Piper nigrum* L.) essential oil. J Food Eng 54:263–269

Ferreira SRS, Nikolov ZL, Doraiswamy LK, Meireles MAA, Petentate A (1999) Supercritical fluid extraction of black pepper (*Piper nigrum* L.) essential oil. J Supercrit Fluids 14:235–245

Fonseca J, Simoes PC, Nunes da Ponte M (2003) An apparatus for high-pressure VLE measurements using a static mixer. Results for (CO_2 + limonene + citral) and (CO_2 + limonene + linalool). J Supercrit Fluids 25:7–17

Francisco JD, Sivik B (2002) Solubility of three monoterpenes, their mixtures and eucalyptus leaf oils in dense carbon dioxide. J Supercrit Fluids 23:11–19

Funazukuri T, Kong C, Kagei S (1998) Effective axial dispersion coefficients in packed beds under supercritical conditions. J Supercrit Fluids 13:169–175

Gamse T, Marr R (2000) High-pressure phase equilibria of the binary systems carvone-carbon dioxide and limonene-carbon dioxide at 303, 313 and 323 K. Fluid Phase Equilib 171:165–174

Gardner DS (1993) Commercial scale extraction of alpha acids and hop oils with compressed CO_2. In: King MB, Bott TR (eds) Extraction of natural products using near-critical solvents. Blackie Academic & Professional, London, UK, pp 84–100

Gaspar F (2002) Extraction of essential oils and cuticular waxes with compressed CO_2: Effect of extraction pressure and temperature. Ind Eng Chem Res 41:2497–2503

Gaspar F, Santos R, King MB (2001) Disruption of glandular trichomes with compressed CO_2: Alternative matrix pre-treatment for CO_2 extraction of essential oils. J Supercrit Fluids 21:11–22

Gaspar F, Lu T, Santos R, Al-Duri B (2003) Modelling the extraction of essential oils with compressed carbon dioxide. J Supercrit Fluids 25:247–260

Germain JC, del Valle JM, de la Fuente JC (2005) Natural convection retards supercritical CO_2 extraction of essential oils and lipids from vegetable substrates. Ind Eng Chem Res 44:2879–2886

Ghoreishi SM, Akgerman A (2004) Dispersion coefficients of supercritical fluid in fixed beds. Sep Purif Technol 39:39–50

Gironi F, Maschietti M (2008) Continuous countercurrent deterpenation of lemon essential oil by means of supercritical carbon dioxide: experimental data and process modeling. Chem Eng Sci 63:651–661

Goodarznia I, Eikani M (1998) Supercritical carbon dioxide extraction of essential oils: Modelling and simulation. Chem Eng Sci 53:1387–1395

Goto M, Sato M, Hirose T (1993) Extraction of peppermint oil by supercritical carbon dioxide. J Chem Eng Jpn 26:401–407

Goto M, Roy BC, Hirose T (1996) Shrinking-core leaching model for supercritical-fluid extraction. J Supercrit Fluids 9:128–133

Goto M, Roy B, Kodama A, Hirose T (1998) Modeling supercritical fluid extraction process involving solute-solid interaction. J Chem Eng Jpn 32:171–177

Hall HK (ed) (2001) Landolt-Börnstein: Numerical data and functional relationships in science and technology – New Series. Group 4: Physical chemistry, Vol. 20: Vapor pressure of chemicals. Subvolume B: Vapor pressure and antoine constants for oxygen containing organic compounds. Springer, Berlin, Germany

Han N-H, Bhakta J, Carbonell RG (1985) Longitudinal and lateral dispersion in packed beds: effect of column length and particle size distribution. Am Inst Chem Eng J 31:277–288

Helmig D, Revermann T, Pollmann J, Kaltschmidt O, Jiménez-Hernández A, Bocquet F, David D (2003) Calibration system and analytical considerations for quantitative sesquiterpene measurements in air. J Chromatogr A 1002:193–211

Hong IK, Rho SW, Lee KS, Lee WH, Yoo KP (1990) Modeling of soybean oil bed extraction with supercritical carbon dioxide. Korean J Chem Eng 7:40–46

Hubert P, Vitzthum OG (1978) Fluid extraction of hops, spices and tobacco with supercritical gases. Angew Chem Int Ed Engl 17:710–715

Hybertson BM (2007) Solubility of the sesquiterpene alcohol patchoulol in supercritical carbon dioxide. J Chem Eng Data 52:235–238

Iwai Y, Hosotani N, Morotomi T, Koga Y, Arai Y (1994) High-pressure vapor-liquid-equilibria for carbon-dioxide plus linalool. J Chem Eng Data 39:900–902

Iwai Y, Morotomi T, Sakamoto K, Koga Y, Arai Y (1996) High-pressure vapor-liquid equilibria for carbon dioxide plus limonene. J Chem Eng Data 41:951–952

Jimenez-Carmona MM, Ubera JL, Luque de Castro MD (1999) Comparison of continous subcritical water extraction and hydrodistillation of marjoram essential oil. J Chromatogr A 855:625–632

Kim KH, Hong J (1999) Equilibrium solubilities of spearmint oil components in supercritical carbon dioxide. Fluid Phase Equilib 164:107–115

Kim KH, Hong J (2002) A mass transfer model for super- and near-critical CO_2 extraction of spearmint leaf oil. Sep Sci Technol 37:2271–2288

King MB, Catchpole O (1993) Physico-chemical data required for the design of near-critical fluid extraction process. In: King MB, Bott TR (eds) Extraction of natural products using near-critical solvents. Blackie Academic & Professional, London, UK, pp 184–231

Kotnik P, Skerget M, Knez Z (2007) Supercritical fluid extraction of chamomile flower heads: Comparison with conventional extraction, kinetics and scale-up. J Supercrit Fluids 43: 192–198

Lack E, Seidlitz H (1993) Commercial scale decaffeination of coffee and tea using supercritical CO_2. In: King MB, Bott TR (eds) Extraction of natural products using near-critical solvents. Blackie Academic & Professional, London, UK, pp 101–139

Langa E, Della Porta G, Palavra AMF, Urieta JS, Mainar A (2009) Supercritical fluid extraction of Spanish sage essential oil: Optimization of the process parameters and modelling. J Supercrit Fluids 49:174–181

Lee CH, Holder GD (1995) Use of supercritical fluid chromatography for obtaining mass transfer coefficients in fluid-solid systems at supercritical conditions. Ind Eng Chem Res 34:906–914

Leeke GA, Santos R, King M (2001) Vapor-liquid equilibria for the carbon dioxide plus carvacrol system at elevated pressures. J Chem Eng Data 46:541–545

Louli V, Folas G, Voutsas E, Magoulas K (2004) Extraction of parsley seed oil by supercritical CO_2. J Supercrit Fluids 30:163–174

Ma YH, Evans LB (1968) Transient diffusion from a well-stirred reservoir to a body of arbitrary shape. J Am Inst Chem Eng 14:956–961

Machmudah S, Sulaswatty A, Sasaki M, Goto M, Hirose T (2006) Supercritical CO_2 extraction of nutmeg oil: Experiments and modeling. J Supercrit Fluids 39:30–39

Marrone C, Poletto M, Reverchon E, Stassi A (1998) Almond oil extraction by supercritical CO_2: Experiments and modelling. Chem Eng Sci 53:3711–3718

Marteau Ph, Obriot J, Tufeu R (1995) Experimental determination of vapor-liquid equilibria of CO_2 + limonene and CO_2 + citral mixtures. J Supercrit Fluids 8:20–24

Martin AJP, Synge R (1941) A new form of chromatogram employing two liquid phases. 1. A theory of chromatography. 2. Application to the micro-determination of the higher mono-amino-acids in proteins. Biochem J 35:1358–1368

Martínez J, Monteiro AR, Rosa PTV, Marques MOM, Meireles M (2003) Multicomponent model to describe extraction of ginger oleoresin with supercritical carbon dioxide. Ind Eng Chem Res 42:1057–1063

Martínez J, Rosa PTV, Meireles MAA (2007) Extraction of clove and vetiver oils with supercritical carbon dioxide: modeling and simulation. Open Chem Eng J 1:1–7

Matos HA, Gomes de Azevedo E, Simoes PC, Carrondo MT, Nunes da Ponte M (1989) Phase equilibria of natural flavours and supercritical solvents. Fluid Phase Equilib 52:357–364

Michielin EMZ, Rosso SR, Franceschi E, Borges GR, Corazza ML, Oliveira JV, Ferreira SRS (2009) High-pressure phase equilibrium data for systems with carbon dioxide, α-humulene and *trans*-caryophyllene. J Chem Thermodyn 41:130–137

Mira B, Blasco M, Subirats S, Berna A (1996) Supercritical CO_2 extraction of essential oils from orange peel. J Supercrit Fluids 9:238–243

Mira B, Blasco M, Berna A, Subirats S (1999) Supercritical CO_2 extraction of essential oil from orange peel. Effect of operation conditions on the extract composition. J Supercrit Fluids 14:95–104

Miraldi E, Ferri S, Franchi GG, Giorgi G (1996) *Peumus boldus* essential oil: New constituents and comparison of oils from leaves of different origin. Fitoterapia 67:227–230

Mišić D, Zizovic I, Stamenić M, Ašanin R, Ristić M, Petrović SD, Skala D (2008) Antimicrobial activity of celery fruit isolates and SFE process modeling. Biochem Eng J 42:148–152

Morotomi T, Iwai Y, Yamaguchi H, Arai Y (1999) High-pressure vapor-liquid equilibria for carbon dioxide plus limonene plus linalool. J Chem Eng Data 44:1370–1372

Moura LS, Corazza ML, Cardozo-Filho L, Meireles MAA (2005) Phase equilibrium measurements for the system fennel (*Foeniculum vulgare*) extract + CO_2. J Chem Eng Data 50:1657–1661

Moyler DA (1993) Extraction of flavours and fragrances with compressed CO_2. In: King MB, Bott TR (eds) Extraction of natural products using near-critical solvents. Blackie Academic & Professional, London, UK, pp 140–183

Mukhopadhyay M (2000) Natural extracts using supercritical carbon dioxide. CRC Press, Boca Raton, FL

Mukhopadhyay M, De SK (1995) Fluid-phase behavior of close molecular-weight fine chemicals with supercritical carbon dioxide. J Chem Eng Data 40:909–913

NIST (2000) Fluid Thermodynamic and Transport Properties (version 5.0). http://www.nist.gov/srd/nist23.htm

Núñez GA, del Valle JM, de la Fuente JC (2010) Solubilities in supercritical carbon dioxide of (2E,6E)-3,7,11-trimethyldodeca-2,6,10-trien-1-ol (farnesol) and (2 S)-5,7-dihydroxy-2-(4-hydroxyphenyl)chroman-4-one (naringenin). J Chem Eng Data 55:3863–3868

Özer EÖ, Platin S, Akman U, Hortaçsu Ö (1996) Supercritical carbon dioxide extraction of spearmint oil from mint-plant leaves. Can J Chem Eng 74:920–928

Papamichail I, Louli V, Magoulas K (2000) Supercritical fluid extraction of celery seed oil. J Supercrit Fluids 18:213–226

Pavlicek J, Richter M (1993) High pressure vapour-liquid equilibrium in the carbon dioxide–α-pinene system. Fluid Phase Equilib 90:125–133

Perakis C, Louli V, Magoulas K (2005) Supercritical fluid extraction of black pepper oil. J Food Eng 71:386–393

Perrut M, Clavier JY, Poletto M, Reverchon E (1997) Mathematical modeling of sunflower seed extraction by supercritical CO_2. Ind Eng Chem Res 36:430–435

Pfaf-Šovljanski II, Grujić OS, Peruničić MB, Cvetković IM, Zeković Z (2005) Supercritical carbon dioxide hop extraction. APTEFF 36:111–120

Pfohl O, Petkov S, Brunner G (2000) PE 2000: a powerful tool to correlate phase equilibria. Herbert Utz Verlag, München, Germany

Podlaski S, Chrobak Z, Wyszkowska Z (2003) The effect of parsley seed hydration treatment and pelleting on seed vigour. Plant Soil Environ 49:114–118
Poling BE, Prausnitz JM, O'Connell J (2000) The properties of gases and liquids, 5th edn. McGraw-Hill, New York
Povh NP, Marques MOM, Meireles MAA (2001) Supercritical CO_2 extraction of essential oil and oleoresin from chamomile (*Chamomilla recutita* L.). J Supercrit Fluids 21:245–256
Puiggené J, Larrayoz MA, Recasens F (1997) Free liquid-to-supercritical fluid mass transfer in packed beds. Chem Eng Sci 52:195–212
Quirin K-W, Gerard D (2007) Supercritical fluid extraction (SFE). In: Ziegler H (ed) Flavourings: production, composition, applications, regulations, 2nd edn. Wiley-VCH, Weinheim, Germany, pp 49–65
Raal JD, Mühlbauer AL (1998) Phase equilibria: measurement and computation. Taylor & Francis, Washington, DC
Raeissi S, Peters CJ (2005) Experimental determination of high-pressure phase equilibria of the ternary system carbon dioxide + limonene + linalool. J Supercrit Fluids 35:10–17
Reis-Vasco EMC, Coelho JAP, Palavra AMF, Marrone C, Reverchon E (2000) Mathematical modelling and simulation of pennyroyal essential oil supercritical extraction. Chem Eng Sci 55:2917–2922
Reverchon E (1996) Mathematical modeling of supercritical extraction of sage oil. J Am Inst Chem Eng 42:1765–1771
Reverchon E (1997) Supercritical fluid extraction and fractionation of essential oils and related products. J Supercrit Fluids 10:1–37
Reverchon E, De Marco I (2006) Supercritical fluid extraction and fractionation of natural matter. J Supercrit Fluids 38:146–166
Reverchon E, De Marco I (2008) Essential oils extraction and fractionation using supercritical fluids. In: Martínez JL (ed) Supercritical fluid extraction of nutraceuticals and bioactive compounds. CRC Press, Boca Raton, FL, pp 305–335
Reverchon E, Marrone C (1997) Supercritical extraction of clove bud essential oil: Isolation and mathematical modeling. Chem Eng Sci 52:3421–3428
Reverchon E, Sesti Osséo L (1994a) Modelling the supercritical extraction of basil oil. In: Perrut M, Brunner G (eds) Proceedings of the third symposium on supercritical fluids, Vol. 2., pp 189–196
Reverchon E, Sesti Osséo L (1994b) Supercritical CO_2 extraction of basil oil: Characterization of products and process modeling. J Supercrit Fluids 7:185–190
Reverchon E, Donsi G, Sesti Osséo L (1993a) Modeling of supercritical fluid extraction from herbaceous matrices. Ind Eng Chem Res 32:2721–2726
Reverchon E, Russo P, Stassi A (1993b) Solubilities of solid octacosane and triacontane in supercritical carbon dioxide. J Chem Eng Data 38:458–460
Reverchon E, Della Porta G, Senatore F (1995a) Supercritical CO_2 extraction and fractionation of lavender essential oil and waxes. J Agr Food Chem 43:1654–1658
Reverchon E, Taddeo R, Della Porta G (1995b) Extraction of sage oil by supercritical CO2: Influence of some process parameters. J Supercrit Fluids 8:302–309
Reverchon E, Daghero J, Marrone C, Mattea M, Poletto M (1999) Supercritical fractional extraction of fennel seed oil and essential oil: Experiments and mathematical modeling. Ind Eng Chem Res 38:3069–3075
Richter M, Sovová H (1993) The solubility of 2 monoterpenes in supercritical carbon-dioxide. Fluid Phase Equilib 85:285–300
Rodrigues VM, Rosa PTV, Marques MOM, Petenate AJ, Meireles MAA (2003) Supercritical extraction of essential oil from aniseed (*Pimpinella anisum* L.) using CO_2: Solubility, kinetics, and composition data. J Agric Food Chem 51:1518–1523
Roy BC, Goto M, Hirose T (1996) Extraction of ginger oil with supercritical carbon dioxide: Experiments and modeling. Ind Eng Chem Res 35:607–612
Ruetsch L, Daghero J, Mattea M (2003) Supercritical extraction of solid matrices. Model formulation and experiments. Lat Am Appl Res 33:103–107

Salimi A, Fatemi S, Zakizadeh Nei Nei H, Safaralie A (2008) Mathematical modeling of supercritical extraction of valerenic acid from *Valeriana officinalis* L. Chem Eng Technol 31:1470–1480

Sanders N (1993) Food legislation and the scope for increased use of near-critical fluid extraction operations in the food, flavouring and pharmaceutical industries. In: King MB, Bott TR (eds) Extraction of natural products using near-critical solvents. Blackie Academic & Professional, London, UK, pp 34–49

Sefidkon F, Dabiri M, Mirmostafa SA (2004) The composition of *Thymus serpyllum* L. oil. J Essent Oil Res 16:184–185

Serrato-Valenti G, Bisio A, Cornara L, Ciarallo G (1997) Structural and histochemical investigation of the glandular trichomes of *Salvia aurea* L. leaves, and chemical analysis of the essential oil. Ann Bot 79:329–336

Simandi B, Deák A, Rónyai E, Yanxiang G, Veress T, Lemberkovics E, Then M, Saa-Kiss A, Vámos-Falusi Z (1999) Supercritical carbon dioxide extraction and fractionation of fennel oil. J Agric Food Chem 47:1635–1640

Simões-Pires CA, Debenedetti S, Spegazzini E, Mentz LA, Matzenbacher NI, Limberger RP, Henriques A (2005) Investigation of the essential oil from eight species of *Baccharis* belonging to sect. Caulopterae (Asteraceae, Astereae): A taxonomic approach. Plant Syst Evol 253:23–32

Skerget M, Knez Z (2001) Modelling high pressure extraction processes. Comput Chem Eng 25:879–886

Sousa EMBD, Chiavone-Filho O, Moreno MT, Silva DN, Marques MOM, Meireles MAA (2002) Experimental results for the extraction of essential oil from *Lippia sidoides* Cham. using pressurized carbon dioxide. Braz J Chem Eng 19:229–241

Sousa EMBD, Martínez J, Chiavone-Filho O, Rosa PTV, Domingos T, Meireles MAA (2005) Extraction of volatile oil from *Croton zehntneri* Pax et Hoff with pressurized CO_2: Solubility, composition and kinetics. J Food Eng 69:325–333

Souza AT, Corazza ML, Cardozo-Filho L, Guirardello R, Meireles MAA (2004) Phase equilibrium measurements for the system clove (*Eugenia caryophyllus*) oil + CO_2. J Chem Eng Data 49:352–356

Sovová H (1994) Rate of the vegetable oil extraction with supercritical CO_2.1. Modeling of extraction curves. Chem Eng Sci 49:409–414

Sovová H (2005) Mathematical model for supercritical fluid extraction of natural products and extraction curve evaluation. J Supercrit Fluids 33:35–52

Sovová H, Jež J (1994) Solubility of menthol in supercritical carbon-dioxide. J Chem Eng Data 39:840–841

Sovová H, Komers R, Kucera J, Jež J (1994a) Supercritical carbon dioxide extraction of caraway essential oil. Chem Eng Sci 49:2499–2505

Sovová H, Kucera J, Jez J (1994b) Rate of vegetable oil extraction with supercritical CO_2. 2. Extraction of grape oil. Chem Eng Sci 49:415–420

Sovová H, Stateva RP, Galushko AA (2001) Essential oils from seeds: Solubility of limonene in supercritical CO_2 and how it is affected by fatty oil. J Supercrit Fluids 20:113–129

Sovová H, Stateva RP, Galushko AA (2007) High-pressure equilibrium of menthol + CO_2. J Supercrit Fluids 41:1–9

Spricigo CB, Pinto LT, Bolzan A, Novais AF (1999) Extraction of essential oil and lipids from nutmeg by liquid carbon dioxide. J Supercrit Fluids 15:253–259

Spricigo CB, Bolzan A, Pinto LT (2001) Mathematical modeling of nutmeg essential oil extraction by liquid carbon dioxide. Lat Am Appl Res 31:397–401

Stahl E, Quirin K-W, Gerard D (1988) Dense gases for extraction and refining. Springer-Verlag, Berlin, Germany

Stamenić M, Zizovic I, Orlović A, Skala D (2008) Mathematical modelling of essential SFE on the micro-scale. Classification of plant material. J Supercrit Fluids 46:285–292

Stassi A, Schiraldi A (1994) Solubility of vegetable cuticular waxes in supercritical CO_2 isothermal calorimetry investigations. Thermochim Acta 246:417–425

Šťastová J, Jež J, Bartlová M, Sovová H (1996) Rate of vegetable oil extraction with supercritical CO_2. 3. Extraction from sea buckthorn. Chem Eng Sci 51:4347–4352
Steffani E, Atti-Santos AC, Atti-Serafini L, Pinto LT (2006) Extraction of ho-sho (*Cinnamomum camphora* Nees and Eberm var. *Linaloolifera fujita*) essential oil with supercritical CO_2: Experiments and modeling. Braz J Chem Eng 23:259–266
Stüber F, Vázquez AM, Larrayoz MA, Recasens F (1996) Supercritical fluid extraction of packed beds: External mass transfer in upflow and downflow operation. Ind Eng Chem Res 35:3618–3628
Stüber F, Julien S, Recasens F (1997) Internal mass transfer in sintered metallic pellets filled with supercritical fluid. Chem Eng Sci 52:3527–3542
Stull DR (1947) Vapor pressures of pure substances organic compounds. Ind Eng Chem 39:517–540
Svoboda K, Svoboda T (2000) Secretory structures of aromatic and medicinal plants. A review and atlas of micrographs. Microscopix Publications, Knighton, UK
Takeuchi TM, Leal PF, Favareto R, Cardozo-Filho L, Corazza ML, Rosa PTV, Meireles MAA (2008) Study of the phase equilibrium formed inside the flash tank used at the separation step of a supercritical fluid extraction unit. J Supercrit Fluids 43:447–459
Tan CS, Liou DC (1989) Axial dispersion of supercritical carbon dioxide in packed beds. Ind Eng Chem Res 28:1246–1250
Tan CS, Liang SK, Liou DC (1988) Fluid-solid mass transfer in a supercritical fluid extractor. Chem Eng J 38:17–22
Teixeira de Souza A, Benazzia T, Boer Grings M, Cabral V, da Silva E, Cardozo-Filho L, Ceva Antunes O (2008) Supercritical extraction process and phase equilibrium of candeia (*Eremanthus erythropappus*) oil using supercritical carbon dioxide. J Supercrit Fluids 47:182–187
Temelli F, O'Connell JP, Chen CS, Braddock RJ (1990) Thermodynamic analysis of supercritical carbon dioxide extraction of terpenes from cold-pressed orange oil. Ind Eng Chem Res 29:618–624
The Good Scents Company (2009a) http://www.thegoodscentscompany.com/data/rw1060851.html
The Good Scents Company (2009b) http://www.thegoodscentscompany.com/data/rw1005091.html
Tufeu R, Subra P, Plateaux C (1993) Contribution to the experimental determination of the phase diagrams of some (carbon dioxide + a terpene) mixtures. J Chem Thermodyn 25:1219–1228
Uquiche E, Huerta E, Sandoval A, del Valle JM. Effect of boldo (*Peumus boldus* M.) pretreatment on the kinetics of supercritical CO_2 essential oil extraction. J Food Eng (submitted)
Vargas RMF, Cassel E, Gomes GMF, Longhi LGS, Atti-Serafini L, Atti-Santos AC (2006) Supercritical extraction of *carqueja* essential oil: Experiments and modeling. Braz J Chem Eng 23:375–382
Vieira de Melo SAB, Pallado P, Guarise GB, Bertucco A (1999) High-pressure vapor-liquid equilibrium data for binary and ternary systems formed by supercritical CO_2, limonene and linalool. Braz J Chem Eng 16:7–17
Villermaux J (1987) Chemical engineering approach to dynamic modelling of linear chromatography: A flexible method for representing complex phenomena from simple concepts. J Chromatogr A 406:11–26
Wagner Z, Pavlicek J (1993) Vapour-liquid equilibrium in the carbon dioxide: p-cymene system at high pressure. Fluid Phase Equilib 90:135–141
Wakao N, Kaguei S (1982) Heat and mass transfer in packed beds. Gordon & Breach, New York
Wakao N, Smith JM (1962) Diffusion in catalyst pellets. Chem Eng Sci 17:825–834
Xing H, Yang Y, Su B, Huang M, Ren Q (2003) Solubility of artemisinin in supercritical carbon dioxide. J Chem Eng Data 48:330–332
Yu D (1998) Solute pulse dispersion in soil columns: a comparison of supercritical CO_2, gaseous and aqueous systems. Ph.D. thesis, University of California at Los Angeles, CA

Zekovic Z, Lepojevic Z, Tolic A (2001) Modeling of the thyme-supercritical carbon dioxide extraction system. I. The influence of carbon dioxide flow rate and grinding degree of thyme. Sep Sci Technol 36:2459–3472

Zetzl C, Brunner G, Meireles MAA (2003) Standardized low-cost batch SFE-units for university education and comparative research. In: Brunner G, Kikic I, Perrut M (eds) Proceedings of the 6th international symposium on supercritical fluids. Institut National Polytechnique de Lorraine, Lorraine, France, pp 577–585

Zizovic I, Stamenić M, Orlović A, Skala D (2005) Supercritical carbon dioxide essential oil extraction of Lamiaceae family species: Mathematical modelling on the micro-scale and process optimization. Chem Eng Sci 60:6747–6756

Zizovic I, Stamenić M, Ivanović J, Orlović A, Ristić M, Djordjević S, Petrović SD, Skala D (2007a) Supercritical carbon dioxide extraction of sesquiterpenes from valerian root. J Supercrit Fluids 43:249–258

Zizovic I, Stamenić M, Orlović A, Skala D (2007b) Supercritical carbon dioxide extraction of essential oils from plants with secretory ducts: Mathematical modelling on the micro-scale. J Supercrit Fluids 39:338–346

Zizovic IT, Stamenić MD, Orlović AM, Skala DU (2007c) Supercritical carbon-dioxide extraction of essential oils and mathematical modelling on the micro-scale. In: Berton LP (ed) Chemical engineering research trends. Nova Science Publishers, New York, pp 221–249